International Tables for Crystallography (2010). Vol. B, Chapter 4.2, pp. 492–539.

4.2. Disorder diffuse scattering of X-rays and neutrons

By F. Frey, H. Boysen and H. Jagodzinski

4.2.1. Introduction

Diffuse scattering of X-rays, neutrons and other particles is an accompanying effect in all diffraction experiments aimed at structure analysis with the aid of elastic scattering. In this case, the momentum exchange of the scattered photon or particle includes the crystal as a whole; the energy transfer involved becomes negligibly small and need not be considered in diffraction theory. Static distortions as a consequence of structural changes cause typical elastic diffuse scattering. Many structural phenomena and processes contribute to diffuse scattering, and a general theory has to include all of them. Hence the exact treatment of diffuse scattering becomes very complex.

Inelastic scattering is due to dynamical fluctuations or ionization processes and may become observable as a 'diffuse' contribution in a diffraction pattern. A separation of elastic from inelastic diffuse scattering is generally possible, but difficulties may result from small energy exchanges that cannot be resolved for experimental reasons. The latter is true for scattering of X-rays by phonons, which have energies of the order of 10^{-2}–10^{-3} eV, values which are considerably smaller than 10 keV, a typical value for X-ray quanta. Another equivalent explanation, frequently forwarded in the literature, is the high speed of X-ray photons, such that the rather slow motion of atoms cannot be 'observed' by them during diffraction. Hence, all movements appear as static displacement waves of atoms, and temperature diffuse scattering is pseudo-elastic for X-rays. This is not true in the case of thermal neutrons, which have energies comparable to those of phonons. Phonon-related or thermal diffuse scattering is discussed separately in Chapter 4.1, *i.e.* the present chapter is mainly concerned with the elastic (or pseudo-elastic other than thermal) part of diffuse scattering. A particularly important aspect concerns diffuse scattering related to phase transitions, in particular the critical diffuse scattering observed at or close to the transition temperature. In simple cases, a satisfactory description may be given with the aid of a 'soft phonon', which freezes at the critical temperature, thus generating typical temperature-dependent diffuse scattering. If the geometry of the lattice is maintained during the transformation (*i.e.* there is no breakdown into crystallites of different cell geometry), the diffuse scattering is very similar to diffraction phenomena described in this chapter. Sometimes, however, very complicated interim stages (ordered or disordered) are observed, demanding a complicated theory for their full explanation (see, *e.g.*, Dorner & Comes, 1977).

Obviously, there is a close relationship between thermodynamics and diffuse scattering in disordered systems representing a stable or metastable thermal equilibrium. From the thermodynamical point of view, the system is then characterized by its grand partition function, which is intimately related to the correlation functions used in the interpretation of diffuse scattering. The latter is nothing other than a kind of 'partial partition function' where two atoms, or two cell occupancies, are fixed such that the sum of all partial partition functions represents the grand partition function. This fact yields the useful correlation between thermodynamics and diffuse scattering mentioned above, which may well be used for a determination of thermodynamical properties of the crystal. This important subject shall not be included here for the following reason: real three-dimensional crystals generally exhibit diffuse scattering by defects and/or disordering effects that are not in thermal equilibrium. They are created during crystal growth, or are frozen-in defects formed at higher temperatures. Hence a thermodynamical interpretation of diffraction data needs a careful study of diffuse scattering as a function of temperature or some other thermodynamical parameters. This can be done in very rare cases only, so the omission of this subject seems justified.

As shown in this chapter, electron-density fluctuations and distribution functions of defects play an important role in the complete interpretation of diffraction patterns. Both quantities may best be studied in the low-angle scattering range. Hence many problems cannot be solved without a detailed interpretation of low-angle diffraction (also called small-angle scattering).

Disorder phenomena in magnetic structures are also not specifically discussed here. Magnetic diffuse neutron scattering and special experimental techniques constitute a large subject by themselves. Many aspects, however, may be analysed along similar lines to those given here.

Glasses, liquids or liquid crystals show typical diffuse diffraction phenomena. Particle-size effects and strains have an important influence on the diffuse scattering. The same is true for dislocations and point defects such as interstitials or vacancies. These defects are mainly described by their strain field, which influences the intensities of sharp reflections like an artificial temperature factor: the Bragg peaks diminish in intensity while the diffuse scattering increases predominantly close to them. These phenomena are less important from a structural point of view, at least in the case of metals or other simple structures. This statement is true as long as the structure of the 'kernel' of defects may be neglected when compared with the influence of the strain field. Whether dislocations in more complicated structures meet this condition is not yet known.

Commensurate and incommensurate modulated structures and quasicrystals frequently show a typical diffuse scattering, a satisfactory explanation of which demands extensive experimental and theoretical study. A reliable structure determination becomes very difficult in cases where the interpretation of diffuse scattering has not been incorporated. Many erroneous structural conclusions have been published in the past. The solution of problems of this kind needs careful thermodynamical consideration as to whether a plausible explanation of the structural data can be given.

For all of the reasons mentioned above, this article cannot be complete. It is hoped, however, that it will provide a useful guide for those who need a full understanding of the crystal chemistry of a given structure.

The study of disorder in crystals by diffuse-scattering techniques can be performed with X-rays, neutrons or electrons. Each of these methods has its own advantages (and disadvantages) and they often can (or have to) be used in a complementary way (*cf.* Chapter 4.3 of this volume). Electron diffraction and microscopy are usually restricted to relatively small regions in space and thus supply information on a local scale, *i.e.* local defect structures. Moreover, electron-microscopy investigations are carried out on thin samples (films), where the disorder could be different from the bulk, and, in addition, could be affected by the high heat load deposited by the impinging electron beam. X-rays and neutrons sample larger crystal volumes and thus provide thermodynamically more important information on *averages* of the disorder. These methods are also better suited to the analysis of long-range correlated cooperative disorder phenomena. On the other hand, electron microscopy and diffraction often allow more direct access to disorder and can therefore provide valuable

information about the underlying model, which can then be used for a successful interpretation of X-ray and neutron diffuse scattering. Basic aspects of electron diffraction and microscopy in structure determination are treated in Chapter 2.5 of this volume.

There is no comprehensive treatment of all aspects of diffuse scattering. Essential parts are treated in the textbooks by James (1954), Wilson (1962), Wooster (1962), Krivoglaz (1969, 1996*a*,*b*), Schwartz & Cohen (1977), Billinge & Thorpe (1998), Schweika (1998), Nield & Keen (2001), Fultz & Howe (2002), Frey (2003) and Welberry (2004); handbook articles have been written by Jagodzinski (1963, 1964*a*,*b*, 1987), Schulz (1982), Welberry (1985) and Moss *et al.* (2003), and a series of relevant papers has been collected by Collongues *et al.* (1977).

Finally, we mention that different symbols and 'languages' are used in the various diffraction methods. Quite a few of the new symbols in use are not really necessary, but some are caused by differences in the experimental techniques. For example, the neutron scattering length b may usually be equated with the atomic form factor f in X-ray diffraction. The differential cross section introduced in neutron diffraction represents the intensity scattered into an angular range dΩ and an energy range dE. The 'scattering law' in neutron work corresponds to the square of an (extended) structure factor; the 'static structure factor', a term used by neutron diffractionists, is nothing other than the conventional Patterson function. The complicated resolution functions in neutron work correspond to the well known Lorentz factors in X-ray diffraction. These have to be derived in order to include all the techniques used in diffuse-scattering work. In this article we try to preserve the most common symbols. In particular, the scattering vector will be denoted as $\mathbf{H}$, which is more commonly used in crystallography than $\mathbf{Q} = 2\pi\mathbf{H}$.

4.2.2. Basic scattering theory

4.2.2.1. General

Diffuse scattering results from deviations from the identity of translationally invariant scattering objects and from long-range correlations in space and time. Fluctuations of scattering amplitudes and/or phase shifts of the scattered wavetrains reduce the maximum capacity of interference (leading to Bragg reflections) and are responsible for the diffuse scattering, *i.e.* scattering parts that are not located in distinct spots in reciprocal space. Unfortunately, the terms 'coherent' and 'incoherent' scattering used in this context are not uniquely defined in the literature. Since all scattering processes are correlated in space and time, there is no incoherent scattering at all in its strict sense. A similar relationship exists for 'elastic' and 'inelastic' scattering. Here pure inelastic scattering would take place if the momentum and the energy were transferred to a single scatterer; on the other hand, an elastic scattering process would demand a uniform exchange of momentum and energy with the whole crystal. Obviously, both cases are idealized and the truth lies somewhere in between. In spite of this, many authors use the term 'incoherent' systematically for the diffuse scattering away from the Bragg peaks when all diffuse maxima or minima are due to structure factors of molecules or atoms only. Although this definition is unequivocal as such, it is physically incorrect. Other authors use the term 'coherent' for Bragg scattering only; all diffuse contributions are then called 'incoherent'. This definition is clear and unique since it considers space and time, but it does not differentiate between incoherent and inelastic. In the case of neutron scattering, both terms are essential and neither can be abandoned.

In neutron diffraction, the term 'incoherent scattering' refers to scattering by uncorrelated nuclear spin orientations or by a random distribution of isotopes of the same element. Hence another definition of 'incoherence' is proposed for scattering processes that are uncorrelated in space and time. In fact, there may be correlations between the spins *via* their magnetic field, but the correlation length in space (and time) may be very small, such that the scattering process appears to be incoherent. Even in these cases, the nuclei contribute to coherent (average structure) and incoherent scattering (diffuse background). Hence the scattering process cannot really be understood by assuming nuclei that scatter independently. For this reason, it seems to be useful to restrict the term 'incoherent' to cases where a random contribution to scattering is realized or, in other words, a continuous function exists in reciprocal space. This corresponds to a δ function in real four-dimensional space. The randomness may be attributed to a nucleus (neutron diffraction) or an atom (molecule). It follows from this definition that the scattering need not be constant, but may be modulated by structure factors of molecules. In this sense we shall use the term 'incoherent', remembering that it is incorrect from a physical point of view.

As mentioned in Chapter 4.1, the theory of thermal neutron scattering must be treated quantum mechanically. In principle, this is also true in the X-ray case. In the classical limit, however, the final expressions have a simple physical interpretation. Generally, the quantum-mechanical nature of the scattering function of thermal neutrons is negligible at higher temperatures and in those cases where energy or momentum transfers are not too large. In almost all disorder problems this classical interpretation is sufficient for the interpretation of diffuse-scattering phenomena. This is not quite true in the case of orientational disorder (plastic crystals) where H atoms are involved.

The basic formulae given below are valid in either the X-ray or the neutron case: the atomic form factor f replaces the coherent scattering length $b_{\rm coh}$ (abbreviated as b). The formulation in the frame of the van Hove correlation function $G(\mathbf{r}, t)$ (classical interpretation, coherent part) corresponds to a treatment by a four-dimensional Patterson function $P(\mathbf{r}, t)$.

The basic equations for the differential cross sections are

$$\frac{\mathrm{d}^2\sigma_{\rm coh}}{\mathrm{d}\Omega\ \mathrm{d}(\hbar\omega)} = N\frac{|\mathbf{k}|}{|\mathbf{k}_0|}\frac{\langle b\rangle^2}{2\pi\hbar}\int_{\mathbf{r}}\int_{t} G(\mathbf{r}, t) \times \exp\{2\pi i(\mathbf{H}\cdot\mathbf{r} - \nu t)\}\ \mathrm{d}\mathbf{r}\,\mathrm{d}t, \quad (4.2.2.1a)$$

$$\frac{\mathrm{d}^2\sigma_{\rm inc}}{\mathrm{d}\Omega\ \mathrm{d}(\hbar\omega)} = N\frac{|\mathbf{k}|}{|\mathbf{k}_0|}\frac{\langle b^2\rangle - \langle b\rangle^2}{2\pi\hbar}\int_{\mathbf{r}}\int_{t} G_{\rm s}(\mathbf{r}, t) \times \exp\{2\pi i(\mathbf{H}\cdot\mathbf{r} - \nu t)\}\ \mathrm{d}\mathbf{r}\,\mathrm{d}t, \quad (4.2.2.1b)$$

where N is the number of scattering nuclei of same chemical species; $\mathbf{k}$, $\mathbf{k}_0$ are the wavevectors after/before scattering and $\omega = 2\pi\nu$.

The integrations over space may be replaced by summations in disordered crystals, except in cases where structural elements exhibit a liquid-like behaviour. Then the van Hove correlation functions are

$$G(\mathbf{r}, t) = \frac{1}{N}\sum_{\mathbf{r}_j,\,\mathbf{r}_{j'}} \delta\{\mathbf{r} - [\mathbf{r}_{j'}(t) - \mathbf{r}_j(0)]\}, \quad (4.2.2.2a)$$

$$G_{\rm s}(\mathbf{r}, t) = \frac{1}{N}\sum_{\mathbf{r}_j} \delta\{\mathbf{r} - [\mathbf{r}_j(t) - \mathbf{r}_j(0)]\}. \quad (4.2.2.2b)$$

$G(\mathbf{r}, t)$ gives the probability that if there is an atom j at $\mathbf{r}_j(0)$ at time zero, there is an *arbitrary* atom j' at $\mathbf{r}_{j'}(t)$ at an *arbitrary* time t, while $G_{\rm s}(\mathbf{r}, t)$ refers to the *same* atom j at $\mathbf{r}_j(t)$ at time t.

Equations (4.2.2.1) may be rewritten using the four-dimensional Fourier transforms of G and $G_{\rm s}$, respectively:

$$S_{\rm coh}(\mathbf{H},\omega)=\frac{1}{2\pi}\int_{\mathbf{r}}\int_{t} G(\mathbf{r},t)\exp\{2\pi i(\mathbf{H}\cdot\mathbf{r}-\nu t)\}\,\mathrm{d}\mathbf{r}\,\mathrm{d}t, \quad (4.2.2.3a)$$

$$S_{\rm inc}(\mathbf{H},\omega)=\frac{1}{2\pi}\int_{\mathbf{r}}\int_{t} G_{\rm s}(\mathbf{r},t)\exp\{2\pi i(\mathbf{H}\cdot\mathbf{r}-\nu t)\}\,\mathrm{d}\mathbf{r}\,\mathrm{d}t, \quad (4.2.2.3b)$$

$$\frac{\mathrm{d}^2\sigma_{\rm coh}}{\mathrm{d}\Omega\,\mathrm{d}(\hbar\omega)}=N\frac{k}{k_0}\langle b\rangle^2 S_{\rm coh}(\mathbf{H},\omega), \quad (4.2.2.4a)$$

$$\frac{\mathrm{d}^2\sigma_{\rm inc}}{\mathrm{d}\Omega\,\mathrm{d}(\hbar\omega)}=N\frac{k}{k_0}[\langle b^2\rangle-\langle b\rangle^2]S_{\rm inc}(\mathbf{H},\omega). \quad (4.2.2.4b)$$

Incoherent scattering cross sections [(4.2.2.3*b*), (4.2.2.4*b*)] refer to one and the same particle (at different times). In particular, plastic crystals (see Section 4.2.5.5) may be studied by means of this incoherent scattering. It should be emphasized, however, that for reasons of intensity only disordered crystals with strong incoherent scatterers can be investigated by this technique. In practice, mostly samples that contain H atoms have been investigated. This topic will not be treated further in this article (see, *e.g.*, Springer, 1972; Lechner & Riekel, 1983). The following considerations are restricted to *coherent* scattering only.

Essentially the same formalism as given by equations (4.2.2.1*a*)–(4.2.2.4*a*) may be described using a generalized Patterson function, which is more familiar to crystallographers:

$$P(\mathbf{r},t)=\int_{\mathbf{r}'}\int_{t'=0}^{\tau}\rho(\mathbf{r}',t')\rho(\mathbf{r}'+\mathbf{r},t'+t)\,\mathrm{d}\mathbf{r}'\,\mathrm{d}t', \quad (4.2.2.5)$$

where ρ is the scattering density and τ denotes the time of observation. The only difference between $G(\mathbf{r},t)$ and $P(\mathbf{r},t)$ is the inclusion of the scattering weight (f or b) in $P(\mathbf{r},t)$. $P(\mathbf{r},t)$ is an extension of the usual spatial Patterson function $P(\mathbf{r})$. Similarly, S is replaced by another function,

$$\begin{aligned}2\pi S(\mathbf{H},\omega)&\equiv|F(\mathbf{H},\omega)|^2\\&=\int_{\mathbf{r}}\int_{t}P(\mathbf{r},t)\exp\{2\pi i(\mathbf{H}\cdot\mathbf{r}-\nu t)\}\,\mathrm{d}\mathbf{r}\,\mathrm{d}t,\end{aligned} \quad (4.2.2.6)$$

which is the Fourier transform of $P(\mathbf{r},t)$. One difficulty arises from neglecting the time of observation. Just as $S(\mathbf{H})$ [$\simeq|F(\mathbf{H})|^2$] is always proportional to the scattering volume V in the framework of kinematical theory or within Born's first approximation [*cf.* equation (4.2.2.1*a*)], so $S(\mathbf{H},\omega)$ [$\simeq|F(\mathbf{H},\omega)|^2$] is proportional to volume *and* observation time. In general, one does not make S proportional to τ, but one normalizes S to be independent of τ as $\tau\rightarrow\infty$: $2\pi S=(1/\tau)|F|^2$. Averaging over time τ gives therefore

$$\begin{aligned}S(\mathbf{H},\omega)=\frac{1}{2\pi}\int_{\mathbf{r}}\int_{t}\left\langle\int_{\mathbf{r}'}\rho(\mathbf{r}',t')\rho(\mathbf{r}'+\mathbf{r},t'+t)\,\mathrm{d}r'\right\rangle_{t'}\\\times\exp\{2\pi i(\mathbf{H}\cdot\mathbf{r}-\nu t)\}\,\mathrm{d}\mathbf{r}\,\mathrm{d}t.\end{aligned} \quad (4.2.2.7)$$

Special cases (see, *e.g.*, Cowley, 1981) are:

(1) *Pure elastic measurement*

$$\begin{aligned}I_{\rm e}\simeq S(\mathbf{H},0)&=\int_{\mathbf{r}}\left[\int_{t}P(\mathbf{r},t)\,\mathrm{d}t\right]\exp\{2\pi i\mathbf{H}\cdot\mathbf{r}\}\,\mathrm{d}\mathbf{r}\\&=\left|\sum_j f_j\langle\exp\{2\pi i\mathbf{H}\cdot\mathbf{r}_j(t)\}\rangle_t\right|^2.\end{aligned} \quad (4.2.2.8)$$

In this type of measurement, the time-averaged 'structure' is determined:

$$\langle\rho(\mathbf{r},t)\rangle_t=\int_{\mathbf{H}}|F(\mathbf{H},0)|\exp\{2\pi i\mathbf{H}\cdot\mathbf{r}\}\,\mathrm{d}\mathbf{H}.$$

The projection along the time axis in real (Patterson) space gives a section in Fourier space at $\omega=0$. True elastic measurement is a domain of neutron scattering. To determine the time-averaged structure of a statistically disordered crystal, dynamical disorder (phonon scattering) may be separated. For liquids or liquid-like systems this kind of scattering technique is rather ineffective, as the time-averaging procedure gives only a uniform particle distribution.

(2) *Integration over frequency (or energy)*

$$\begin{aligned}I_{\rm tot}\simeq\int_{\omega}|F(\mathbf{H},\omega)|^2\,\mathrm{d}\omega&=\int_{\omega}\int_{\mathbf{r}}\int_{t}P(\mathbf{r},t)\\&\times\exp\{2\pi i(\mathbf{H}\cdot\mathbf{r}-\nu t)\}\,\mathrm{d}\mathbf{r}\,\mathrm{d}t\,\mathrm{d}\omega\\&=\int_{\mathbf{r}}P(\mathbf{r},0)\exp\{2\pi i\mathbf{H}\cdot\mathbf{r}\}\,\mathrm{d}\mathbf{r}\end{aligned} \quad (4.2.2.9)$$

(*cf.* the properties of δ functions). In such an experiment, one determines the Patterson function for $t=0$, *i.e.* the instantaneous structure (a 'snapshot' of the correlation function): a projection in Fourier space along the energy axis gives a section in direct (Patterson) space at $t=0$. An energy integration is automatically performed in a conventional X-ray diffraction experiment ($|\mathbf{k}|\simeq|\mathbf{k}_0|$). One should bear in mind that in a real experiment there is, of course, an average over both the sample volume and the time of observation.

In most practical cases, averaging over time is equivalent to averaging over space: the total diffracted intensity may be regarded as the sum of the intensities from a large number of independent regions due to the limited coherence of a beam. At any time these regions take all possible configurations. Therefore, this sum of intensities is equivalent to the sum of intensities from any one region at different times,

$$\begin{aligned}\langle I_{\rm tot}\rangle_t&=\left\langle\sum_j\sum_{j'}f_jf_{j'}\exp\{2\pi i\mathbf{H}\cdot(\mathbf{r}_j-\mathbf{r}_{j'})\}\right\rangle_t\\&=\sum_{j,j'}f_jf_{j'}\langle\exp\{2\pi i\mathbf{H}\cdot(\mathbf{r}_j-\mathbf{r}_{j'})\}\rangle_t.\end{aligned} \quad (4.2.2.9a)$$

From the basic formulae one also derives the well known results for X-ray or neutron scattering by a periodic arrangement of particles in space [*cf.* equation (4.1.3.2) of Chapter 4.1]:

$$\frac{\mathrm{d}\sigma}{\mathrm{d}\Omega}=N\frac{(2\pi)^3}{V_{\rm c}}\sum_{\mathbf{h}}|F(\mathbf{H})|^2\delta(\mathbf{H}-\mathbf{G}), \quad (4.2.2.10)$$

$$F(\mathbf{H})=\sum_j f_j(\mathbf{H})\exp\{-W_j\}\exp\{2\pi i\mathbf{H}\cdot\mathbf{r}_j\}. \quad (4.2.2.11)$$

$F(\mathbf{H})$ denotes the Fourier transform of one cell (structure factor); $\mathbf{G}$ is the reciprocal-lattice vector and W is the Debye–Waller factor; the f's are assumed to be real.

The evaluation of the intensity expressions (4.2.2.6), (4.2.2.8) or (4.2.2.9), (4.2.2.9*a*) for a disordered crystal must be performed in terms of statistical relationships between scattering factors and/or atomic positions.

4.2.2.2. X-ray and neutron scattering

From these basic scattering formulae some conclusions on the relative merits of X-rays and neutrons can be drawn. Both X-rays and thermal neutrons possess wavelengths of the order of interatomic distances and are thus well suited to the study of the atomic structure of condensed matter. Besides this, there are fundamental differences that make one or the other the radiation of choice for a particular problem or enable them to be used with advantage in a complementary manner. These differences are well documented in a number of textbooks on diffraction and are widely exploited in the determination of average structures. One fundamental difference is related to the interaction with matter: while X-rays are scattered by the electrons, neutrons are scat-

tered by the atomic nuclei (we are disregarding magnetic interactions in this chapter), *i.e.* X-rays probe the distribution of charges, which (in particular for light atoms) may not coincide with that of the nuclei. This fact forms the basis for the well known X − N technique in the analysis of Bragg intensities. No such studies of disorder diffuse scattering have been performed up to now, but may be a challenge for the future. As a consequence of the different size of the scattering objects, the scattering amplitude falls off with increasing scattering vector $|\mathbf{H}| = (\sin\theta)/\lambda$ for X-rays (the form factor), while it is constant for neutrons. Since for a complete interpretation of diffuse scattering high Q values are generally required, neutrons have their advantages in this respect. The scattering intensity varies as Z^2 (Z = number of electrons) for X-rays and more-or-less erratically for neutrons, for which it also depends on the specific isotope. This imposes problems for X-rays when trying to detect light elements (in particular H and O) in the presence of heavy elements or discriminating neighbouring elements in the periodic table (*e.g.* Al/Si/Mg, Fe/Co/Ni). On the other hand, these differences in scattering power can be used to identify the atomic species taking part in the disorder by comparing the intensity distributions observed with both methods. The contrast can be further enhanced by marking selected atoms by isotope substitution for neutrons or by using anomalous dispersion for X-rays.

In many practical cases, the complementarities of the two methods can be exploited by using them simultaneously. Some illustrative examples can be found in Boysen & Frey (1998).

Another important difference is in the energies given by the dispersion laws $E_x = \hbar ck$ and $E_n = (\hbar^2/2m)k^2$ for X-rays and neutrons, respectively, where c is the velocity of light, m is the neutron mass and $k = 2\pi/\lambda$ is the wavevector. For a typical wavelength, λ =1.54 Å (Cu $K\alpha$) ($k = 4.08$ Å^{-1}), $E_x = 8$ keV and E_n = 35 meV, *i.e.* the energies differ by almost six orders of magnitude. This means that neutron energies are similar to those of typical collective lattice excitations, which may therefore be determined more easily by neutron spectroscopy. The basic question of whether the underlying disorder is of static or dynamic origin can be answered using neutrons alone, *e.g.* by comparing the 'integral' (= elastic + inelastic) scattered intensity (*i.e.* without energy analysis, using a two-axis diffractometer) with the purely elastic intensity by placing an analyser crystal set to zero energy transfer in the diffracted beam (using a triple-axis diffractometer) or using time-of-flight methods. The high energy resolution of Mössbauer radiation can also be used for this purpose. Owing to the very low available intensities, however, this technique has only been applied occasionally. In the elastic mode, diffracted neutron intensities are also usually rather weak. The decision can, however, also be made simply by comparing the positions of the intensity maxima in reciprocal space. This follows from a consideration of the relative changes of the momentum transfer (the wavevector) in the two cases. For example, for an energy change $\Delta E = E_f - E_i$ (the subscripts refer to final and incident energies) of 1 meV, one obtains a change in the scattered wavevector Δk_f of 2×10^{-6} Å^{-1} for X-rays and 0.06 Å^{-1} for neutrons. In a two-axis experiment where the detector does not discriminate energies, *i.e.* without prior knowledge of the real energies, the distribution of diffuse intensities has to be drawn as if the scattering had been elastic ($\Delta E = 0$). In other words, the signal appears at a position displaced by Δk_f. From the estimations above it is clear that only in the neutron case can a measurable effect be expected.

Other specific features of neutrons include their magnetic moment (magnetic scattering is still a domain of neutrons, although progress is now being made with synchrotron radiation) and (nuclear) spin and isotope incoherent scattering processes (which allow the determination of the self-correlation functions). It is possible to separate the spin-incoherent part and distinguish between nuclear and magnetic scattering using polarization analysis. For most elements scattering and absorption is much weaker for neutrons, allowing larger samples to be analysed and sample environments (furnaces, pressure cells, electric and magnetic fields, special atmospheres *etc.*) to be handled much more easily. Differences in the experimental techniques for X-ray and neutron scattering are discussed in Section 4.2.8.

4.2.3. Qualitative treatment of structural disorder

4.2.3.1. Basic mathematics

Any structure analysis of disordered structures should start with a qualitative interpretation of diffuse scattering. This may be achieved with the aid of Fourier transforms and convolutions. A thorough mathematical treatment of Fourier transforms is given in Chapter 1.3 of this volume; here we give a simple short overview of the practical use of Fourier transforms, convolutions, their algebraic operations and examples of functions which are frequently used in diffraction physics (see, *e.g.*, Patterson, 1959; Jagodzinski, 1987). For simplicity, the following modified notation is used in this section: functions in real space are represented by lower-case letters, *e.g.* $a(\mathbf{r})$, $b(\mathbf{r})$, ... except for $F(\mathbf{r})$ [also, more frequently, denoted as $\rho(\mathbf{r})$] and $P(\mathbf{r})$, which are used as general symbols for a structure and the Patterson function, respectively; functions in reciprocal space are represented by capital letters $A(\mathbf{H})$, $B(\mathbf{H})$; and $\mathbf{r}$ and $\mathbf{H}$ are general vectors in real and reciprocal space, respectively. H, K, L denote continuous variables in reciprocal space; integer values are given by the commonly used symbols h, k, l. $Hx + Ky + Lz$ is the scalar product $\mathbf{H}\cdot\mathbf{r}$; d$\mathbf{r}$ and d$\mathbf{H}$ indicate integrations in three dimensions in real and reciprocal space, respectively. Even for X-rays, the electron density $\rho(\mathbf{r})$ will generally be replaced by the scattering potential $a(\mathbf{r})$. Consequently, anomalous contributions to scattering may be included if complex functions $a(\mathbf{r})$ are admitted. In the neutron case $a(\mathbf{r})$ refers to a quasi-potential. Using this notation we obtain the scattered amplitude

$$A(\mathbf{H}) = \int_{\mathbf{r}} a(\mathbf{r}) \exp\{2\pi i \mathbf{H}\cdot\mathbf{r}\}\, \mathrm{d}\mathbf{r}, \qquad (4.2.3.1a)$$

$$a(\mathbf{r}) = \int_{\mathbf{H}} A(\mathbf{H}) \exp\{-2\pi i \mathbf{H}\cdot\mathbf{r}\}\, \mathrm{d}\mathbf{H} \qquad (4.2.3.1b)$$

(constant factors are omitted).

$a(\mathbf{r})$ and $A(\mathbf{H})$ are reversibly and uniquely determined by Fourier transformation. Consequently, equations (4.2.3.1) may simply be replaced by $a(\mathbf{r}) \leftrightarrow A(\mathbf{H})$, where the double-headed arrow represents the two integrations given by (4.2.3.1) and means: $A(\mathbf{H})$ is the Fourier transform of $a(\mathbf{r})$ and *vice versa.* The following relations may easily be derived from (4.2.3.1):

$$a(\mathbf{r}) + b(\mathbf{r}) \leftrightarrow A(\mathbf{H}) + B(\mathbf{H}) \quad \text{(law of addition)}, \qquad (4.2.3.2)$$

$$\beta a(\mathbf{r}) \leftrightarrow \beta A(\mathbf{H}) \quad \text{(law of scalar multiplication)}, \qquad (4.2.3.3)$$

where β is a scalar quantity.

On the other hand, the multiplication of two functions does not yield a relation of similar symmetrical simplicity:

$$a(\mathbf{r})b(\mathbf{r}) \leftrightarrow \int A(\mathbf{H}')B(\mathbf{H}-\mathbf{H}')\, \mathrm{d}\mathbf{H}' = A(\mathbf{H}) * B(\mathbf{H}), \qquad (4.2.3.4a)$$

$$a(\mathbf{r}) * b(\mathbf{r}) = \int a(\mathbf{r}')b(\mathbf{r}-\mathbf{r}')\, \mathrm{d}\mathbf{r}' \leftrightarrow A(\mathbf{H})B(\mathbf{H}) \qquad (4.2.3.4b)$$

(the laws of convolution and multiplication).

For simplicity, the complete convolution integral is abbreviated as $a(\mathbf{r}) * b(\mathbf{r})$. Since $a(\mathbf{r})b(\mathbf{r}) = b(\mathbf{r})a(\mathbf{r})$,

$$\int A(\mathbf{H}')B(\mathbf{H}-\mathbf{H}')\, \mathrm{d}\mathbf{H}' = \int B(\mathbf{H}')A(\mathbf{H}-\mathbf{H}')\, \mathrm{d}\mathbf{H}'$$

and *vice versa.* The convolution operation is commutative in either space.

The distribution law $a(b+c) = ab + ac$ is valid for the convolution as well:

$$a(\mathbf{r}) * [b(\mathbf{r}) + c(\mathbf{r})] = a(\mathbf{r}) * b(\mathbf{r}) + a(\mathbf{r}) * c(\mathbf{r}). \quad (4.2.3.5)$$

The associative law of multiplication does not hold if mixed products (convolution and multiplication) are used:

$$a(\mathbf{r}) * [b(\mathbf{r})c(\mathbf{r})] \neq [a(\mathbf{r}) * b(\mathbf{r})]c(\mathbf{r}). \quad (4.2.3.6)$$

From equations (4.2.3.1) one has

$$\begin{aligned} a(\mathbf{r} - \mathbf{r}_0) &\leftrightarrow A(\mathbf{H}) \exp\{2\pi i \mathbf{H} \cdot \mathbf{r}_0\}, \\ A(\mathbf{H} - \mathbf{H}_0) &\leftrightarrow a(\mathbf{r}) \exp\{-2\pi i \mathbf{H}_0 \cdot \mathbf{r}\} \end{aligned} \quad (4.2.3.7)$$

(the law of displacements).

Since symmetry operations are well known to crystallographers in reciprocal space as well, the law of inversion is only mentioned here:

$$a(-\mathbf{r}) \leftrightarrow A(-\mathbf{H}). \quad (4.2.3.8)$$

Consequently, if $a(\mathbf{r}) = a(-\mathbf{r})$, then $A(\mathbf{H}) = A(-\mathbf{H})$. In order to calculate the intensity, the complex conjugate $A^+(\mathbf{H})$ is needed:

$$a^+(\mathbf{r}) \leftrightarrow A^+(-\mathbf{H}), \quad (4.2.3.9a)$$

$$a^+(-\mathbf{r}) \leftrightarrow A^+(\mathbf{H}). \quad (4.2.3.9b)$$

Equations (4.2.3.9) yield the relationship $A^+(-\mathbf{H}) = A(\mathbf{H})$ ('Friedel's law') if $a(\mathbf{r})$ is a *real* function. The multiplication of a function with its conjugate is given by

$$a(\mathbf{r}) * a^+(-\mathbf{r}) \leftrightarrow |A(\mathbf{H})|^2,$$

with

$$a(\mathbf{r}) * a^+(-\mathbf{r}) = \int a(\mathbf{r}')a(\mathbf{r}' - \mathbf{r})\,\mathrm{d}\mathbf{r}' = P(\mathbf{r}). \quad (4.2.3.10)$$

Note that $P(\mathbf{r}) = P(-\mathbf{r})$ is not valid if $a(\mathbf{r})$ is complex. Consequently $|A(-\mathbf{H})|^2 \neq |A(\mathbf{H})|^2$. This is shown by evaluating $A(-\mathbf{H})A^+(-\mathbf{H})$,

$$A(-\mathbf{H})A^+(-\mathbf{H}) \leftrightarrow a(-\mathbf{r}) * a^+(\mathbf{r}) = P(-\mathbf{r}). \quad (4.2.3.11)$$

Equation (4.2.3.11) is very useful for the determination of the contribution of anomalous scattering to diffuse reflections.

Most of the diffuse-diffraction phenomena observed may be interpreted qualitatively or even semiquantitatively in a very simple manner using a limited number of important Fourier transforms, which are given below.

4.2.3.2. Fourier transforms

(1) *Normalized Gaussian function*

$$(\pi^{3/2}\alpha\beta\gamma)^{-1} \exp\{-(x/\alpha)^2 - (y/\beta)^2 - (z/\gamma)^2\}. \quad (4.2.3.12)$$

This plays an important role in statistics. Its Fourier transform is again a Gaussian:

$$\exp\{-\pi^2(\alpha^2H^2 + \beta^2K^2 + \gamma^2L^2)\}. \quad (4.2.3.12a)$$

The three parameters α, β, γ determine the width of the curve. Small values of α, β, γ represent a broad maximum in reciprocal space but a narrow one in real space and *vice versa*. The constant has been chosen such that the integral of the Gaussian is unity in real space. The product of two Gaussians in reciprocal space,

$$\begin{aligned} &\exp\{-\pi^2(\alpha_1^2H^2 + \beta_1^2K^2 + \gamma_1^2L^2)\} \\ &\quad \times \exp\{-\pi^2(\alpha_2^2H^2 + \beta_2^2K^2 + \gamma_2^2L^2)\} \\ &\quad = \exp\{-\pi^2[(\alpha_1^2 + \alpha_2^2)H^2 + (\beta_1^2 + \beta_2^2)K^2 \\ &\qquad + (\gamma_1^2 + \gamma_2^2)L^2]\} \end{aligned} \quad (4.2.3.12b)$$

again represents a Gaussian of the same type, but with a sharper profile. Consequently, its Fourier transform, which is given by the convolution of the transforms of the two Gaussians, is itself a Gaussian with a broader maximum. It may be concluded from this discussion that the Gaussian with $\alpha, \beta, \gamma \to 0$ is a δ function in real space and its Fourier transform is unity in reciprocal space.

(2) δ *'functions'*

For a proper definition see, *e.g.*, Cowley (1981). Here the term is used with the relaxed definition $\delta(\mathbf{r}) = 1$ if $\mathbf{r} = 0$ and zero elsewhere.

$$\delta(\mathbf{r}) \leftrightarrow 1 \text{ and } \delta(\mathbf{H}) \leftrightarrow 1$$

and

$$\delta(\mathbf{r} - \mathbf{r}_0) \leftrightarrow \exp\{2\pi i \mathbf{H} \cdot \mathbf{r}_0\}.$$

The convolution of two δ functions is again a δ function.

(3) *Lattices*

Lattices in real and reciprocal space may be described by δ functions:

$$l(\mathbf{r}) = \sum_{\mathbf{n}} \delta(\mathbf{r} - \mathbf{n})$$

and

$$L(\mathbf{H}) = \sum_{\mathbf{h}} \delta(\mathbf{H} - \mathbf{G}),$$

where $\mathbf{n} = n_1\mathbf{a} + n_2\mathbf{b} + n_3\mathbf{c}$ and $\mathbf{G} = h\mathbf{a}^* + k\mathbf{b}^* + l\mathbf{c}^*$ represent the components of the translation vectors in real and reciprocal space, respectively. The Fourier transforms of lattices with orthogonal basis vectors of unit length and an infinite number of points in all three dimensions correspond to each other. In the following the relation $l(\mathbf{r}) \leftrightarrow L(\mathbf{H})$ is used in this generalized sense.

The Fourier transforms of *finite* lattices with N_1, N_2, N_3 nodes in the basic directions $\mathbf{a}$, $\mathbf{b}$, $\mathbf{c}$ are given by

$$\frac{\sin \pi N_1 H}{\sin \pi H} \frac{\sin \pi N_2 K}{\sin \pi K} \frac{\sin \pi N_3 L}{\sin \pi L}, \quad (4.2.3.13)$$

which is a periodic function in reciprocal space, but, strictly speaking, nonperiodic in real space. It should be pointed out that the correspondence of lattices in either space is valid only if the origin coincides with a δ function. This fact may easily be understood by applying the law of displacement given in equation (4.2.3.7).

(4) *Box functions*

The Fourier transform of a box function $b(\mathbf{r})$ with unit height is

$$b(\mathbf{r}) \leftrightarrow \frac{\sin \pi\alpha H}{\pi H} \frac{\sin \pi\beta K}{\pi K} \frac{\sin \pi\gamma L}{\pi L}. \quad (4.2.3.14)$$

α, β, γ describe its extension in the three dimensions. This function is real as long as the centre of symmetry is placed at the origin, otherwise the law of displacement has to be used. The convolution of the box function with its inverse is needed for the calculation of intensities:

$$\begin{aligned} t(\mathbf{r}) &= b(\mathbf{r}) * b(-\mathbf{r}) \\ &\leftrightarrow \left(\frac{\sin \pi\alpha H}{\pi H}\right)^2 \left(\frac{\sin \pi\beta K}{\pi K}\right)^2 \left(\frac{\sin \pi\gamma L}{\pi L}\right)^2. \end{aligned} \quad (4.2.3.15)$$

$t(\mathbf{r})$ is a generalized three-dimensional 'pyramid' of doubled basal length when compared with the corresponding length of the box function. The top of the pyramid has a height given by the number of unit cells covered by the box function. Obviously, the box function generates a particle size in real space by multiplying the infinite lattice $l(\mathbf{r})$ by $b(\mathbf{r})$. Fourier transformation yields a particle-size effect well known in diffraction. Correspondingly, the termination effect of a Fourier synthesis is caused by multiplication by a box function in reciprocal space, which causes a broadening of maxima in real space.

(5) *Convolutions*

It is often very useful to elucidate the convolution given in equations (4.2.3.4) by introducing the corresponding pictures in real or reciprocal space. Since $1 \cdot f(\mathbf{r}) = f(\mathbf{r})$, $\delta(\mathbf{H}) * F(\mathbf{H}) = F(\mathbf{H})$, the convolution with a δ function must result in an identical picture of the second function, although the function is used as $f(-\mathbf{r})$ in the integrals of equations (4.2.3.4), $f(\mathbf{r} - \mathbf{r}')$ with $\mathbf{r}'$ as variable in the integral of convolution. The convolution with $f(-\mathbf{r})$ brings the integral into the form

$$\int f(\mathbf{r}')\, f(\mathbf{r}' - \mathbf{r})\, \mathrm{d}\mathbf{r}', \tag{4.2.3.16}$$

which is known as the Patterson (or self- or auto-convolution) function and represents the generalized Patterson function including anomalous scattering [*cf.* equation (4.2.3.10)].

The change of the variable in the convolution integral may sometimes lead to confusion if certain operations are applied to the arguments of the functions entering the integral. Hence it is useful to mention the invariance of the convolution integral with respect to a change of sign, or a displacement, respectively, if applied to $\mathbf{r}'$ in both functions. Consequently, the convolution with the inverted function $a(\mathbf{r}) * b(-\mathbf{r})$ may be determined as follows:

$$\begin{aligned} b'(\mathbf{r}) &= b(-\mathbf{r}), \\ a(\mathbf{r}) * b(-\mathbf{r}) &= a(\mathbf{r}) * b'(\mathbf{r}) = \int a(\mathbf{r}')b'(\mathbf{r} - \mathbf{r}')\, \mathrm{d}\mathbf{r}', \\ &= \int a(\mathbf{r}')b(\mathbf{r}' - \mathbf{r})\, \mathrm{d}\mathbf{r}' = P'(\mathbf{r}). \end{aligned} \tag{4.2.3.17}$$

This equation means that the second function is displaced into the positive direction by $\mathbf{r}$, then multiplied by the first function and integrated. In the original meaning of the convolution, the operation represents a displacement of the second function in the positive direction and an inversion at the displaced origin before multiplication and subsequent integration. On comparing the two operations it may be concluded that $P'(\mathbf{r}) \neq P'(-\mathbf{r})$ if the second function is acentric. For real functions both have to be acentric. In a similar way, it may be shown that the convolution

$$\begin{aligned} a(\mathbf{r} - \mathbf{m}) * b(\mathbf{r} - \mathbf{m}') &= \int_{\mathbf{r}'} a(\mathbf{r}' - \mathbf{m})b(\mathbf{r} - \mathbf{m}' - \mathbf{r}')\, \mathrm{d}\mathbf{r}' \\ &= \int_{\mathbf{r}''} a(\mathbf{r}'')b(\mathbf{r} - \mathbf{m}' - \mathbf{m} - \mathbf{r}'')\, \mathrm{d}\mathbf{r}''. \end{aligned} \tag{4.2.3.18}$$

Equation (4.2.3.18) indicates a displacement by $\mathbf{m}' + \mathbf{m}$ with respect to the convolution of the undisplaced functions. Consequently,

$$\delta(\mathbf{r} - \mathbf{m}) * \delta(\mathbf{r} - \mathbf{m}') = \delta(\mathbf{r} - \mathbf{m} - \mathbf{m}'). \tag{4.2.3.19}$$

Obviously, the commutative law of convolution is obeyed; on the other hand, the convolution with the inverted function yields

$$\delta(\mathbf{r} - \mathbf{m}' + \mathbf{m}),$$

indicating that the commutative law (interchange of $\mathbf{m}$ and $\mathbf{m}'$) is violated because of the different signs of $\mathbf{m}$ and $\mathbf{m}'$.

The effectiveness of the method outlined above may be greatly improved by introducing further Fourier transforms of useful functions in real and reciprocal space (Patterson, 1959).

4.2.3.3. General formulation of a disorder problem

From these basic concepts the generally adopted method in a disorder problem is to try to separate the scattering intensity into two parts, namely one part $\langle\rho\rangle$ from an average periodic structure where formulae (4.2.2.10), (4.2.2.11) apply and a second part $\Delta\rho$ resulting from fluctuations from this average (see, *e.g.*, Schwartz & Cohen, 1977). One may write this formally as

$$\rho = \langle\rho\rangle + \Delta\rho, \tag{4.2.3.20}$$

where $\langle\rho\rangle = \langle\rho_\mathrm{c}\rangle * l$ is defined to be time-independent and periodic in space and $\langle\Delta\rho\rangle = 0$. $\langle\rho_\mathrm{c}\rangle = (1/N)\sum_i \rho_i$ is the density of the average unit cell obtained by the projection of all unit cells into a single one. Fourier transformation gives the average amplitude,

$$\langle A\rangle = \langle F\rangle L = \sum_i \langle F\rangle \exp\{2\pi i\mathbf{H}\cdot\mathbf{r}_i\}, \tag{4.2.3.21a}$$

where $\langle F\rangle$ is the usual structure factor (4.2.2.11). The difference structure $\Delta\rho$ leads to the difference amplitude,

$$\begin{aligned} \Delta A = A - \langle A\rangle &= \sum_i (F_i - \langle F\rangle)\exp\{2\pi i\mathbf{H}\cdot\mathbf{r}_i\} \\ &= \sum_i \Delta F_i \exp\{2\pi i\mathbf{H}\cdot\mathbf{r}_i\}. \end{aligned} \tag{4.2.3.21b}$$

Because cross terms $\langle\rho\rangle * \Delta\rho$ vanish by definition, the Patterson function is

$$\begin{aligned} &[\langle\rho(\mathbf{r})\rangle + \Delta\rho(\mathbf{r})] * [\langle\rho(-\mathbf{r})\rangle + \Delta\rho(-\mathbf{r})] \\ &\quad = [\langle\rho(\mathbf{r})\rangle * \langle\rho(-\mathbf{r})\rangle] + [\Delta\rho(\mathbf{r}) * \Delta\rho(-\mathbf{r})]. \end{aligned} \tag{4.2.3.22}$$

Fourier transformation gives

$$I \simeq |\langle F\rangle|^2 + |\Delta F|^2, \tag{4.2.3.23a}$$

$$|\Delta F|^2 \simeq \langle |F|^2\rangle - |\langle F\rangle|^2. \tag{4.2.3.23b}$$

Since $\langle\rho\rangle$ is periodic, the first term in (4.2.3.23*a*) describes Bragg scattering,

$$I_\mathrm{B} = \langle A\rangle\langle A^*\rangle = |\langle F\rangle|^2 L, \tag{4.2.3.24}$$

where $\langle F\rangle$ plays the normal role of a structure factor of *one* cell of the averaged structure. The second term corresponds to diffuse scattering,

$$I_\mathrm{D} = \langle \Delta A \Delta A^*\rangle = \left\langle \sum_i \sum_j \Delta F_i \Delta F_j^* \exp\{2\pi i\mathbf{H}\cdot(\mathbf{r}_i - \mathbf{r}_j)\}\right\rangle. \tag{4.2.3.25}$$

In many cases, diffuse interferences are centred exactly at the positions of the Bragg reflections. It is then a serious experimental problem to decide whether the observed intensity distribution is due to Bragg scattering obscured by crystal-size limitations or due to other scattering phenomena.

If disordering is exclusively time-dependent, $\langle\rho\rangle$ represents the time average, whereas $\langle F\rangle$ gives the pure elastic scattering part [*cf.* (4.2.2.8)] and ΔF refers to inelastic scattering only.

4.2.3.4. General aspects of diffuse scattering

Diffuse scattering may be classified in various ways which may be related to specific aspects of the intensity distribution, *e.g.* according to the type of disorder: substitutional (or density or chemical) or displacive. The general expression (4.2.3.25), which may be rewritten as

$$I_{\rm D} = \left\langle \sum_k \left(\sum_i \Delta F_i \Delta F_{i+k} \right) \exp\{2\pi i \mathbf{H}\cdot\mathbf{r}_k\} \right\rangle = \sum_k \langle \Delta F \Delta F^* \rangle_k \exp\{2\pi i \mathbf{H}\cdot\mathbf{r}_k\}, \quad (4.2.3.26)$$

where $\mathbf{r}_k = \mathbf{r}_i - \mathbf{r}_j$, contains the difference structure factor ΔF, which may formally be written as

$$\Delta F = (\Delta f)\exp\{2\pi i \mathbf{H}\cdot(\mathbf{r}+\Delta\mathbf{r})\},$$

where (Δf) denotes a fluctuation of the scattering density (the form factor in the case of X-rays and the scattering length in the case of neutrons; note that this may include vacancies) and $\Delta\mathbf{r}$ denotes a fluctuation of the position, *i.e.* they refer to substitutional and displacive disorder, respectively. Although the two types often occur together in real crystals, they may be discriminated through their different dependence on the modulus of the scattering vector $\mathbf{H}$. This may be seen by considering the diffuse scattering of completely random fluctuations, *i.e.* without any correlations. For substitutional disorder one easily derives from (4.2.3.26)

$$I_{\rm D} = N\langle \Delta F^2 \rangle = N\langle \Delta f^2 \rangle,$$

while for displacive fluctuations with small amplitudes $\Delta\mathbf{r}$ the exponential may be expanded:

$$\exp\{2\pi i \mathbf{H}\cdot\Delta\mathbf{r}_i\} \simeq (1 + 2\pi i \mathbf{H}\cdot\Delta\mathbf{r}_i + \ldots),$$

leading to

$$I_{\rm D} = Nf^2 \sum_k \sum_i (2\pi\mathbf{H}\cdot\Delta\mathbf{r}_i)(2\pi\mathbf{H}\cdot\Delta\mathbf{r}_{i+k}) \exp\{2\pi i \mathbf{H}\cdot\mathbf{r}_k\} \quad (4.2.3.27)$$

and

$$I_{\rm D} = Nf^2 4\pi^2 H^2 \langle \Delta r_i^2 \rangle_i. \quad (4.2.3.28)$$

Hence in the substitutional case the diffuse intensity is constant throughout reciprocal space, while in the displacive case it increases with H^2, *i.e.* it is zero near the origin. Any correlations will modulate this intensity, but will not change this general behaviour.

A second classification is related to the dimensionality of the disorder: one-dimensional disorder between two-dimensionally ordered objects (planes) leading to diffuse streaks perpendicular to the planes, two-dimensional disorder between one-dimensionally ordered objects (chains) leading to diffuse planes and general three-dimensional disorder.

These different types of disorder will be further discussed separately in the next paragraphs.

From the derivation in Section 4.2.3.3, one may note that information about an averaged disordered structure is contained in the Bragg scattering governed by

$$\langle F \rangle = \sum_i n_i f_i \exp\{2\pi\mathbf{H}\cdot\mathbf{r}_i\} T_i(\mathbf{H}), \quad (4.2.3.29)$$

where $T_i(\mathbf{H})$ is the Debye–Waller factor. Back-transformation to real space gives

$$\langle \rho \rangle = \sum_i n_i f_i \delta(\mathbf{r}-\mathbf{r}_i) * \text{p.d.f.}_i(\mathbf{r}-\mathbf{r}_i), \quad (4.2.3.30)$$

i.e. each average position is convoluted with p.d.f.$_i(\mathbf{r}-\mathbf{r}_i)$, the probability density function, which is the Fourier transform of $T_i(\mathbf{H})$. Any disorder model derived from the diffuse scattering must therefore comply with the p.d.f., *i.e.* this may and should be used to validate these models.

4.2.3.5. Types of diffuse scattering

4.2.3.5.1. Substitutional fluctuations, occupational disorder

As mentioned above, a completely random distribution of chemical species leads to a uniform distribution of diffuse intensity, which is also called monotonic Laue scattering. For example, for a binary alloy with scattering densities f_1 and f_2 and concentrations c_1 and c_2 this is simply given by $I_{\rm D} \propto c_1 c_2 (f_1 - f_2)^2$. Several authors use this, *i.e.* the intensity of a random distribution of occupancies, to define a so-called Laue unit, and therewith to put the general diffuse scattering on a relative scale.

Any deviations from the monotonic Laue scattering may be due either to the scattering factor of the objects (*e.g.* molecules) or to short-range-order correlations. For example, for a simple defect pair with distance $\mathbf{R}$ we have

$$I_{\rm D} \propto c_1 c_2 (f_1 - f_2)^2 [1 + \cos(2\pi\mathbf{H}\cdot\mathbf{R})], \quad (4.2.3.31a)$$

or for more general short-range order

$$I_{\rm D} \propto c_1 c_2 (f_1 - f_2)^2 \sum_n \alpha_n \cos(2\pi\mathbf{H}\cdot\mathbf{r}_n), \quad (4.2.3.31b)$$

where α_n are Warren–Cowley short-range-order parameters, as will be discussed in more detail in Section 4.2.5.4.

For a periodic modulation $\Delta f_n = f_A \cos(2\pi\mathbf{K}\cdot\mathbf{r}_n)$

$$I_{\rm D} \propto f_A^2 \left| \sum_n \left[\exp\{2\pi i(\mathbf{H}+\mathbf{K})\cdot\mathbf{r}_n\} + \exp\{2\pi i(\mathbf{H}-\mathbf{K})\cdot\mathbf{r}_n\} \right] \right|^2 \propto f_A^2 \sum_G \delta(\mathbf{H} - \mathbf{G} \pm \mathbf{K}), \quad (4.2.3.32)$$

where $\mathbf{G}$ is a reciprocal-lattice vector.

Hence a harmonic density modulation of a structure in real space leads to pairs of satellites in reciprocal space. Each main reflection is accompanied by a pair of satellites in the directions $\mp\Delta\mathbf{H}$ with phases $\mp 2\pi\varphi$. The reciprocal lattice may then be written in the following form:

$$L(\mathbf{H}) + \frac{\alpha}{2} L(\mathbf{H}+\Delta\mathbf{H}) \exp\{2\pi i \Phi\} + \frac{\alpha}{2} L(\mathbf{H}-\Delta\mathbf{H}) \exp\{2\pi i(-\Phi)\}, \quad (4.2.3.33)$$

where $0 \le \alpha \le 1$. Fourier transformation yields

$$l(\mathbf{r})\left[1 + \frac{\alpha}{2}\exp\{2\pi i(\Delta\mathbf{H}\cdot\mathbf{r}+\Phi)\} + \frac{\alpha}{2}\exp\{-2\pi i(\Delta\mathbf{H}\cdot\mathbf{r}+\Phi)\}\right] = l(\mathbf{r})[1 + \alpha\cos(2\pi\Delta\mathbf{H}\cdot\mathbf{r}+\Phi)]. \quad (4.2.3.34)$$

Equation (4.2.3.34) describes the lattice modulated by a harmonic density wave. Since phases cannot be determined by intensity measurements, there is no possibility of obtaining any information on the phase relative to the sublattice. From (4.2.3.34) it is obvious that the use of higher orders of harmonics does not change the situation. If $\Delta\mathbf{H}$ is not rational, such that no $n\Delta\mathbf{H}$ (n = integer) coincides with a main reflection in reciprocal space, the modulated structure is incommensurate with the basic lattice and the phase of the density wave becomes meaningless. The same is true for the relative phases of the various orders of harmonic modulations of the density. This uncertainty even remains valid for commensurate density modulations of the sublattice, because coinciding higher-order harmonics in reciprocal space cause the same difficulty; higher-order coefficients cannot uniquely be separated from lower ones, consequently structure determination becomes impossible unless phase-determination methods are applied. Fortunately, density modulations of pure harmonic character are impossible for chemical reasons; they may be approximated by disorder phenomena for the averaged structure only. If diffuse scattering is taken into

account, the situation is changed considerably: A careful study of the diffuse scattering alone, although difficult in principle, will yield the necessary information about the relative phases of density waves (Korekawa, 1967).

4.2.3.5.2. Displacement fluctuations, displacive disorder

Displacement modulations are more complicated, even in a primitive structure. The Fourier transform of a longitudinal or a transverse displacement wave has to be calculated and this procedure does not result in a function of similar simplicity. Formally, a periodic modulation $\Delta\mathbf{r}_n = \mathbf{a}\cos(2\pi\mathbf{K}\cdot\mathbf{r}_n)$ leads to

$$I_{\rm D} \propto (2\pi\mathbf{H}\cdot\mathbf{a})^2 \sum_{\mathbf{G},\nu} A_\nu \delta(\mathbf{H}-\mathbf{G}\pm\nu\mathbf{K}), \qquad (4.2.3.35)$$

where $\mathbf{a}$ is the amplitude of the displacement wave with $\mathbf{a}=\alpha\mathbf{e}$ and $\mathbf{e}$ is the polarization vector: $|\mathbf{e}|=1$. Equation (4.2.3.35) denotes a set of satellites whose amplitudes are described by Bessel functions of νth order, where ν represents the order of the satellites. The intensity of the satellites increases with the magnitude of the product $\mathbf{H}\cdot\mathbf{a}$. This means that a single harmonic displacement causes an infinite number of satellites. They may be unobservable at low diffraction angles as long as the amplitudes are small. If the displacement modulation is incommensurate there are no coincidences with reflections of the sublattice. Consequently, the reciprocal space is completely covered with an infinite number of satellites, or, in other words, with diffuse scattering. This is a clear indication that incommensurate displacement modulations belong to the category of disordered structures. Statistical fluctuations of amplitudes of the displacement waves cause additional diffuse scattering, regardless of whether the period is commensurate or incommensurate (Overhauser, 1971; Axe, 1980). Fluctuations of 'phases' (*i.e.* periods) cause a broadening of satellites in reciprocal space but no change in their integrated intensities as long as the changes are not correlated with fluctuation periods. The broadening of satellite reflections increases with the order of the satellites and $(\mathbf{H}\cdot\mathbf{a})$. Obviously, there is no fundamental difference in the calculation of diffuse scattering with an ordered supercell of sufficient size.

4.2.3.5.3. Clusters and domains

Many disorder problems may be treated qualitatively in terms of coarsened structures that are made up of clusters or domain-like order extending along one or more directions in space. Common crystals are made up of 'mosaic individuals' which are separated irregularly by unspecified defects such as dislocations, small-angle boundaries, micro-strain fields and other defects. This 'real' crystallinity is not covered by the term 'disorder'. Clustering is, in a structural sense, not a very well defined term, but refers to general agglomerations of atoms, vacancies, defects or atomic groups due to preferred chemical bonding or due to some kind of exsolution processes. In general, the term 'cluster' is used to describe some inhomogeneity in a basic matrix structure. The term 'domain' usually implies either a spatially varying structure forming separate blocks, such as occurring in twin domains, or a spatial variation of a physical property (*e.g.* magnetic moment), which may be visualized by different configurations (see, *e.g.*, Frey, 1997). Structural domains may be chemically homogeneous, as is the case in twin domain structures, or heterogeneous, which occurs, *e.g.*, in feldspars with their complicated Ca/Na and Al/Si distributions. A definition of a domain structure may be given by symmetry arguments or, equivalently, by the order-parameter concept. Individual domains of the coarsened structure may be derived from a, possibly hypothetical, high-symmetry aristophase obeying the concept of symmetry groups. A lower symmetry of the domain is either due to loss of a point-group symmetry element (twin domains) or due to loss of a translational symmetry element of the aristophase, giving rise to the formation of out-of-phase domains. The special case of antiphase domains is related to a violation of a translational vector $\mathbf{t}$ in the aristophase by regular or irregular insertion of lattice displacements $\frac{1}{2}\mathbf{t}$. Shear domains, which are related by other fractional parts of $\mathbf{t}$, may be explained by cooperative gliding of structural building blocks, for example coordination polyhedra. Colour (black-and-white) symmetry has to be used for magnetic domain structures and may also be used for chemical domain ordering. While preserving the same lattice, the disordered (usually high-temperature) phase, which is specified by grey, decomposes into black and white domains, possibly embedded in the grey matrix. However, the term 'atomic cluster' is frequently used in this context. Domains can exhibit a new order by themselves, thus creating new symmetries of the superstructure. The boundaries between different domains are apparently essential and may even be used for a definition of a domain. This does not mean that the boundaries or domain walls are simple atomic planes rather than extended intermediate structural states which mellow the transition from one domain to the next one. Thus extended walls may carry a 'gradient' structure between neighbouring differently oriented domains and may be treated as new domains with their own structure. If misfits at the planes of coincidence are accompanied by remarkable straining, an array of dislocations may destroy the exact symmetry relation between the individuals. There is a stepwise transition from fully coherent domains to fully incoherent crystal parts. As long as coherency between the individuals is preserved, domain structures can be treated simply by means of Fourier transforms and characteristic features of the disorder problem may be extracted from diffuse patterns.

Quite generally, the scattering density for a general arrangement of domains may be written as (Boysen, 1995; Frey, 1997)

$$[\rho_1 * l_1][b_1^1 * d_1^1 + b_1^2 * d_1^2 + \ldots] + [\rho_2 * l_2][b_2^1 * d_2^1 + b_2^2 * d_2^2 + \ldots] + \ldots, \qquad (4.2.3.36)$$

where $\rho_i = \rho_i(\mathbf{r})$ is the structure of the unit cell of domain i, $l_i(\mathbf{r})$ is the lattice function, $b_i^j(\mathbf{r})$ is the shape function (which is unity in the region of domain i with size j and zero elsewhere) and $d_i^j(\mathbf{r}) = \sum \delta(\mathbf{r}-\mathbf{m}_i^j)$ is the distribution function ($\mathbf{m}_i^j$ are the centres of the domains). Note again that domain walls may be included in this formulation as separate 'domains'. Fourier transformation yields the scattering amplitude

$$[F_1 L_1] * [B_1^1 D_1^1 + B_1^2 D_1^2 + \ldots] + [F_2 L_2] * [B_2^1 D_2^1 + B_2^2 D_2^2 + \ldots] + \ldots, \qquad (4.2.3.37)$$

where $F_i = F_i(\mathbf{H})$ is the usual structure factor, $L_i(\mathbf{H})$ is the lattice function in reciprocal space, $B_i^j(\mathbf{H})$ and $D_i^j(\mathbf{H})$ are the Fourier transforms of the shape and distribution function, respectively, and the intensity is

$$\sum_i \Big|[F_i L_i] * \Big[\sum_j B_i^j D_i^j\Big]\Big|^2 + 2\sum_{i\neq k}[F_i L_i] * \Big[\sum_j B_i^j D_i^j\Big][F_k^+ L_k^+] * \Big[\sum_j B_k^{j+} D_k^{j+}\Big]. \qquad (4.2.3.38)$$

The first term represents sharp or diffuse reflections that are modified by the convolution with the Fourier transforms of the shape and distribution function (more correctly, with the Fourier transforms of the corresponding Patterson functions), while the second (cross) term generally leads to smaller additional changes. It should be emphasized that this separation does not correspond to the separation into Bragg and diffuse scattering. Although a further mathematical treatment of this very general expression does not seem to be easy, some qualitative or even semi-quantitative conclusions may be drawn:

(1) If the d_i^j are coherent with l_i (*i.e.* the $\mathbf{m}_i^j$ coincide with lattice points $\sum m_i\mathbf{a}_i$), the convolution with the second term in (4.2.3.38) is meaningless and we obtain sharp (basic) Bragg

reflections. This means that domain sizes and distributions cannot be determined from the widths of the Bragg reflections. One has to rely on the second term in this case.

(*a*) If, in addition, the d_i^j are strictly periodic (which implies equal sizes b_i), superlattice reflections occur that accompany the basic reflections as *satellites*. If the periodicity is *commensurate* with the basic lattice, higher-order satellites may coincide with basic reflections. Hence care must be taken even in the determination of the average structure.

(*b*) If the periodicity in (*a*) is not perfect (there are small fluctuations of domain sizes), the satellites will be broadened.

(*c*) If the distribution of domain sizes is completely random, this will degenerate into a continuous intensity distribution (diffuse streaks). Note, however, that a completely random distribution cannot be realized, since the domains have a *finite* size, *i.e.* there will always be some kind of modulation of the streak.

(2) If the d_i^j are incoherent, the second terms vanish and the broadening effect of the convolution in the first term becomes effective, *i.e.* the domain size and distribution can be determined directly from the widths of the basic Bragg reflections. This situation may be encountered more frequently in real systems, as usually the fluctuating widths of the domain walls lead to a loss of coherence between different domains of the same type. Nevertheless, one has to be careful if relatively small domain sizes are present, since accidental coincidences may occur that lead to different broadening of different reflections. The problem of coherence effects in these cases is discussed and exemplified by Boysen (2007).

(3) Interferences between domains of *different* kinds may lead to specific extinction rules (governing the distribution of sharp and diffuse reflections). Some examples are given below.

(4) The general reciprocity between direct and reciprocal space means that narrow objects in real space correspond to broad features in reciprocal space and *vice versa*. In particular, for domain walls, which are usually thin in one direction and extended in the other two, we expect a broad feature in one direction (perpendicular to the wall) and narrow ones in the perpendicular directions, *i.e.* streaks. For a single layer (with an ideal interface) this streak will be uniform, *i.e.* without modulations. In order to estimate domain sizes W, the square of the Fourier transform of a box function (for a special direction $\mathbf{H}$)

$$B^2(H) = [\sin(\pi WH)/\pi H]^2 \qquad (4.2.3.39)$$

may be used to estimate the half widths of the peaks. Hence measuring the peak broadening in all directions of reciprocal space will give full information about the shape of the domains.

(5*a*) The situation becomes slightly more complicated when strain effects are present. For small extensions of the strained volume, *e.g.* inside a domain wall, it may be convenient to treat the whole wall as one unit cell, *i.e.* simply calculate the sum over all atoms directly. A strained lattice may generally be written

$$l_s(\mathbf{r}) = \sum_m \delta\big[\mathbf{r} - \textstyle\sum m_i \mathbf{a}_i - \mathbf{s}(m)\big], \qquad (4.2.3.40)$$

where the function $\mathbf{s}(m)$ describes the displacement variation in the different cells. Fourier transformation gives

$$L_s(\mathbf{H}) = \sum_m \exp\{2\pi i \mathbf{H} \cdot \textstyle\sum m_i \mathbf{a}_i\} \exp\{2\pi i \mathbf{H} \cdot \mathbf{s}(m)\}. \qquad (4.2.3.41)$$

For a harmonic (sinusoidal) wave $\mathbf{s} = \mathbf{z}_0 \sin(2\pi m/M + \varphi)$, where $\mathbf{z}_0$, φ and M are the amplitude, the phase and the period of the wave, one gets (Korekawa, 1967)

$$L_s(\mathbf{H}) = \sum_m J_m(2\pi \mathbf{H} \cdot \mathbf{z}_0) \exp\{2\pi i m\varphi\} L(H - m/M), \quad (4.2.3.41a)$$

i.e. a set of satellites m weighted by Bessel functions of order m. The intensity of the zeroth order (Bragg peak) thus decreases with $\mathbf{H}$, while higher orders become more important. Again, one has to be careful with possible coincidences. This dependence on the scattering vector $\mathbf{H}$ holds for all other functional forms of $\mathbf{s}(m)$ as well and is therewith fundamentally different to the behaviour of the size effect, which gives the same contribution to all Bragg reflections, like in the case of density fluctuations. This difference may therefore be used to distinguish between the two effects.

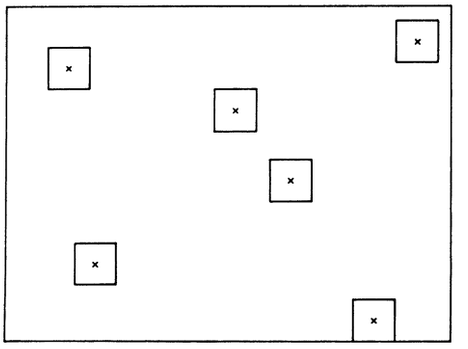

Fig. 4.2.3.1. Model of the two-dimensional distribution of point defects, causing changes in the surroundings.

(5*b*) Again, fluctuations of amplitude and phase lead to a broadening (diffuse tails) of the satellites. A general function $\mathbf{s}(m)$ may be analysed by expanding it into a Fourier series. For very long wavelengths (M) the satellites approach the basic Bragg peaks and cannot be observed easily. The case of a linear strain may be approximated by a sinusoidal modulation with very large wavelength, *i.e.* we will essentially observe a broadening of the Bragg peaks only. Then the strain ε may be estimated from the measured width $\Delta\mathbf{H}$:

$$\varepsilon = \Delta d/d = \Delta H/H.$$

Example: Clusters in a periodic lattice (low concentrations)

The exsolution of clusters of equal sizes is considered. The lattice of the host is undistorted, structure F_1, and the clusters have the same lattice but a different structure, F_2. A schematic drawing is shown in Fig. 4.2.3.1. Two different structures are introduced:

$$F_1(\mathbf{r}) = \sum_\nu \delta(\mathbf{r} - \mathbf{r}_\nu) * F_\nu(\mathbf{r}),$$

$$F_2(\mathbf{r}) = \sum_\mu \delta(\mathbf{r} - \mathbf{r}_\mu) * F_\mu(\mathbf{r}).$$

Their Fourier transforms are the structure factors $F_1(\mathbf{H})$, $F_2(\mathbf{H})$ of the matrix and the exsolved clusters, respectively. The boxes in Fig. 4.2.3.1 indicate the clusters, which may be represented by box functions $b(\mathbf{r})$ in the simplest case. It should be pointed out, however, that a more complicated shape means nothing other than a replacement of $b(\mathbf{r})$ by another shape function $b'(\mathbf{r})$ and its Fourier transform $B'(\mathbf{H})$. The distribution of clusters is represented by

$$d(\mathbf{r}) = \sum_{\mathbf{m}} \delta(\mathbf{r} - \mathbf{m}),$$

where $\mathbf{m}$ refers to the centres of the box functions (the crosses in Fig. 4.2.3.1). The problem is therefore defined by

$$l(\mathbf{r}) * F_1(\mathbf{r}) + [l(\mathbf{r})b(\mathbf{r})] * [F_2(\mathbf{r}) - F_1(\mathbf{r})] * d(\mathbf{r}). \qquad (4.2.3.42a)$$

The incorrect addition of $F_1(\mathbf{r})$ to the areas of clusters $F_2(\mathbf{r})$ is compensated by subtracting the same contribution from the second term in equation (4.2.3.42*a*). In order to determine the diffuse scattering, the Fourier transformation of (4.2.3.42*a*) is performed:

$$L(\mathbf{H})F_1(\mathbf{H}) + [L(\mathbf{H}) * B(\mathbf{H})][F_2(\mathbf{H}) - F_1(\mathbf{H})]D(\mathbf{H}). \quad (4.2.3.42b)$$

The intensity is given by

$$\left|L(\mathbf{H})F_1(\mathbf{H}) + [L(\mathbf{H}) * B(\mathbf{H})][F_2(\mathbf{H}) - F_1(\mathbf{H})]D(\mathbf{H})\right|^2. \quad (4.2.3.42c)$$

Evaluation of equation (4.2.3.42*c*) yields three terms (where c.c. means complex conjugate):

(i) $|L(\mathbf{H})F_1(\mathbf{H})|^2$

(ii) $\{[L(\mathbf{H})F_1(\mathbf{H})][L(\mathbf{H}) * B(\mathbf{H})] \times [F_2(\mathbf{H}) - F_1(\mathbf{H})]D(\mathbf{H}) + \text{c.c.}\}$

(iii) $|[L(\mathbf{H}) * B(\mathbf{H})][F_2(\mathbf{H}) - F_1(\mathbf{H})]D(\mathbf{H})|^2$.

The first two terms represent modulated lattices [multiplication of $L(\mathbf{H})$ by $F_1(\mathbf{H})$]. Consequently, they cannot contribute to diffuse scattering, which is completely determined by the third term. Fourier transformation of this term gives

$$\begin{aligned}&[l(\mathbf{r})b(\mathbf{r})] * \Delta F(\mathbf{r}) * d(\mathbf{r}) * [l(\mathbf{r})b(\mathbf{r})] * \Delta F^+(-\mathbf{r}) * d(-\mathbf{r})\\ &\quad = [l(\mathbf{r})b(\mathbf{r})] * [l(\mathbf{r})b(\mathbf{r})] * \Delta F(\mathbf{r}) * \Delta F^+(-\mathbf{r}) * d(\mathbf{r}) * d(-\mathbf{r})\\ &\quad = [l(\mathbf{r})t(\mathbf{r})] * \Delta F(\mathbf{r}) * \Delta F^+(-\mathbf{r}) * d(\mathbf{r}) * d(-\mathbf{r}), \quad (4.2.3.43a)\end{aligned}$$

where $l(\mathbf{r}) = l(-\mathbf{r})$, $b(\mathbf{r}) = b(-\mathbf{r})$ and $\Delta F = F_2 - F_1$. According to equation (4.2.3.15) and its subsequent discussion, the convolution of the two expressions in square brackets was replaced by $l(\mathbf{r})t(\mathbf{r})$, where $t(\mathbf{r})$ represents the 'pyramid' of n-fold height discussed above and n is the number of unit cells within $b(\mathbf{r})$. $d(\mathbf{r}) * d(-\mathbf{r})$ is the Patterson function of the distribution function $d(\mathbf{r})$. Its usefulness may be recognized by considering the two possible extreme solutions, namely the random and the strictly periodic distribution.

If no fluctuations of domain sizes are admitted, the minimum distance between two neighbouring domains is equal to the length of the domain in the corresponding direction. This means that the distribution function cannot be completely random. In one dimension, the solution of a random distribution of particles of a given size on a finite length shows that the distribution functions exhibit periodicities that depend on the average free volume of one particle (Zernike & Prins, 1927). Although the problem is more complicated in three dimensions, there should be no fundamental difference in the exact solutions.

On the other hand, it may be shown that the convolution of a pseudo-random distribution may be obtained if the average free volume is large. This is shown in Fig. 4.2.3.2(*a*) for the particular case of a cluster smaller than one unit cell. A strictly periodic distribution function (a superstructure) may result, however, if the volume of the domain and the average free volume are equal. Obviously, the practical solution for the self-convolution of the distribution function (which is the Patterson function) lies somewhere in between, as shown in Fig. 4.2.3.2(*b*). If a harmonic periodicity damped by a Gaussian is assumed, this self-convolution of the distribution in real space may be considered to consist of two parts, as shown in Figs. 4.2.3.2(*c*), (*d*). Note that the two different solutions result in completely different diffraction patterns:

(i) The geometrically perfect lattice extends to distances that are large when compared with the correlation length of the distribution function. Then the Patterson function of the distribution function concentrates at the positions of the basic lattice, which is given by multiplication by the lattice $l(\mathbf{r})$. The corresponding convolution in reciprocal space gives the same contribution to all Bragg reflections (Fig. 4.2.3.2*e*).

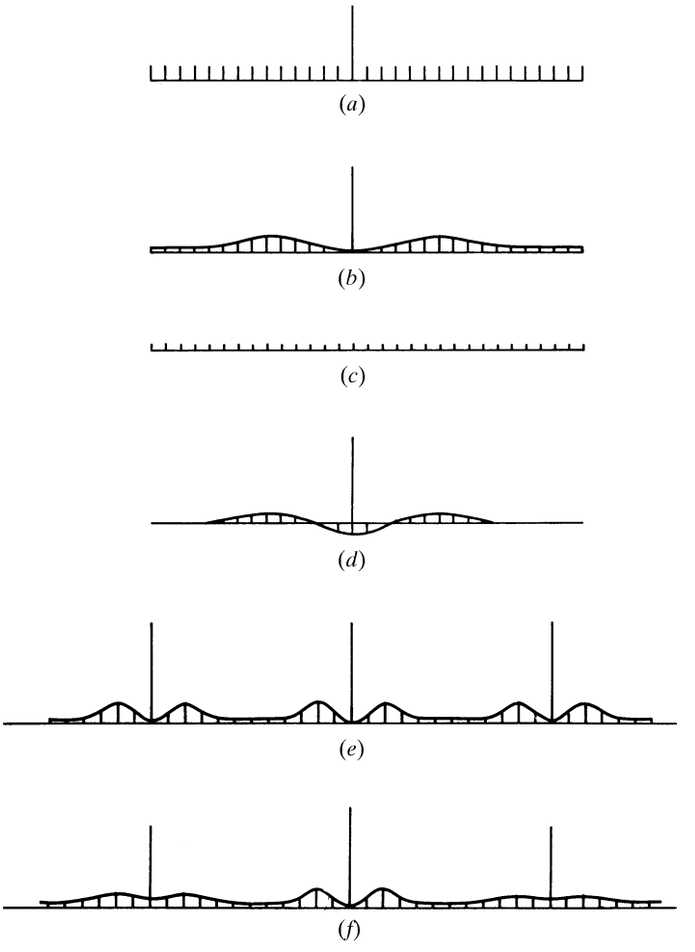

Fig. 4.2.3.2. One-dimensional Patterson functions of various point-defect distributions: (*a*) random distribution; (*b*) influence of finite volume of defects on the distribution function; (*c*), (*d*) decomposition of (*b*) into a periodic (*c*) and a convergent (*d*) part; (*e*) Fourier transform of (*c*) + (*d*); (*f*) changes of (*e*) if the centres of the defects show major deviations from the origins of the lattice.

(ii) There is no perfect lattice geometry. In this case, a continuous Patterson function results. Fourier transformation yields an influence that is now restricted primarily to the reflection 000, *i.e.* to the low-angle diffraction range.

Figs. 4.2.3.2(*e*), (*f*) show the different diffraction patterns of the diffuse scattering that is concentrated around the Bragg maxima. Although the discussion of the diffuse scattering was restricted to the case of identical domains, the introduction of a distribution of domain sizes does not influence the diffraction pattern essentially, as long as the fluctuation of sizes is small compared with the average volume of domain sizes and no strong correlation exists between domains of any size (a size-independent random distribution).

A complete qualitative discussion of the diffraction pattern may be carried out by investigating the Fourier transform of (4.2.3.43*a*):

$$[L(\mathbf{H}) * T(\mathbf{H})]|\Delta F(\mathbf{H})|^2|D(\mathbf{H})|^2. \quad (4.2.3.43b)$$

The first factor in (4.2.3.43*b*) describes the particle-size effect of a domain containing the influence of a surrounding strain field and the new structure of the domains precipitated from the bulk. $D(\mathbf{H})$ has its characteristic variation near the Bragg peaks (Figs. 4.2.3.2*e*,*f*) and is less important in between. For domain structure determination, intensities near the Bragg peaks should be avoided. Note that equation (4.2.3.43*b*) may be used for measurements using anomalous scattering in both the centric and the acentric case.

Solution of the diffraction problem. In equation (4.2.3.43*b*) $\Delta F(\mathbf{H})$ is replaced by its average,

$$\langle \Delta F(\mathbf{H}) \rangle = \sum_{\mu} p_{\mu} \Delta F_{\mu}(\mathbf{H}),$$

where p_{μ} represents the *a priori* probability of a domain of type μ. This replacement becomes increasingly important if small clusters (domains) have to be considered. Applications of the formulae to Guinier–Preston zones are given by Guinier (1942) and Gerold (1954); a similar application to clusters of vacancies in spinels with an excess of Al_2O_3 was outlined by Jagodzinski & Haefner (1967).

Although refinement procedures are possible in principle, the number of parameters entering the diffraction problem becomes increasingly large if more clusters or domains (of different sizes) have to be introduced. Another difficulty results from the large number of diffraction data which must be collected to perform a reliable structure determination. There is no need to calculate the first two terms in equation (4.2.3.42*c*) which contribute to the sharp Bragg peaks only, because their intensity is simply described by the averaged structure factor $|\langle F(\mathbf{H}) \rangle|^2$. These terms may therefore be replaced by

$$|L(\mathbf{H})|^2 |\langle F(\mathbf{H}) \rangle|^2$$

with

$$|\langle F(\mathbf{H}) \rangle|^2 = \Big| \sum_{\mu} p_{\mu} F_{\mu}(\mathbf{H}) \Big|^2, \qquad (4.2.3.43c)$$

where p_{μ} is the *a priori* probability of the structure factor $F_{\mu}(\mathbf{H})$. It should be emphasized here that (4.2.3.43*c*) is independent of the distribution function $d(\mathbf{r})$ or its Fourier transform $D(\mathbf{H})$.

While a number of solutions to the diffraction problem may be found in the literature for one-dimensional (1D) disorder (1D distribution functions) (see, *e.g.*, Jagodzinski, 1949*a*,*b*,*c*; Cowley, 1976*a*,*b*; Adlhart, 1981; Pflanz & Moritz, 1992), these become increasingly more complicated with increasing dimensionality. These types are therefore discussed separately in the following.

4.2.3.5.4. One-dimensional disorder

This lamellar (1D) type of disorder is common in many crystals for energetic reasons. For example, most of the important rock-forming minerals exhibit such disorder behaviour. Therefore we give some extended introduction to this field. To illustrate the application of the formalism outlined above, we start with a simple example of domains of an identical structure $\rho(\mathbf{r})$ displaced relative to each other by an arbitrary fault vector $\mathbf{\Delta}$ (Boysen *et al.*, 1991). If $t(\mathbf{r})$ describes the regions of one domain, then $1 - t(\mathbf{r})$ describes those of the displaced domains and the complete structure may be written

$$t(\mathbf{r})[l(\mathbf{r}) * \rho(\mathbf{r})] + [1 - t(\mathbf{r})][l(\mathbf{r} - \mathbf{\Delta}) * \rho(\mathbf{r})].$$

Introducing $t'(\mathbf{r}) = 2t(\mathbf{r}) - 1$, this may be rewritten as

$$[l(\mathbf{r}) + l(\mathbf{r} - \mathbf{\Delta})] * \rho(\mathbf{r})/2 = t'(\mathbf{r})\{[l(\mathbf{r}) - l(\mathbf{r} - \mathbf{\Delta})] * \rho(\mathbf{r})\}/2.$$

Fourier transformation yields

$$L(\mathbf{H})[1 + \exp\{2\pi i \mathbf{\Delta} \cdot \mathbf{r}\}]F(\mathbf{H})/2 + T'(\mathbf{H}) * L(\mathbf{H})[1 - \exp\{2\pi i \mathbf{\Delta} \cdot \mathbf{r}\}]F(\mathbf{H})/2.$$

The first term describes sharp reflections due to the multiplication with the lattice function $L(\mathbf{H})$, while the second term gives diffuse reflections due to the convolution with $T'(\mathbf{H})$. The corresponding intensities are

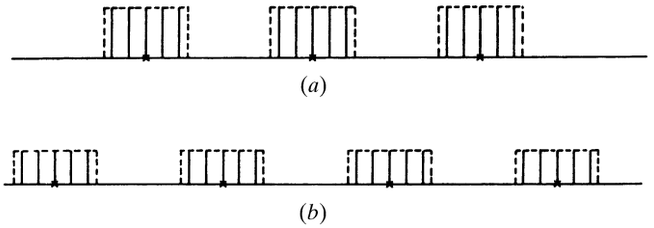

Fig. 4.2.3.3. Periodic array of domains consisting of two different atoms, represented by different heights. (*a*) Distribution of domain type 1, (*b*) distribution of domain type 2.

$$I_{\mathrm{S}} \propto 1 + \cos(2\pi \mathbf{\Delta} \cdot \mathbf{H}) \text{ and } I_{\mathrm{D}} \propto 1 - \cos(2\pi \mathbf{\Delta} \cdot \mathbf{H}).$$

In the general case, all reflections consist of a superposition of sharp and diffuse intensities. Note that the well known separation of sharp and diffuse intensities for antiphase domains is obtained if $\mathbf{\Delta}$ equals $\frac{1}{2}$ times a lattice vector.

(1) *Periodic distribution of lamellar domains*

Here $d(\mathbf{r})$ is one-dimensional and can easily be calculated: a periodic array of two types of lamellae having the same basic lattice $l(\mathbf{r})$ but different structures is shown in Fig. 4.2.3.3. The sizes of the two types of lamellae may be different. The structure of the first domain type is given by a convolution with $F_1(\mathbf{r})$ (Fig. 4.2.3.3*a*) and that of the second domain type by $F_2(\mathbf{r})$ (Fig. 4.2.3.3*b*). Introducing $\langle F(\mathbf{r}) \rangle$ and $\Delta F(\mathbf{r})$, the structure in real space is described by

$$\begin{aligned}[l(\mathbf{r})b_1(\mathbf{r})] * d(\mathbf{r}) * F_1(\mathbf{r}) + [l(\mathbf{r})b_2(\mathbf{r})] * d(\mathbf{r}) * F_2(\mathbf{r}) \\ = \{[l(\mathbf{r})b_1(\mathbf{r}) + l(\mathbf{r})b_2(\mathbf{r})] * d(\mathbf{r})\} * \langle F(\mathbf{r}) \rangle \\ + [l(\mathbf{r})b_1(\mathbf{r}) - l(\mathbf{r})b_2(\mathbf{r})] * d(\mathbf{r}) * \Delta F(\mathbf{r}). \qquad (4.2.3.44a)\end{aligned}$$

Obviously, the first term in curly brackets in equation (4.2.3.44*a*) is no more than $l(\mathbf{r})$ itself and $d(\mathbf{r})$ is strictly periodic. $b_1(\mathbf{r})$ and $b_2(\mathbf{r})$ are box functions, mutually displaced by $\pm(n_1 + n_2)/2$ unit cells in the stacking direction [n_1, n_2 are the numbers of cells covered by $b_1(\mathbf{r})$ and $b_2(\mathbf{r})$, respectively].

Fourier transformation of equation (4.2.3.44*a*) yields

$$L(\mathbf{H})\langle F(\mathbf{H}) \rangle + \{L(\mathbf{H}) * [B_1(\mathbf{H}) - B_2(\mathbf{H})]\} D(\mathbf{H}) \Delta F(\mathbf{H}). \qquad (4.2.3.44b)$$

The first term in equation (4.2.3.44*b*) gives the normal sharp reflections of the average structure, while the second describes superlattice reflections [sublattice $L_{\mathrm{s}}(\mathbf{H}) = D(\mathbf{H})$ in reciprocal space], multiplied by $\Delta F(\mathbf{H})$ and another 'structure factor' generated by the convolution of the reciprocal lattice $L(\mathbf{h})$ with $[B_1(\mathbf{H}) - B_2(\mathbf{H})]$ (*cf.* Fig. 4.2.3.3). Since the centres of $b_1(\mathbf{r})$ and $b_2(\mathbf{r})$ are mutually displaced, the expression in square brackets includes extinctions if $b_1(\mathbf{r})$ and $b_2(\mathbf{r})$ represent boxes equal in size. These extinctions are discussed below. It should be pointed out that $L_{\mathrm{s}}(\mathbf{H})$ and its Fourier transform $l_{\mathrm{s}}(\mathbf{r})$ are commensurate with the basic lattice as long as no change of the translation vector at the interface of the lamellae occurs. Obviously, $L_{\mathrm{s}}(\mathbf{H})$ becomes incommensurate in the general case of a slightly distorted interface. Considerations of this kind play an important role in the discussion of modulated structures.

No assumption has been made so far about the position of the interface. This point is meaningless only in the case of a strictly periodic array of domains (with no diffuse scattering). Therefore it seems to be convenient to introduce two basis vectors parallel to the interface in real space, which demand a new reciprocal vector perpendicular to them defined by $(\mathbf{a}' \times \mathbf{b}')/V'$, where $\mathbf{a}'$, $\mathbf{b}'$ are the new basis vectors and V' is the volume of the supercell. As long as the new basis vectors are commensurate with the original lattice, the direction of the new reciprocal vector $\mathbf{c}'^*$, perpendicular to $\mathbf{a}'$, $\mathbf{b}'$, passes through the Bragg points of the original reciprocal lattice and the reciprocal lattice of the superlattice

remains commensurate as long as V' is a multiple of V ($V' = mV$, m = integer). Since the direction of **c** is arbitrary to some extent, there is no clear rule about the assignment of superlattice reflections to the original Bragg peaks. This problem becomes very important if extinction rules of the basic lattice and the superlattice have to be described together.

Example

We consider a b.c.c. structure with two kinds of atoms (1, 2) with a strong tendency towards superstructure formation (CsCl-type ordering). According to equations (4.2.3.43*b*,*c*) and (4.2.3.44*b*), in the case of negligible short-range order we obtain the following expressions for sharp and diffuse scattering (where c = concentration):

$$I_S = |cf_1(\mathbf{H}) + (1-c)f_2(\mathbf{H})|^2 \quad \text{for } h+k+l = 2n,$$
$$I_D = c(1-c)|f_1(\mathbf{H}) - f_2(\mathbf{H})|^2 \quad \text{elsewhere.}$$

With increasing short-range order the sharp reflections remain essentially unaffected, while the diffuse ones concentrate into diffuse maxima at **h** with $h+k+l = 2n+1$. This process is treated more extensively below. As long as the domains exhibit no clear interface, it is useful to describe the ordering process with the two possible cell occupations of a pair of different atoms; then contributions of equal pairs may be neglected with increasing short-range order. Now the two configurations 1, 2 and 2, 1 may be given with the aid of the translation $\frac{1}{2}(\mathbf{a}+\mathbf{b}+\mathbf{c})$. Hence the two structure factors are

$$F_1 \text{ and } F_2 = F_1 \exp\{\pi i(h+k+l)\}.$$

Since the two structure factors occur with the same probability, the equations for sharp and diffuse reflections become

$$I_S = \tfrac{1}{4}|F_1(\mathbf{H})|^2[1 + \exp\{\pi i(h+k+l)\}]^2,$$
$$I_D = \tfrac{1}{4}|F_1(\mathbf{H})|^2[1 - \exp\{\pi i(h+k+l)\}]^2.$$

It is well recognized that no sharp reflections may occur for $h+k+l = 2n+1$, and the same holds for the diffuse scattering if $h+k+l = 2n$. This extinction rule for diffuse scattering is due to suppression of the contributions of equal pairs. The situation becomes different for lamellar structures. Let us first consider the case of lamellae parallel to (100). The ordered structure is formed by an alternating sequence of monoatomic layers consisting of atoms of types 1 or 2. Hence the interface between two neighbouring domains is a pair of equal layers 1, 1 or 2, 2, which are not equivalent. Each interface of type 1 (2) may be described by an inserted layer of type 1 (2) and the chemical composition differs from 1:1 if one type of interface is preferred. Since the contribution of equal pairs has been neglected in deriving the extinction rule of diffuse scattering (see above), this rule is no longer valid. Because of the lamellar structure the diffuse intensity is concentrated into streaks parallel to (00l). Starting from the diffuse maximum (010), the diffuse streak passes over the sharp reflection 011 to the next diffuse one 012 *etc.*, and the extinction rule is violated as long as one of the two interfaces is predominant. Therefore, the position of the interface determines the extinction rule in this orientation.

A completely different behaviour is observed for lamellae parallel to (110). This structure is described by a sequence of equal layers containing atoms 1 and 2. The interface between two domains (exchange of the two different atoms) is now nothing other than the displacement parallel to the layer of the original one in the ordered sequence. Calculation of the two structure factors would involve displacements $\pm\frac{1}{2}(\mathbf{a}-\mathbf{b})$. Starting from the diffuse reflection 001, the diffuse streak parallel to (HH0) passes through (111), (221), (331), ...; *i.e.* through diffuse reflections only. On the other hand, rows (HH2) going through (002), (112), (222), ... do not show any diffuse scattering. Hence we have a new extinction rule for diffuse scattering originating from the orientation of interfaces. This fact is rather important in structure determination. For various reasons, lamellar interfaces show a strong tendency towards a periodic arrangement. In diffraction the diffuse streak then concentrates into quite sharp superstructure reflections. These are not observed on those rows of the reciprocal lattice that are free from diffuse scattering. The same extinction law is not valid in the case of the (100) orientation of the interfaces. Summarizing, we may state that three types of extinction rules have to be considered:

(*a*) Normal extinctions for the average structure.

(*b*) Extinction of the difference structure factors for diffuse scattering.

(*c*) Extinctions caused by the ordering process itself.

(2) *Lamellar system with two different structures, where* $\langle F(\mathbf{H})\rangle$ *and* $\Delta F(\mathbf{H})$ *do not obey any systematic extinction law*

The convolution of the second term in equation (4.2.3.44*b*) (*cf.* Fig. 4.2.3.3) may be represented by a convolution of the Fourier transform of a box function $B_1(\mathbf{H})$ with the reciprocal superlattice. Since $B_1(\mathbf{H})$ is given by $\sin(\pi m_s H)/(\pi H)$, where m_s is the number of cells in the supercell, the reader might believe that the result of the convolution may easily be determined quantitatively: this assumption is not correct because of the slow convergence of $B_1(\mathbf{H})$. The systematic concidences of the maxima, or minima, of $B_1(\mathbf{H})$ with the points of the superlattice in the commensurate case cause considerable changes in intensities, especially in the case of a small domain thickness. For this reason, an accurate calculation of the amplitudes of the satellites is necessary (Jagodzinski & Penzkofer, 1981):

(*a*) Bragg peaks of the basic lattice

$$I \simeq |\langle F(\mathbf{H})\rangle|^2; \qquad (4.2.3.45a)$$

(*b*) satellites: $\nu = 2n$ (n = integer except 0)

$$I \simeq |2\sin\pi\nu C/[\sin\pi\nu/(N_1+N_2)]\Delta F(\mathbf{H})|^2; \qquad (4.2.3.45b)$$

(*c*) satellites: $\nu = 2n+1$

$$I \simeq |2\cos\pi\nu C/[\sin\pi\nu/(N_1+N_2)]\Delta F(\mathbf{H})|^2. \qquad (4.2.3.45c)$$

Here ν is the order of the satellites, $C = \frac{1}{2}(N_1 - N_2)/(N_1 + N_2)$, and N_1 and N_2 are the number of cells within $b_1(\mathbf{r})$ and $b_2(\mathbf{r})$, respectively.

Obviously, there is again a systematic extinction rule for even satellites if $N_1 = N_2$.

Equation (4.2.3.45*b*) indicates an increasing intensity of first even-order satellites with increasing C. Intensities of first even and odd orders become nearly equal if $N_2 \simeq \frac{1}{2}N_1$. Smaller values of N_2 result in a decrease of intensities of both even and odd orders (no satellites occur if $N_2 = 0$). The denominators in equations (4.2.3.45*b*,*c*) indicate a decrease in intensity with increasing order of the satellites. The quantitative behaviour of the intensities needs a more detailed discussion of the numerator in equations (4.2.3.45*b*,*c*) with increasing order of the satellites. Obviously, there are two kinds of extinction rules to be taken into account: systematic absences for the various orders of satellites, and the usual extinctions for $\langle F(\mathbf{H})\rangle$ and $\Delta F(\mathbf{H})$. Each has to be considered separately in order to arrive at reliable conclusions. This different behaviour of the superlattice reflections (satellites) and that of the basic lattice may be represented by a multidimensional group-theoretical representation, as has been shown by de Wolff (1974), Janner & Janssen (1980*a*,*b*), de Wolff *et al.* (1981) and others.

(3) *Nonperiodic system of lamellar domains*

Following the discussion of equations (4.2.3.43), one may conclude that the fluctuations of domain sizes cause a broadening of satellites if the periodic distribution function has to be

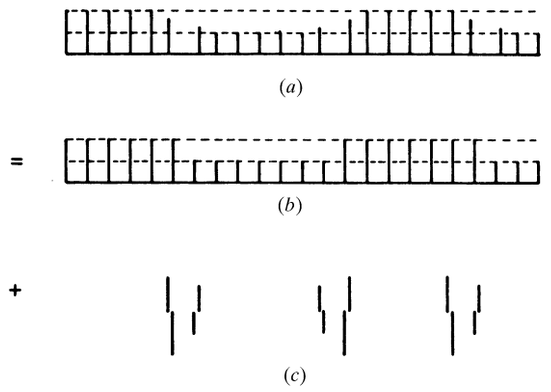

Fig. 4.2.3.4. Influence of distortions at the boundary of domains and separation into two parts; for discussion see text.

replaced by a statistical one. In this case, the broadening effect increases with the order of the satellites. The intensities, however, are completely determined by the distribution function and can be estimated by calculating the intensities of the perfectly ordered array, as approximated by the distribution function.

A careful check of $\langle F(\mathbf{H})\rangle$ and $\Delta F(\mathbf{H})$ in equations (4.2.3.45) shows that the position of the interface plays an important role in the intensities of the satellites. Since this position determines the origin of the unit cells in the sublattice, we have to choose this origin for the calculation of $F(\mathbf{H})$ and $\Delta F(\mathbf{H})$. This involves phase factors which are meaningless for integral values of $\mathbf{H}$ (i) if the average $\langle F(\mathbf{H})\rangle$ refers to different structures with arbitrary origin or (ii), which is important for practical cases, where no change occurs in the origin of related structures for neighbouring domains that are bound to an origin by general convention (*e.g.* a centre of symmetry). This statement is no longer true for non-integral values of $\mathbf{H}$, which are needed for the calculation of intensities of satellites. The intensities of satellites become different for different positions of the interface even in the absence of a relative displacement between neighbouring domains with respect to an origin by convention. This statement may be extended to nonperiodic distribution functions. Consequently, one may conclude that the study of diffuse scattering yields information on the interfacial scattering. For slightly different structures at the interface two cases are important:

(i) the two structures are related by symmetry (*e.g.* by a twin law); and

(ii) the difference between the two structures cannot be described by a symmetry operation.

In structures based on the same sublattice, the first case seems to be more important, because two different structures with the same sublattice are improbable. In the first case there is an identical sublattice if the symmetry operation in question does not influence the plane of intergrowth, *e.g.* a mirror plane should coincide with the plane of intergrowth. Since we have two inequivalent mirror planes in any sublattice, there are two such planes. It is assumed that no more than one unit cell of both domains at the interface has a slightly different structure without any change of geometry of the unit cell, and the number of unit cells is equal because of the equivalence of both domain structures (twins). Fig. 4.2.3.4(*a*) shows a picture of this model; Figs. 4.2.3.4(*b*), (*c*) explain that this structure may be described by two contributions:

(i) The first term is already given by equation (4.2.3.45) for $N_1 = N_2$, consequently only odd orders of satellites are observed.

(ii) The second term may be described by a superlattice containing $2N_1$ cells with an alternating arrangement of interfaces, correlated by the relevant plane of symmetry.

In real space, the second term may be constructed by convolution of the one-dimensional superlattice with two difference structures displaced by $\mp N_1/2$ units of the sublattice; its Fourier transformation yields

$$L_s(\mathbf{H})[\Delta F_i(\mathbf{H})\exp\{2\pi i N_1 H/2\} + \Delta F_i'(\mathbf{H})\exp\{-2\pi i N_1 H/2\}], \quad (4.2.3.46)$$

where ΔF_i, $\Delta F_i'$ correspond to the Fourier transforms of the contributions shown in Fig. 4.2.3.4(*c*). Since $H = \nu/N_1$, there are alternating contributions to the νth satellite which may be calculated more accurately by taking into account the symmetry operations. The important difference between equations (4.2.3.45) and (4.2.3.46) is the missing decrease in intensity with increasing order of the satellites. Consequently, one may conclude that the interface contributes to low- and high-order satellites as well, but its influence prevails for high-order satellites. Similar considerations may be made for two- and three-dimensional distributions of domains. A great variety of extinction rules may be found depending on the type of order approximated by the distribution under investigation.

(4) *Two kinds of lamellar domains with variable size distribution*

The preceding discussion of the diffuse scattering from domains is obviously restricted to relatively small fluctuations of domain sizes. This is specifically valid if the most probable domain size does not differ markedly from the average size. This condition is violated in the case of order–disorder phenomena. It may happen that the smallest ordered area is the most probable one, although the average is considerably larger. This may be shown for a lamellar structure of two types of layers correlated by a (conditional) pair probability $p_{\mu\mu'}(\mathbf{1})$. As shown below, a pair at distance $\mathbf{m}$ occurs with the probability $p_\mu p_{\mu\mu'}(\mathbf{m})$, which may be derived from the pair probability of nearest neighbours $p_\mu p_{\mu\mu'}(\mathbf{1})$. (In fact only one component of vector $\mathbf{m}$ is relevant in this context.) The problem will be restricted to two kinds of layers (μ, $\mu' = 1, 2$). Furthermore, it will be symmetric in the sense that the pair probabilities obey the following rules:

$$p_{11}(\mathbf{m}) = p_{22}(\mathbf{m}), \quad p_{12}(\mathbf{m}) = p_{21}(\mathbf{m}). \quad (4.2.3.47)$$

It may be derived from equation (4.2.3.47) that the *a priori* probabilities p_μ of a single layer are $\frac{1}{2}$ and

$$p_{11}(\mathbf{0}) = p_{22}(\mathbf{0}) = 1, \quad p_{12}(\mathbf{0}) = p_{21}(\mathbf{0}) = 0.$$

With these definitions and the general relation

$$p_{11}(\mathbf{m}) + p_{12}(\mathbf{m}) = p_{22}(\mathbf{m}) + p_{21}(\mathbf{m}) = 1,$$

the *a priori* probability of a domain containing m layers of type 1 may be calculated with the aid of $p_{11}(\mathbf{1})$ [$0 \le p_{11}(\mathbf{1}) \le 1$]:

$$p_\mu = \tfrac{1}{2}p_{11}(\mathbf{1})^{m-1}[1 - p_{11}(\mathbf{1})]. \quad (4.2.3.48)$$

Hence the most probable size of domains is a single layer, because a similar relation holds for layers of type 2. Since the average thickness of the domains is strongly dependent on $p_{11}(\mathbf{1})$ [infinite for $p_{11}(\mathbf{1}) = 1$ and one layer for $p_{11}(\mathbf{1}) = 0$], it may become very large in the latter case. Consequently, there are extremely large fluctuations if $p_{11}(\mathbf{1})$ is small but different from zero.

It may be concluded from equation (4.2.3.48) that the function $p_{11}(\mathbf{m})$ decreases monotonically with increasing $\mathbf{m}$, approaching $\frac{1}{2}$ with $\mathbf{m} \to \infty$. It is apparent that this cannot be true for a finite crystal if $p_{11}(\mathbf{m})$ is unity (a structure of two types of domains) or zero (a superstructure of alternating layers). In either case, the crystal should consist of a single domain of type 1 or 2, or one of the possible superstructures 1212 ..., 2121 ..., respectively. Hence one has to differentiate between long-range order, where two equivalent solutions have to be considered, and short-range order, where $p_{11}(\mathbf{m})$ approaches the *a priori* probability $\frac{1}{2}$ for large m. This behaviour of $p_{11}(\mathbf{m})$ and $p_{12}(\mathbf{m})$, which may also be

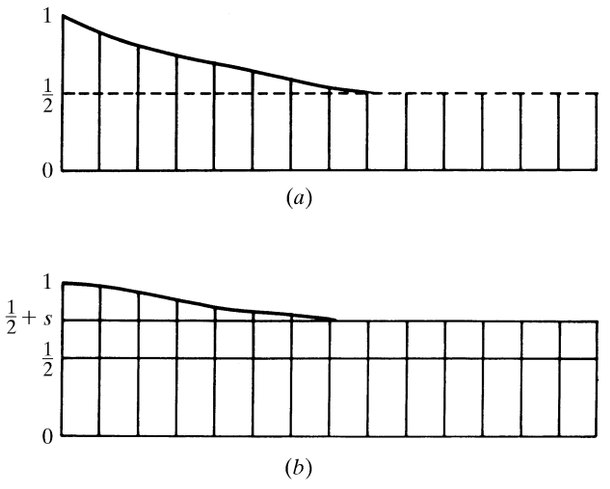

Fig. 4.2.3.5. Behaviour of $p_{11}(\mathbf{m})$ and $p_{12}(\mathbf{m})$ in mixed crystals (unmixing): (*a*) upper curve: short-range order only; (*b*) lower curve: long-range order.

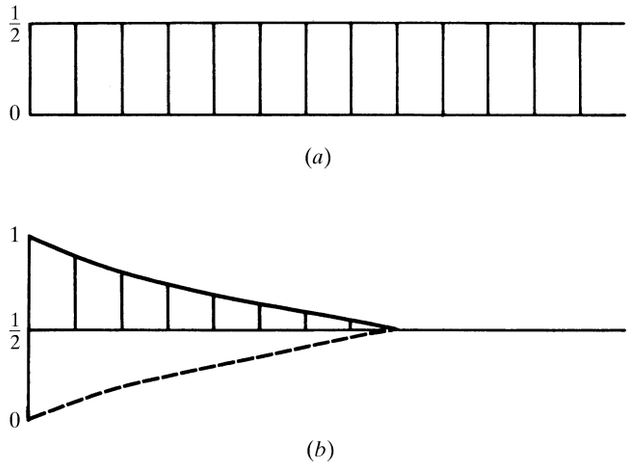

Fig. 4.2.3.6. Decomposition of Fig. 4.2.3.5(*a*) into (*a*) a periodic and (*b*) a rapidly convergent part.

expressed by equivalent correlation functions, is shown in Figs. 4.2.3.5(*a*) (short-range order) and 4.2.3.5(*b*) (long-range order, quantified by the parameter s). $p_{11}(\mathbf{m})$ approaches $\frac{1}{2}+s$ for large m with $s = 0$ in the case of short-range order, while $p_{12}(\mathbf{m})$ becomes $\frac{1}{2}-s$. Obviously, a strict correlation between $p_{11}(\mathbf{1})$ and s exists, and this has to be calculated. For a qualitative interpretation of the diffraction pictures this correlation may be derived from the diffraction pattern itself. The $p_{\mu\mu'}(\mathbf{m})$ are separable into a strictly periodic and a monotonically decreasing term approaching zero in both cases. This behaviour is shown in Figs. 4.2.3.6(*a*), (*b*). The periodic term contributes to sharp Bragg scattering. In the case of short-range order, the symmetry relations given in equation (4.2.3.47) are valid. The convolution in real space yields with factors $t(\mathbf{r})$ (equation 4.2.3.43*a*):

$$\begin{aligned}
&\tfrac{1}{2}t(\mathbf{r})\left[\sum_{\mathbf{m}}\delta(\mathbf{r}+\mathbf{m})p'_{11}(\mathbf{m})\right] * F_1(\mathbf{r}) * F_1(-\mathbf{r})\\
&\quad+\tfrac{1}{2}t(\mathbf{r})\left[\sum_{\mathbf{m}}\delta(\mathbf{r}+\mathbf{m})p'_{12}(\mathbf{m})\right] * F_1(\mathbf{r}) * F_2(-\mathbf{r})\\
&\quad+\tfrac{1}{2}t(\mathbf{r})\left[\sum_{\mathbf{m}}\delta(\mathbf{r}+\mathbf{m})p'_{21}(\mathbf{m})\right] * F_2(\mathbf{r}) * F_1(-\mathbf{r})\\
&\quad+\tfrac{1}{2}t(\mathbf{r})\left[\sum_{\mathbf{m}}\delta(\mathbf{r}+\mathbf{m})p'_{22}(\mathbf{m})\right] * F_2(\mathbf{r}) * F_2(-\mathbf{r}),
\end{aligned}$$

where $p'_{\mu\mu'}(\mathbf{m})$ are factors attached to the δ functions:

$$\begin{aligned}
p'_{11}(\mathbf{m}) &= p_{11}(\mathbf{m}) - \tfrac{1}{2} = p'_{22}(\mathbf{m}),\\
p'_{12}(\mathbf{m}) &= p'_{21}(\mathbf{m}) = -p'_{11}(\mathbf{m}).
\end{aligned}$$

The positive sign of $\mathbf{m}$ in the δ functions results from the convolution with the inverted lattice (*cf.* Patterson, 1959). Fourier transformation of the four terms given above yields the four corresponding expressions with $\mu, \mu' = 1, 2$:

$$\tfrac{1}{2}\left[T(\mathbf{H}) * \sum_{\mathbf{m}} p'_{\mu\mu'}(\mathbf{m})\exp\{-2\pi i\mathbf{H}\cdot\mathbf{m}\}\right]F_\mu(\mathbf{H})F^+_{\mu'}(\mathbf{H}). \qquad (4.2.3.49a)$$

Now the summation over $\mathbf{m}$ may be replaced by an integral if the factor $l(\mathbf{m})$ is added to $p'_{\mu\mu'}(\mathbf{m})$, which may then be considered as the smoothest continuous curve passing through the relevant integer values of $\mathbf{m}$:

$$\sum \rightarrow \int l(\mathbf{m})p'_{\mu\mu'}(\mathbf{m})\exp\{-2\pi i\mathbf{H}\cdot\mathbf{m}\}\,\mathrm{d}\mathbf{m}.$$

Since both $l(\mathbf{m})$ and $p'_{\mu\mu'}(\mathbf{m})$ are symmetric in our special case, we obtain

$$\sum = L(\mathbf{H}) * P'_{\mu\mu'}(\mathbf{H}).$$

Insertion of the sum in equation (4.2.3.49*a*) results in

$$\tfrac{1}{2}[L(\mathbf{H}) * T(\mathbf{H}) * P'_{\mu\mu'}(\mathbf{H})]F_\mu(\mathbf{H})F^+_{\mu'}(\mathbf{H}). \qquad (4.2.3.49b)$$

Using all symmetry relations for $p'_{\mu\mu'}(\mathbf{m})$ and $P'_{\mu\mu'}(\mathbf{H})$, respectively, we obtain for the diffuse scattering after summing over μ, μ'

$$I_{\mathrm{D}} \simeq [L(\mathbf{H}) * T(\mathbf{H}) * P'_{11}(\mathbf{H})]|\Delta F(\mathbf{H})|^2 \qquad (4.2.3.50)$$

with $\Delta F(\mathbf{H}) = \frac{1}{2}[F_1(\mathbf{H}) - F_2(\mathbf{H})]$.

It should be borne in mind that $P'_{11}(\mathbf{H})$ decreases rapidly if $p'_{11}(\mathbf{r})$ decreases slowly and *vice versa.* It is interesting to compare the different results from equations (4.2.3.43*b*) and (4.2.3.50). Equation (4.2.3.50) indicates diffuse maxima at the positions of the sharp Bragg peaks, while the multiplication by $D(\mathbf{H})$ causes satellite reflections in the neighbourhood of Bragg maxima. Both equations contain the factor $|\Delta F(\mathbf{H})|^2$, indicating the same influence of the two structures. More complicated formulae may be derived for several cell occupations. In principle, a result similar to equation (4.2.3.50) will be obtained, but more interdependent correlation functions $p_{\mu\mu'}(\mathbf{r})$ have to be introduced. Consequently, the behaviour of diffuse intensities becomes more differentiated in so far as all $p'_{\mu\mu'}(\mathbf{r})$ are now correlated with the corresponding $\Delta F_\mu(\mathbf{r})$, $\Delta F_{\mu'}(-\mathbf{r})$. Hence the method of correlation functions becomes increasingly ineffective with an increasing number of correlation functions. Here the cluster method seems to be more convenient and is discussed below.

(5) *Lamellar domains with long-range order: tendency to exsolution*

The Patterson function of a disordered crystal exhibiting long-range order is shown in Fig. 4.2.3.5(*b*). Now $p_{11}(\infty)$ converges against $\frac{1}{2}+s$ and the *a priori* probability changes correspondingly. Since $p_{12}(\infty)$ becomes $\frac{1}{2}-s$, the symmetry relation given in equation (4.2.3.47) is violated: $p_{11}(\mathbf{r}) \neq p_{22}(\mathbf{r})$ for a finite crystal; it is evident that another crystal shows long-range order with the inverted correlation function, $p_{22}(\infty) = \frac{1}{2}+s$, $p_{21}(\infty) = \frac{1}{2}-s$, such that the symmetry $p_{11}(\mathbf{r}) = p_{22}(\mathbf{r})$ is now valid for an assembly of finite crystals only. According to Fig. 4.2.3.5(*b*), there is a change in the intensities of the Bragg peaks.

$$\begin{aligned}
I_1 &\simeq |(\tfrac{1}{2}+s)F_1(\mathbf{H}) + (\tfrac{1}{2}-s)F_2(\mathbf{H})|^2,\\
I_2 &\simeq |(\tfrac{1}{2}+s)F_2(\mathbf{H}) + (\tfrac{1}{2}-s)F_1(\mathbf{H})|^2,
\end{aligned} \qquad (4.2.3.51)$$

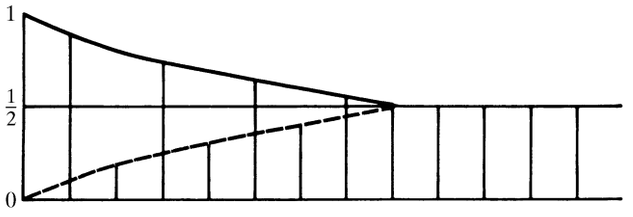

Fig. 4.2.3.7. The same distribution (*cf.* Fig. 4.2.3.5) in the case of superstructure formation.

where I_1, I_2 represent the two solutions discussed for the assembly of crystals and have to be added with the probability $\frac{1}{2}$; the intensities of sharp reflections become

$$I = (I_1 + I_2)/2. \tag{4.2.3.52}$$

Introducing equation (4.2.3.51) into (4.2.3.52), we obtain

$$I \simeq |\tfrac{1}{2}[F_1(\mathbf{H}) + F_2(\mathbf{H})]|^2 + s^2|F_1(\mathbf{H}) - F_2(\mathbf{H})^2|^2. \tag{4.2.3.53a}$$

$s = 0$ corresponds to the well known behaviour of sharp reflections, $s = \frac{1}{2}$ (maximum long-range order) gives

$$I \simeq \tfrac{1}{2}[|F_1(\mathbf{H})|^2 + |F_2(\mathbf{H})|^2]. \tag{4.2.3.53b}$$

This result reveals some difficulties for the determination of the averaged structure as long as s is different from zero or $\frac{1}{2}$, since in the former case the use of integrated sharp Bragg intensities yields a correct average structure. If $s = \frac{1}{2}$, a correct structure determination can only be performed with a refinement allowing for an incoherent superposition of two different structures. Having subtracted all periodic contributions to $p_{\mu\mu'}(\mathbf{r})$, new functions that describe the remaining nonperiodic parts have to be introduced (Fig. 4.2.3.6*b*). In order to obtain a clear overview of intensities, $p'_{\mu\mu'}(\mathbf{r})$ is again defined:

$$p'_{\mu\mu'}(\mathbf{r}) = cp_{\mu\mu'}(\mathbf{r}) - p_{\mu\mu'}(\infty),$$

where c should be chosen such that $p_{\mu\mu'}(\mathbf{0}) = 1$. By this definition a very simple behaviour of the diffuse scattering is obtained:

$$p'_{11}(\mathbf{r}) : \tfrac{1}{2} - s; \quad p'_{12}(\mathbf{r}) : -(\tfrac{1}{2} - s);$$
$$p'_{22}(\mathbf{r}) : \tfrac{1}{2} + s; \quad p'_{21}(\mathbf{r}) : -(\tfrac{1}{2} + s).$$

With the definitions introduced above it is found that

$$p'_{11}(\mathbf{r}) = p'_{22}(\mathbf{r}).$$

The diffuse scattering is given by

$$I_{1\mathrm{D}}(\mathbf{H}) = (\tfrac{1}{4} - s^2)|F_1(\mathbf{H}) - F_2(\mathbf{H})|^2[P'_{11}(\mathbf{H}) * L(\mathbf{H})]. \tag{4.2.3.54}$$

Since equation (4.2.3.54) is symmetrical with respect to an interchange of F_1 and F_2, the same result is obtained for $I_{2\mathrm{D}}$. Diffuse reflections occur in the positions of the sharp ones; the integrated intensities of sharp and diffuse reflections are independent of the special shape of $P'_{11}(\mathbf{H})$, hence

$$1 = \int P'_{11}(\mathbf{H}) \exp\{2\pi i \mathbf{0} \cdot \mathbf{H}\}\, \mathrm{d}\mathbf{H} = \int P'_{11}(\mathbf{H})\, \mathrm{d}\mathbf{H}$$

since $p_{11}(\mathbf{0}) = 1$.

(6) *Lamellar domains with long-range order: tendency to superorder*

So far it has been tacitly assumed that the crystal shows a preference for equal neighbours. If there is a reversed tendency (*i.e.* pairs of unequal neighbours are more probable), the whole procedure outlined above may be repeated as shown in Fig. 4.2.3.7 for the one-dimensional example. With the same probability of an unlike pair as used for the equal pair in the preceding example, the order process approaches an alternating structure such that the even-order neighbours have the same pair probabilities, while the odd ones are complementary for equal pairs (Fig. 4.2.3.7). In order to calculate intensities, it is necessary to introduce a new lattice with the doubled lattice constant and the corresponding reciprocal lattice with $b^{*\prime} = b^*/2$. In order to describe the probability $p_{\mu\mu'}(\mathbf{r})$, one has to introduce two lattices in real space – the normal lattice with the undisplaced origin and the displaced one. Fourier transformation of the new functions yields the following very similar results:

Sharp Bragg reflections

(*a*) $k' =$ even

$$I_{\mathrm{S}} = |\tfrac{1}{2}[F_1(\mathbf{H}) + F_2(\mathbf{H})]|^2. \tag{4.2.3.55a}$$

(*b*) $k' =$ odd

$$I_{\mathrm{S}} = s^2|\tfrac{1}{2}[F_1(\mathbf{H}) - F_2(\mathbf{H})]|^2. \tag{4.2.3.55b}$$

Diffuse reflections

(*c*) $k' =$ odd

$$I_{\mathrm{D}} = (\tfrac{1}{4} - s^2)|\tfrac{1}{2}[F_1(\mathbf{H}) - F_2(\mathbf{H})]|^2. \tag{4.2.3.55c}$$

In contrast to (5), this is the better situation for the determination of the averaged structure, which may be performed without any difficulty regardless of whether s is different from zero or not. For this purpose, even reflections (or reflections in the old setting) may be used. The inclusion of odd reflections in the structure determination of the superstructure is also possible if convenient **H**-independent scaling factors are introduced in order to compensate for the loss in intensity which is unavoidable for the integration of the diffuse scattering.

A few comments should be made on the physical meaning of the formulae derived above. All formulae may be applied to the general three-dimensional case, where long-range and short-range order is a function of the relevant thermodynamical parameters. In practice, long-range order will never be realized in a real crystal consisting of mosaic blocks which may behave as small subunits in order–disorder transitions. Another reason to assume partly incoherent areas in single crystals is the possible presence of strains or other distortions at the interfaces between domains, which should cause a decrease of the averaged areas of coherent scattering. All these effects may lead to diffuse scattering in the neighbourhood of Bragg peaks, similar to the diffuse scattering caused by domain structures. For this reason, an incoherent treatment of domains is probably more efficient, although considerable errors in intensity measurements may occur. A very careful study of line profiles is generally useful in order to decide between the various possibilities.

4.2.3.5.5. Two-dimensional disorder

The subject of two-dimensional disorder refers to predominantly one-dimensional structural elements, *e.g.* extended macromolecules and chain- or column-like structural units. A short introduction to this subject and some examples taken from inorganic structures are given in Section 4.2.5.3. Most important in this context, however, would be a treatment of disorder diffuse scattering of polymer/fibre structures. These are subjects in their own right and are treated in Chapter 4.5 of this volume and in Chapter 19.5 of Volume F.

4.2.3.5.6. Three-dimensional disorder

The solution of three-dimensional disorder problems is generally more demanding, although it may start with the formulation given above. Various algorithms have been developed to tackle these problems at least approximately, most of them restricted to particular models. Both real-space (cluster) and reciprocal-space (fluctuation wave) methods are employed and will be briefly addressed in Section 4.2.5.4. The more recently

developed approaches using computer simulations are described in Section 4.2.7.

Here we give only some general remarks on order–disorder problems.

Correlation functions in three dimensions may have very complicated periodicities; hence careful study is necessary to establish whether or not they may be interpreted in terms of a superlattice. If so, extinction rules have to be determined in order to obtain information on the superspace group. In the literature these are often called modulated structures (see Section 4.2.6) because a sublattice, as determined by the basic lattice, and a superlattice may well be defined in reciprocal space: reflections of a sublattice including (000) are formally described by a multiplication by a lattice having larger lattice constants (the superlattice) in reciprocal space; in real space this means a convolution with the Fourier transform of this lattice (the sublattice). In this way, the averaged structure is generated in each of the subcells (the superposition or 'projection' of all subcells into a single one). Obviously, the Patterson function of the averaged structure contains little information in the case of small subcells. Hence it is advisable to include the diffuse scattering of the superlattice reflections at the beginning of any structure determination.

N subcells in real space are assumed, each of them representing a kind of a complicated 'atom' that may be equal by translation or other symmetry operation. Once a superspace group has been determined, the usual extinction rules of space groups may be applied, remembering that the 'atoms' themselves may have systematic extinctions. Major difficulties arise from the existence of different symmetries of the subgroup and the supergroup. Since the symmetry of the supercell is lower in general, all missing symmetry elements may cause domains corresponding to the missing symmetry element: translations cause antiphase domains in their generalized sense; other symmetry elements cause twins generated by rotations, mirror planes or the centre of symmetry. If all these domains are small enough to be detected by a careful study of line profiles, using diffraction methods with a high resolution power, the structural study may be facilitated by introducing scaling factors for groups of reflections affected by the possible domain structures.

4.2.3.6. Symmetry

If disorder problems involving completely different structures (exsolutions *etc.*) are excluded, in general the symmetry of the diffuse-scattering pattern is the same as that of the Bragg peaks, *i.e.* it corresponds to the point group of the space group of the average structure. Only under specific directional growth conditions are deviations from this rule conceivable (although seemingly not very common). On the other hand, the symmetry of the underlying disorder model in direct space may be lower than that of the space group of the average structure (it is usually a subgroup of the space group of the average structure). The overall symmetry in reciprocal space is then restored by employing the missing (point-group) symmetry elements, which have therefore to be used in the calculation of the full diffraction pattern.

From these arguments, some specific disorder models may be classified according to the irreducible representations of the space group of the average structure. While for general wavevectors in the Brillouin zone no further restrictions appear, for high-symmetry directions consideration of the irreducible representations of the little co-group of the wavevector can help to identify the different symmetries of the disorder model. This becomes particularly evident when the modulation-wave approach is used as shown *e.g.* by Welberry & Withers (1990) and Welberry & Butler (1994). Of particular value are observed extinction rules, which may be calculated by group-theoretical methods as developed by Perez-Mato *et al.* (1998) for the extinctions occurring in inelastic neutron-scattering experiments. In favourable cases, the analysis of such extinctions alone can lead to a unique determination of the disorder model (see, *e.g.*, Aroyo *et al.*, 2002).

4.2.4. General guidelines for analysing a disorder problem

In general, the structure determination of a disordered crystal should start in the usual way by solving the average structure. The effectiveness of this procedure strongly depends on the distribution of integrated intensities of sharp and diffuse reflections. In cases where the integrated intensities of Bragg peaks are predominant, the maximum information can be drawn from the averaged structure. The observations of fractional occupations of lattice sites, split positions and anomalous large and anharmonic displacement parameters are indications of the disorder involved. Since these aspects of disorder phenomena in the averaged structure may be interpreted very easily, a detailed discussion of this matter is not given here (see any modern textbook of X-ray crystallography). Therefore, the anomalies of the average structure can give valuable hints on the underlying disorder and, *vice versa*, can be used to check the final disorder model derived from the diffuse scattering.

Difficulties may arise from the intensity integration, which should be carried out very carefully to separate the Bragg peaks from the diffuse contributions, *e.g.* by using a high-resolution diffraction method. The importance of this may be understood from the following argument. The averaged structure is determined by the coherent superposition of different structure factors. This interpretation is true if there is a strictly periodic subcell with long-range order that allows for a clear separation of sharp and diffuse scattering. There are important cases, however, where this procedure cannot be applied without loss of information.

(*a*) The diffuse scattering (other than thermal diffuse scattering) is concentrated near the Bragg peaks for a large number of reflections. Because of the limited resolution power of conventional single-crystal methods, the separation of sharp and diffuse scattering is impossible. Hence, the conventional study of integrated intensities does not really lead to an averaged structure. In this case, a refinement should be tried using an incoherent superposition of different structure factors (from the average structure and the difference structure). Application of this procedure is subject to conditions which have to be checked very carefully before starting the refinement: first, it is necessary to estimate the amount of diffuse scattering not covered by intensity integration of the 'sharp' reflections. Since loss in intensity, hidden in the background scattering, is underestimated very frequently, it should be checked whether nearly coinciding sharp and diffuse maxima are modulated by the same structure factor. It may be difficult to meet this condition in some cases; *e.g.* this condition is fulfilled for antiphase domains but the same is not true for twin domains.

(*b*) The concentration of diffuse maxima near Bragg peaks is normally restricted to domain structures with a strictly periodic sublattice. Cases deviating from this rule are possible. Since they are rare, they are omitted here. Even structures with small deviations from the average structure do not necessarily lead to structure factors for diffuse scattering that are proportional to those of the average structure. This has been shown in the case of a twin structure correlated by a mirror plane, where the reflections of a zone only have equal structure factors (Cowley & Au, 1978). This effect causes even more difficulties for orthogonal lattices, where the two twins have reflections in exactly the same positions, although differing in their structure factors. In this particular case, the incoherent or coherent treatment in refinements may be seriously hampered by strains originating from the boundary. Unsatisfactory refinements may be explained in this way but this does not improve their reliability.

The integrated intensity within a Brillouin zone of any structure is independent of atomic positions if the atomic form factors remain unchanged by structural fluctuations. Small deviations of atomic form factors owing to electron-density changes of valence electrons are neglected. Consequently, the integrated diffuse intensities remain unchanged if the average structure is not altered by the degree of order. The latter condition is obeyed in cases where a geometrical long-range order of the lattice is independent of the degree of order, and no long-range order in the structure exists. This law is extremely useful for the interpretation of diffuse scattering. Unfortunately, intensity integration over coinciding sharp and diffuse maxima does not necessarily lead to a structure determination of the corresponding undistorted structure. This integration may be useful for antiphase domains without major structural changes at the boundaries. In all other cases, the deviations of domains (or clusters) from the averaged structure determine the intensities of maxima, which are no longer correlated with those of the average structure.

If the integrated intensity of diffuse scattering is comparable with, or even larger than, those of the Bragg peaks, it is useful to begin the interpretation with a careful statistical study of the diffuse intensities. Intensity statistics can be applied in a way similar to the intensity statistics in classical structure determination. The following rules are briefly discussed in order to enable a semiquantitative interpretation of the essential features of disorder.

(1) First, it is recommended that the integrated intensities are studied in certain areas of reciprocal space.

(2) Since low-angle scattering is very sensitive to fluctuations of densities, the most important information can be drawn from its intensity behaviour. If there is at least a one-dimensional sublattice in reciprocal space without diffuse scattering, it may often be concluded that there is no important low-angle scattering either. This law is subject to the condition of a sufficient number of reflections obeying this extinction rule without any exception.

(3) If the diffuse scattering shows maxima and minima, it should be checked whether the maxima observed may be approximately assigned to a lattice in reciprocal space. Obviously, this condition can hardly be met exactly if these maxima are modulated by a kind of structure factor, which causes displacements of maxima proportional to the gradient of this structure factor. Hence this influence may well be estimated from a careful study of the complete diffuse diffraction pattern.

It should then be checked whether the corresponding lattice represents a sub- or a superlattice of the structure. An increase of the width of reflections as a function of increasing $|\mathbf{H}|$ indicates strained clusters of this sub- or superlattice.

(4) The next step is to search for extinction rules for the diffuse scattering. The simplest is the lack of low-angle scattering, which has already been mentioned above. Since diffuse scattering is generally given by equation (4.2.3.23*b*),

$$I_{\rm D}(\mathbf{H}) = \langle |F(\mathbf{H})|^2 \rangle - |\langle F(\mathbf{H}) \rangle|^2 = \sum_\mu p_\mu |F_\mu(\mathbf{H})|^2 - \Big| \sum_\mu p_\mu F_\mu(\mathbf{H}) \Big|^2,$$

it may be concluded that this condition is fulfilled in cases where all structural elements participating in disorder differ by translations only (stacking faults, antiphase domains *etc.*). They add phase factors to the various structure factors, which may become $n2\pi$ (n = integer) for specific values of the reciprocal vector $\mathbf{H}$. If all p_μ are equivalent by symmetry

$$p \sum_\mu |F_\mu(\mathbf{H})|^2 - \left[p \sum_\mu F_\mu(\mathbf{H}) \right] \left[p \sum_\mu F_\mu^+(\mathbf{H}) \right] = 0.$$

Other possibilities for vanishing diffuse scattering may be derived in a similar manner for special reflections if glide operations are responsible for disorder. Since we are concerned with disordered structures, these glide operations need not necessarily be a symmetry operation of the lattice. It should be pointed out, however, that all these extinction rules of diffuse scattering are a kind of 'anti'-extinction rule, because they are valid for reflections having maximum intensity for the sharp reflections unless the structure factor itself vanishes.

(5) Furthermore, it is important to plot the integrated intensities of sharp and diffuse scattering as a function of the reciprocal coordinates, at least in a semiquantitative way. If the ratio of integrated intensities remains constant in the statistical sense, we are predominantly concerned with a density phenomenon. It should be pointed out, however, that a particle-size effect of domains behaves like a density phenomenon (the density changes at the boundary!).

If the ratio of 'diffuse' to 'sharp' intensities increases with diffraction angle, we have to take into account atomic displacements. A careful study of this ratio yields very important information on the number of displaced atoms. The result has to be discussed separately for domain structures if the displacements are equal in the subcells of a single domain but different for the various domains. In the case of two domains with displacements of all atoms, the integrated intensities of sharp and diffuse reflections become statistically equal for large $|\mathbf{H}|$. Other rules may be derived from statistical considerations.

(6) The next step of a semiquantitative interpretation is to check the intensity distribution of diffuse reflections in reciprocal space. In general this modulation is simpler than that of the sharp reflections. Hence it is frequently possible to start a structure determination with diffuse scattering. This method is extremely helpful for one- and two-dimensional disorder where partial structure determinations yield valuable information, even for the evaluation of the average structure.

(7) In cases where no sub- or superlattice belonging to the diffuse scattering can be determined, a careful check of integrated intensities in the neighbourhood of Bragg peaks should again be performed. If systematic absences are found, the disorder is most probably restricted to specific lattice sites which may also be found in the average structure. The accuracy, however, is much lower here. If no such effects correlated with the average structure are observed, the disorder problem is related to a distribution of molecules or clusters with a structure differing from the average structure. As pointed out in Section 4.2.3.1, the problem of the representative structure(s) of the molecule(s) or the cluster(s) should be solved. Furthermore, their distribution function(s) is (are) needed. In this particular case, it is very useful to start with a study of diffuse intensity at low diffraction angles in order to acquire information about density effects. Despite the contribution to sharp reflections, one should remember that the level of information derived from the average structure may be very low (*e.g.* small displacements, low concentrations *etc.*).

(8) A Patterson picture – or strictly speaking a difference Patterson ($|\Delta F|^2$ Fourier synthesis) – may be very useful in this case. This method is promising in the case of disorder in molecular structures where the molecules concerned are at least partly known. Hence the interpretation of the difference Patterson may start with some internal molecular distances. Nonmolecular structures show some distances of the average structure. Consequently, a study of the important distances will yield information on displacements or replacements in the average structure. For a detailed study of this matter the reader is referred to the literature (Schwartz & Cohen, 1977).

Although it is highly improbable that exactly the same diffraction picture will be found, the use of an atlas of optical transforms (Wooster, 1962; Harburn *et al.*, 1975; Welberry & Withers, 1987) may be helpful at the beginning of any study of

diffuse scattering. Alternatively, computer simulations may be helpful, as discussed in Section 4.2.7. The most important step is the separation of the distribution function from the molecular scattering. Since this information may be derived from a careful comparison of low-angle diffraction with the remaining sharp reflections, this task is not too difficult. If the influence of the distribution function is unknown, the reader is strongly advised to disregard the immediate neighbourhood of Bragg peaks in the first step of the interpretation. Obviously information may be lost in this way but, as has been shown in the past, much confusion caused by an attempt to interpret the scattering near the Bragg peaks with specific structural properties of a cluster or molecular model is avoided. The inclusion of this part of diffuse scattering can be made after a complete interpretation of the change of the influence of the distribution function on diffraction in the wide-angle region.

4.2.5. Quantitative interpretation

4.2.5.1. Introduction

In these sections, quantitative interpretations of the elastic part of X-ray and neutron diffuse scattering are outlined. Although similar relations are valid for the magnetic scattering of neutrons, this particular topic is excluded. Obviously, all disorder phenomena are strongly temperature-dependent if thermal equilibrium is reached. Consequently, the interpretation of diffuse scattering should include a statistical thermodynamical treatment. Unfortunately, no quantitative theory for the interpretation of structural phenomena is so far available: all quantitative solutions introduce formal order parameters such as correlation functions or distributions of defects. At low temperatures (*i.e.* with a low concentration of defects) the distribution function plays the dominant role in diffuse scattering. With increasing temperature the number of defects increases with corresponding strong interactions between them. Therefore, correlations become increasingly important, and phase transformations of first or higher order may occur which need a separate theoretical treatment. In many cases, large fluctuations of structural properties occur that are closely related to the dynamical properties of the crystal. Theoretical approximations are possible, but their presentation is far beyond the scope of this article. Hence we restrict ourselves to formal parameters in the following.

Point defects or limited structural units, such as molecules, clusters of finite size *etc.*, may only be observed in diffraction if there is a sufficiently large number of defects. This statement is no longer true in high-resolution electron diffraction, where single defects may be observed either by diffraction or by optical imaging if their contrast is high enough. Hence electron microscopy and diffraction are valuable methods in the interpretation of disorder phenomena.

The arrangement of a finite assembly of structural defects is described by its structure and its three-dimensional (3D) distribution function. Structures with a strict 1D periodicity (chain-like structures) need a 2D distribution function, while for structures with a 2D periodicity (layers) a 1D distribution function is sufficient. Since the distribution function is the dominant factor in statistics with correlations between defects, we define the dimensionality of disorder as that of the corresponding distribution function. This definition is more effective in diffraction problems because the dimension of the disorder problem determines the dimension of the diffuse scattering: 1D diffuse streaks, 2D diffuse layers or a general 3D diffuse scattering.

Strictly speaking, completely random distributions cannot be realized, as shown in Section 4.2.3. They occur approximately if the following conditions are satisfied:

(1) The average volume of all defects including their surrounding strain fields NcV_d (where N is the number of unit cells, c is the concentration of defects and V_d is the volume of the defect with $V_d > V_c$, V_c being the volume of the unit cell) is small in comparison with the total volume NV_c of the crystal, or $V_c \gg cV_d$.

(2) Interactions between the defects are negligible. These conditions, however, are valid in very rare cases only, *i.e.* where small concentrations and vanishing strain fields are present. Remarkable exceptions from this rule are real point defects without interactions, such as isotope distribution (which can be studied by neutron diffraction) or the system AuAg at high temperature.

As already mentioned, disorder phenomena may be observed in thermal equilibrium. Two completely different cases have to be considered:

(1) The concentration of defects is given by the chemical composition, *i.e.* impurities in a closed system.

(2) The number of defects increases with temperature and also depends on pressure or other parameters, *i.e.* interstitials, voids, static displacements of atoms, stacking faults, dislocations *etc.*

In many cases, the defects do not occur in thermal equilibrium. Nevertheless, their diffuse scattering is temperature-dependent because of the anomalous thermal movements at the boundary of the defect. Hence the observation of a temperature-dependent behaviour of diffuse scattering cannot be taken as a definite criterion of thermal equilibrium without further careful interpretation.

Ordering of defects may take place in a very anisotropic manner. This is demonstrated by the huge number of examples of 1D disorder. As shown by Jagodzinski (1963), this type of disorder cannot occur in thermal equilibrium for the infinite crystal. This type of disorder is generally formed during crystal growth or mechanical deformation. Similar arguments may be applied to 2D disorder. This is a further reason why the Ising model can hardly ever be used to obtain interaction energies of structural defects. From these remarks it becomes clear that order parameters are formal parameters without strict thermodynamical meaning.

The following section is organized as follows: first we discuss the simple case of 1D disorder where reliable solutions of the diffraction problem are available. Intensity calculations for diffuse scattering from 2D disorder by chain-like structures follow. Finally, the 3D case is treated, where formal solutions of the diffraction problem have been tried and applied successfully to metallic systems to some extent. A short concluding section concerns the special phenomenon of orientational disorder.

4.2.5.2. Layered structures: one-dimensional disorder

As has been pointed out above, it is often useful to start the interpretation of diffuse scattering by checking the diffraction pattern with respect to the dimensionality of the disorder concerned. Since each disordered direction in the crystal demands a violation of the corresponding Laue condition, this question may easily be answered by looking at the diffuse scattering. Diffuse streaks in reciprocal space are due to a one-dimensional violation of the Laue conditions, and will be called one-dimensional disorder. This kind of order is typical for layer structures, but it is frequently observed in cases where several sequences of layers do not differ in the interactions of next-nearest neighbours. Typical examples are structures which may be described in terms of close packing, *e.g.* hexagonal and cubic close packing.

For a quantitative interpretation of diffuse streaks we need one-dimensional correlation functions, which may be determined uniquely if a single independent correlation function is active. According to equation (4.2.3.50), Fourier transformation yields the information required. In all other cases, a specific model has to be suggested for a full interpretation of diffuse streaks. It is worth noting that disorder parameters can be defined uniquely

only if the diffraction pattern allows for a differentiation between long-range and short-range order. This question can be answered at least partly by studying the line width of sharp reflections at very good resolution. Since integrated intensities of sharp reflections have to be separated from the diffuse scattering, this question is of outstanding importance in most cases. Inclusion of diffuse parts in the diffraction pattern during intensity integration of sharp reflections may lead to serious errors in the interpretation of the average structure.

The existence of diffuse streaks in more than one direction of reciprocal space means that the diffraction problem is no longer one-dimensional. Sometimes the problem may be treated independently if the streaks are sharp and no interference effects are observed in the diffraction pattern in areas where the diffuse streaks do overlap. In all other cases, there are correlations between the various directions of one-dimensional disorder which can be determined with the aid of a model covering more than one of the pertinent directions of disorder.

Before starting the discussion of the quantitative solution of the one-dimensional problem, some remarks should be made about the usefulness of quantitative disorder parameters. It is well known from statistical thermodynamics that a one-dimensional system cannot show long-range order above $T = 0$ K. Obviously, this statement is in contradiction with many experimental observations of long-range order even in layer structures. The reason for this behaviour is given by the following arguments, which are valid for any structure. Let us assume a structure with strong interactions at least in two directions. From the theoretical treatment of the two-dimensional Ising model it is known that such a system shows long-range order below a critical temperature T_c. This statement is true even if the layer is finite, although the strict thermodynamic behaviour is not really critical in the thermodynamical sense. A three-dimensional crystal can be constructed by adding layer after layer. Since each layer has a typical two-dimensional free energy, the full statistics of the three-dimensional crystal may be calculated by introducing a specific free energy for the various stackings of layers. Obviously, this additional energy also has to include terms describing potential and entropic energies. They may be formally developed into contributions of next, next-but-one *etc.* nearest neighbours. The contribution to entropy must include configurational and vibrational parts, which are strongly coupled. As long as the layers are finite, there is a finite probability of a fault in the stacking sequence of layers which approaches zero with increasing extension of the layers. Consequently, the free energy of a change in the favourite stacking sequence becomes infinite quadratically with the size of the layer. Therefore, the crystal should be either completely ordered or disordered; the latter case can only be realized if the free energies of one or more stacking sequences are exactly equal (this is very rare but is possible over a small temperature range during phase transformations). An additional positive entropy associated with a deviation from the periodic stacking sequence may lead to a kind of competition between entropy and potential energy, in such a way that periodic sequences of faults result. This situation occurs in the transition range of two structures differing only in their stacking sequence. On the other hand, one must assume that defects in the stacking sequence may occur if the size of the layers is small. This situation occurs during crystal growth, but one should remember that the number of stacking defects should decrease with increasing size of the growing crystal. Apparently, this rearrangement of layers may be suppressed as a consequence of relaxation effects. The growth process itself may influence the propagation of stacking defects and, consequently, the determination of stacking-fault probabilities, with the aim of interpreting the chemical bonding, seems to be irrelevant in most cases.

The quantitative solution of the diffraction problem of one-dimensional disorder follows a method similar to the Ising model. As long as next-nearest neighbours alone are considered, the solution is very simple if only two possibilities for the structure factors are to be taken into account. Introducing the probability of equal pairs 1 and 2, α, one arrives at the known solution for the *a priori* probability p_μ and *a posteriori* probabilities $p_{\mu\mu'}(\mathbf{m})$, respectively. In the one-dimensional Ising model with two spins and the interaction energies $(U \mp \Delta U)/k_B T$, defining the pair probability $[\alpha = p_{11}(\mathbf{1})]$ as

$$\alpha = \frac{\exp\{\pm \Delta U/k_B T\}}{[\exp\{+\Delta U/k_B T\} + \exp\{-\Delta U/k_B T\}]},$$

the full symmetry is $p_1 = p_2 = \frac{1}{2}$ and $p_{11}(\mathbf{m}) = p_{22}(\mathbf{m})$.

Consequently

$$p_{12}(\mathbf{m}) = p_{22}(\mathbf{m}) = 1 - p_{11}(\mathbf{m}).$$

The scattered intensity is given by

$$I(\mathbf{H}) = L(h,k) \sum_{\mathbf{m}} \langle FF_m^+ \rangle (N - |m|) \exp\{-2\pi i m l\}, \qquad (4.2.5.1)$$

where $\mathbf{m} = m\mathbf{c}$, N is the number of unit cells in the $\mathbf{c}$ direction and $\langle FF^+ \rangle$ depends on λ_1, λ_2, which are the eigenvalues of the matrix

$$\begin{pmatrix} \alpha & 1-\alpha \\ 1-\alpha & \alpha \end{pmatrix}.$$

From the characteristic equation

$$\lambda^2 - 2\alpha\lambda - 1 + 2\alpha = 0 \qquad (4.2.5.2)$$

one has

$$\lambda_1 = 1; \quad \lambda_2 = 2\alpha - 1. \qquad (4.2.5.2a)$$

λ_1 describes a sharp Bragg reflection (from the average structure) which need not be calculated. Its intensity is simply proportional to $\langle F(\mathbf{H}) \rangle$. The second characteristic value yields a diffuse reflection in the same position if the sign is positive ($\alpha > 0.5$) and in a position displaced by $\frac{1}{2}$ in reciprocal space if the sign is negative ($\alpha < 0.5$). Because of the symmetry conditions only $p_{11}(\mathbf{m})$ is needed; it may be determined with the aid of the boundary conditions

$$p_{11}(\mathbf{0}) = 1, \quad p_{11}(\mathbf{1}) = \alpha,$$

and the general relation

$$p_{\mu\mu'}(\mathbf{m}) = c'_{\mu\mu'} \lambda_1^m + c''_{\mu\mu'} \lambda_2^m.$$

The final solution of our problem yields simply

$$p_{11}(\mathbf{m}) = \tfrac{1}{2} + \tfrac{1}{2}\lambda_2^m = p_{22}(\mathbf{m}),$$
$$p_{12}(\mathbf{m}) = \tfrac{1}{2} - \tfrac{1}{2}\lambda_2^m = p_{21}(\mathbf{m}).$$

The calculation of the scattered intensity is now performed with the general formula

$$I(\mathbf{H}) = L(h,k) \sum_m \sum_{\mu,\mu'} p_\mu p_{\mu\mu'}(\mathbf{m}) F_\mu F_{\mu'}^+ (N - |m|) \exp\{-2\pi i m l\}. \qquad (4.2.5.3)$$

Evaluation of this expression yields

$$I(\mathbf{H}) = L(h,k) \sum_m (N - |m|) \exp\{-2\pi i m l\} \times [|\tfrac{1}{2}(F_1 + F_2)|^2 \lambda_1^m + |\tfrac{1}{2}(F_1 - F_2)|^2 \lambda_2^m]. \qquad (4.2.5.4)$$

Since the characteristic solutions of the problem are real,

$$I(\mathbf{H}) = L(\mathbf{G})|(F_1 + F_2)/2|^2 + L(h,k)|(F_1 - F_2)/2|^2 \times \frac{1 - |\lambda_2|^2}{1 - 2\lambda_2 \cos 2\pi l + |\lambda_2|^2}. \quad (4.2.5.5)$$

The particle-size effect has been neglected in (4.2.5.5). This result confirms the fact mentioned above that the sharp Bragg peaks are determined by the averaged structure factor and the diffuse ones by its mean-square deviation.

For the following reason there are no examples of quantitative applications: two different structures generally have different lattice constants, so the original assumption of an undisturbed lattice geometry is not valid. The only case known to the authors is the typical lamellar structure of plagioclases reported by Jagodzinski & Korekawa (1965). The authors interpret the well known 'Schiller effect' as a consequence of optical diffraction. Hence, the size of the lamellae is of the order of 2000 Å. This long-period superstructure cannot be explained in terms of next-nearest-neighbour interactions. In principle, however, the diffraction effects are similar: instead of the diffuse peak as described by the second term in equation (4.2.5.5), satellites of first and second order *etc.* accompanying the Bragg peaks are observed. The study of this phenomenon (Korekawa & Jagodzinski, 1967) has in the meantime found a quantitative interpretation (Burandt *et al.*, 1992; Kalning *et al.*, 1997).

Obviously, the symmetry relation used in the formulae discussed above is only valid if the structures described by the F_μ are related by symmetries such as translations, rotations or combinations of the two. The type of symmetry has an important influence on the diffraction pattern.

(1) *Translation parallel to the ordered layers*

If the translation vector between the two layers in question is such that $2\Delta\mathbf{r}$ is a translation vector parallel to the layer, there are two relevant structure factors:

$$F_1, F_2 = F_1 \exp\{2\pi i \mathbf{H} \cdot \Delta\mathbf{r}\}.$$

$\mathbf{H} \cdot \Delta\mathbf{r}$ may be either an integer or an integer + $\frac{1}{2}$. Since any integer may be neglected because of the translation symmetry parallel to the layer, we have $F_1 = F_2$ in the former case and $F_1 = -F_2$ in the latter. As a consequence, either the sharp reflections given in equation (4.2.5.4) vanish, or the same is true for the diffuse ones. Hence the reciprocal lattice may be described in terms of two kinds of lattice rows, sharp and diffuse, parallel to the reciprocal coordinate l.

Disorder of this type is observed very frequently. One of the first examples was wollastonite, $CaSiO_3$, studied by Jefferey (1953). Here the reflections with $k = 2n$ are sharp Bragg peaks without any diffuse scattering. Diffuse streaks parallel to (h00), however, are detected for $k = 2n + 1$. In the light of the preceding discussion, the translation vector is $\frac{1}{2}\mathbf{b}$ and the plane of ordered direction (the plane of intergrowth of the two domains) is (100). Hence the displacement is parallel to this plane. Since the intensity of the diffuse lines does not vary according to the structure factor involved, the disorder cannot be random. The maxima observed are approximately in the position of a superstructure generated by large domains without faults in the stacking sequence mutually displaced by $\frac{1}{2}\mathbf{b}$ (antiphase domains). This complicated ordering behaviour is typical for 1D order and may easily be explained by the above-mentioned fact that an infinitely extended interface between two domains causes an infinite unfavourable energy (Jagodzinski, 1964*b*, p. 188). Hence a growing crystal should become increasingly ordered. This consideration explains why the agreement between a 1D disorder theory and experiment is often so poor.

Examples where more than one single displacement vector occur are common. If these are symmetrically equivalent all symmetries have to be considered. The most important cases of displacements differing only by translation are the well known close-packed structures (see below). A very instructive example is the mineral maucherite (approximately Ni_4As_3). According to Jagodzinski & Laves (1947), the structure has the following disorder parameters: interface (001), displacement vectors [000], [$\frac{1}{2}$00], [0$\frac{1}{2}$0], [$\frac{1}{2}\frac{1}{2}$0]. From equation (4.2.5.5) we obtain

$$\langle F(\mathbf{H})\rangle = [1 + \exp\{\pi i h\} + \exp\{\pi i k\} + \exp\{\pi i (h + k)\}]/4.$$

Hence there are sharp reflections for h, k = even and diffuse ones otherwise. Further conclusions may be drawn from the average structure.

(2) *Translation perpendicular to the ordered layers*

If the translation is $\mathbf{c}/2$ the structure factors are

$$F_2 = F_1 \exp\{2\pi i l\},$$
$$F_1 = F_2 \text{ for } l = \text{even},$$
$$F_1 = -F_2 \text{ for } l = \text{odd}.$$

There are sharp ($l = 2n$) *and* diffuse ($l = 2n + 1$) reflections on all reciprocal-lattice rows discussed above.

Since the sharp and diffuse reflections occur on the same reciprocal line, the behaviour is completely different compared with the preceding case. In general, a component of any displacement vector perpendicular to the interface gives rise to a change in chemical composition, as shown in the next example: in a binary system consisting of A and B atoms with a tendency towards an alternating arrangement of A and B layers, any fault in the sequence $BABAB|BABAB|B$ increases the number of B atoms (or A atoms). In general, such kinds of defects will lead to an interface with a different lattice constant, at least in the direction perpendicular to the interface. Consequently, the exact displacement vectors of $\frac{1}{2}$, $\frac{1}{3}$, $\frac{1}{4}$ are rare. Since ordered structures should be realized in the 1D case, incommensurate superstructures will occur; these are very abundant during ordering processes. An interesting example has been reported and interpreted by Cowley (1976*a*,*b*), where the displacement vector has a translational period of $\frac{1}{4}$ perpendicular to the plane of intergrowth. Reflections 00l and 22l with l = 4n are sharp, all remaining reflections more or less diffuse. Since the maxima ($\bar{1}11$), ($\bar{1}33$) show a systematically different behaviour, there is also a displacement component parallel to the plane of intergrowth in question. A semiquantitative interpretation was given in his papers.

(3) *Rotations*

Layers related by a twofold rotation parallel to **c** may easily be discussed by simply considering their structure factors. Since the layers do not obey the twofold symmetry, their structure factors are generally different; unless they become equal accidentally there are sharp and diffuse reflections according to the values of $\langle F\rangle$ and ΔF, respectively. Obviously, $F_1 = F_2$ is valid only if $h = k = 0$; consequently there is just one reciprocal-lattice row free from diffuse scattering.

(4) *Asymmetric case*

In the asymmetric case, the symmetry conditions used above are no longer valid:

$$p_1 \neq p_2, \quad p_{12} \neq p_{21}, \quad p_{11} \neq p_{22}.$$

However, there is one condition which may be derived from the invariance of the numbers of pairs in the relevant and its opposite direction:

$$p_\mu p_{\mu\mu'}(\mathbf{m}) = p_{\mu'} p_{\mu'\mu}(-\mathbf{m}).$$

This equation does not require that $p_{\mu\mu'}(\mathbf{m})$ should be symmetric in $\mathbf{m}$. The calculation of characteristic values yields

$$\lambda_1 = 1, \qquad \lambda_2 = (\alpha_1 + \alpha_2) - 1. \quad (4.2.5.6)$$

The *a priori* probabilities are now different from $\frac{1}{2}$ and may be calculated by considering $p_{\mu\mu'}(\mathbf{m}) \rightarrow p_{\mu'}(\mathbf{m} \rightarrow \infty)$:

$$p_1 = \alpha_1/(\alpha_1 + \alpha_2); \quad p_2 = \alpha_2/(\alpha_1 + \alpha_2).$$

The intensity is given by an expression very similar to (4.2.5.5):

$$\begin{aligned} I(\mathbf{H}) = {} & L(\mathbf{G})|[\alpha_1/(\alpha_1 + \alpha_2)]F_1 + [\alpha_2/(\alpha_1 + \alpha_2)]F_2|^2 \\ & + L(h,k)|[\alpha_1/(\alpha_1 + \alpha_2)]F_1 - [\alpha_2/(\alpha_1 + \alpha_2)]F_2|^2 \\ & \times (1 - |\lambda_2|^2)/(1 - 2\lambda_2 \cos 2\pi l + |\lambda_2|^2). \end{aligned} \tag{4.2.5.7}$$

Again, there are sharp Bragg reflections and diffuse ones in the same positions or in a displaced position depending on the sign of λ_2.

From a discussion of the next-nearest-neighbour Ising model, one may conclude that a detailed study of the qualitative behaviour of sharp and diffuse reflections may give additional information on the symmetry of the layers involved.

In the case of translations between neighbouring layers not fulfilling the condition $\mathbf{h} \cdot \mathbf{r}$ = integer, where $\mathbf{r}$ is parallel to the layer, more than two structure factors have to be taken into account. If $n\mathbf{h} \cdot \mathbf{r}$ = integer, where n is the smallest integer fulfilling the said condition, n different structure factors have to be considered. The characteristic equation has formally to be derived with the aid of an $n \times n$ matrix containing internal symmetries, which may be avoided by adding the phase factors $\varepsilon = \exp\{2\pi i \mathbf{H} \cdot \mathbf{r}/n\}$, $\varepsilon^+ = \exp\{-2\pi i \mathbf{H} \cdot \mathbf{r}/n\}$ to the probability of pairs. The procedure is allowed if the displacements $\mathbf{r}$ and $-\mathbf{r}$ are admitted only for neighbouring layers. The matrix yielding the characteristic values may then be reduced to

$$\begin{pmatrix} \alpha_1\varepsilon & (1-\alpha_1)\varepsilon^+ \\ (1-\alpha_2)\varepsilon & \alpha_2\varepsilon^+ \end{pmatrix}$$

and yields the characteristic equation

$$\lambda^2 - \lambda(\alpha_1\varepsilon + \alpha_2\varepsilon^+) - 1 + \alpha_1 + \alpha_2 = 0. \tag{4.2.5.8}$$

Equation (4.2.5.8) gives sharp Bragg reflections for $\mathbf{H} \cdot \mathbf{r}/n$ = integer; the remaining diffuse reflections are displaced according to the phase of the complex characteristic value. Equation (4.2.5.8) has been used in many cases. Qualitative examples are the mixed-layer structures published by Hendricks & Teller (1942). An example of a four-layer-type structure is treated by Dubernat & Pezerat (1974). A first quantitative treatment with good agreement between theory and experimental powder diffraction data has been given by Dorner & Jagodzinski (1972) for the binary system TiO_2–SnO_2. In the range of the so-called spinodal decomposition, the chemical compositions of the two domains and the average lengths of the two types of domains could be determined. Another quantitative application was reported by Jagodzinski & Hellner (1956) for the transformation of $RhSn_2$ into a very complicated mixed-layer type. A good agreement of measured and calculated diffuse scattering (with asymmetric line profiles and displacement of maxima) could be found over a wide angular range of single-crystal diffraction.

4.2.5.2.1. Stacking disorder in close-packed structures

From an historical point of view, stacking disorder in close-packed systems is most important. The three relevant positions of ordered layers are represented by the atomic coordinates $|0,0|$, $|\frac{1}{3},\frac{2}{3}|$, $|\frac{2}{3},\frac{1}{3}|$ in the hexagonal setting of the unit cell, or simply by the figures 1, 2, 3 in the same sequence. Structure factors F_1, F_2, F_3 refer to the corresponding positions of the same layer:

$$F_2 = F_1 \exp\{2\pi i(h-k)/3\},$$
$$F_3 = F_1 \exp\{-2\pi i(h-k)/3\},$$

hence

$$F_1 = F_2 = F_3 \quad \text{if } h - k \equiv 0 \pmod 3.$$

According to the above discussion, the indices 1, 2, 3 define the reciprocal-lattice rows exhibiting sharp reflections only, as long as the distances between the layers are exactly equal. The symmetry conditions caused by the translation are normally

$$p_1 = p_2 = p_3, \qquad p_{11} = p_{22} = p_{33},$$
$$p_{12} = p_{23} = p_{31}, \quad p_{13} = p_{21} = p_{32}.$$

For the case of close packing of spheres and some other problems any configuration of $\mathbf{m}$ layers determining the *a posteriori* probability $p_{\mu\mu'}(\mathbf{m})$, $\mu = \mu'$, has a symmetrical counterpart where μ is replaced by $\mu' + 1$ (if $\mu' = 3$, $\mu' + 1 = 1$).

In this particular case, $p_{12}(\mathbf{m}) = p_{13}(\mathbf{m})$ and equivalent relations generated by translation.

Nearest-neighbour interactions do not lead to an ordered structure if the principle of close packing is obeyed (no pairs are in equal positions) (Hendricks & Teller, 1942; Wilson, 1942). Extension of the interactions to next-but-one or more neighbours may be carried out by introducing the method of matrix multiplication developed by Kakinoki & Komura (1954, 1965) or the method of overlapping clusters (Jagodzinski, 1954). The latter procedure is outlined in the case of interactions between four layers. A given set of three layers may occur in the following 12 combinations:

$$123, 231, 312; \quad 132, 213, 321;$$
$$121, 232, 313; \quad 131, 212, 323.$$

Since three of them are equivalent by translation, only four representatives have to be introduced:

$$123; \quad 132; \quad 121; \quad 131.$$

In the following, the new indices 1, 2, 3, 4 are used for these four representatives for the sake of simplicity.

In order to construct the statistics layer by layer, the next layer must belong to a triplet starting with the same two symbols with which the preceding one ended, *e.g.* 123 can only be followed by 231 or 232. In a similar way, 132 can only be followed by 321 or 323. Since both cases are symmetrically equivalent, the probabilities α_1 and $1 - \alpha_1$ are introduced. In a similar way, 121 may be followed by 212 or 213 *etc.* For these two groups the probabilities α_2 and $1 - \alpha_2$ are defined. The different translations of groups are considered by introducing the phase factors as described above. Hence the matrix for the characteristic equation may be set up as follows. As a representative cluster of each group the one having the number 1 at the centre is chosen, *e.g.* 312 is the representative for the group 123, 231, 312; in a similar way 213, 212 and 313 are the remaining representatives. Since this arrangement of three layers is equivalent by translation, it may be assumed that the structure of the central layer is not influenced by the statistics to a first approximation. The same arguments hold for the remaining three groups. On the other hand, the groups 312 and 213 are equivalent by rotation only. Consequently, their structure factors may differ if the influence of the two neighbours has to be taken into account. A different situation exists for the groups 212 and 313, which are correlated by a centre of symmetry, which causes different corresponding structure factors. It should be pointed out, however, that the structure factor is invariant as long as there is no influence of neighbouring layers on the structure of the central layer. The latter is often observed in close-packed metal structures or in compounds like

ZnS, SiC and others. For the calculation of intensities $p_\mu p_{\mu\mu'}$ and $F_\mu F^+_{\mu'}$ are needed.

According to the following scheme of sequences, any sequence of pairs is correlated with the same phase factor for FF^+ due to translation if both members of the pair belong to the same group. Consequently, the phase factor may be attached to the sequence probability such that FF^+ remains unchanged and the group may be treated as a single element in the statistics. In this way, the reduced matrix for the solution of the characteristic equation is given by

F_μ	$F^+_{\mu'}$ (1) 312, 123(ε^+), 231(ε)	(2) 212, 323(ε^+), 131(ε)	(3) 213, 321(ε^+), 132(ε)	(4) 313, 121(ε^+), 232(ε)
(1) 312, 123(ε), 231(ε^+)	$\alpha_1\varepsilon^+$	0	0	$(1-\alpha_1)\varepsilon^+$
(2) 212, 323(ε), 131(ε^+)	$(1-\alpha_2)\varepsilon^+$	0	0	$\alpha_2\varepsilon^+$
(3) 213, 321(ε), 132(ε^+)	0	$(1-\alpha_2)\varepsilon$	$\alpha_1\varepsilon$	0
(4) 313, 121(ε), 232(ε^+)	0	$\alpha_2\varepsilon$	$(1-\alpha_2)\varepsilon$	0

It should be pointed out that clusters 1 and 3 describe a cubic arrangement of three layers in the case of simple close packing, while clusters 2 and 4 represent the hexagonal close packing. There may be a small change in the lattice constant c perpendicular to the layers. Additional phase factors then have to be introduced in the matrix for the characteristic equation and a recalculation of the constants is necessary. As a consequence, the reciprocal-lattice rows $(h-k)\equiv 0\,(\mathrm{mod}\ 3)$ become diffuse if $l\neq 0$ and the diffuseness increases with l. Similar behaviour results for the remaining reciprocal-lattice rows.

There are three solutions of the diffraction problem:

(1) If $h - k = 0$ (mod 3), $\varepsilon = +1$, there are two quadratic equations:

$$\begin{aligned}\lambda^2-(\alpha_1+\alpha_2)\lambda-1+\alpha_1+\alpha_2&=0,\\ \lambda^2-(\alpha_1-\alpha_2)\lambda+1-\alpha_1-\alpha_2&=0,\end{aligned}\qquad(4.2.5.9)$$

with solutions

$$\lambda_1=1,\qquad \lambda_2=\alpha_1+\alpha_2-1,$$
$$\lambda_{3/4}=\frac{\alpha_1-\alpha_2}{2}\pm\left[\frac{(\alpha_1-\alpha_2)^2}{4}-1+\alpha_1-\alpha_2\right]^{1/2}.\qquad(4.2.5.10)$$

λ_1 and λ_2 are identical with the solution of the asymmetric case of two kinds of layers [*cf.* equation (4.2.5.6)]. They yield sharp reflections for l = integer and diffuse ones in a position determined by the sequence probabilities α_1 and α_2 (with a position of either l = integer or $l = \frac{1}{2}$ + integer, respectively). The remaining two characteristic values may be given in the form $\lambda = |\lambda|\exp\{2\pi i\varphi\}$, where φ determines the position of the reflection. If the structure factors of the layers are independent of the cluster, λ_2, λ_3 and λ_4 become irrelevant because of the new identity of the F's and there is no diffuse scattering. Weak diffuse intensities on the lattice rows $h - k = 0$ (mod 3) may be explained in terms of this influence.

(2) The remaining two solutions for $\varepsilon = \exp\{\pm 2\pi i(h-k)/3\}$ are equivalent and result in the same characteristic values. They have been discussed explicitly in the literature; the reader is referred to the papers of Jagodzinski (1949*a*,*b*,*c*, 1954).

In order to calculate the intensities, one has to reconsider the symmetry of the clusters, which is different to the symmetry of the layers. Fortunately, a threefold rotation axis is invariant against the translations, but this is not true for the remaining symmetry operations in the layer if there are any more. Since we have two pairs of inequivalent clusters, namely 312, 213 and 212, 313, there are only two different *a priori* probabilities $p_1 = p_3$ and $p_2 = p_4 = \frac{1}{2}(1 - 2p_1)$.

The symmetry conditions of the new clusters may be determined using 'probability trees' as described by Wilson (1942) and Jagodzinski (1949*b*). For example: $p_{11} = p_{33}$, $p_{22} = p_{44}$, $p_{13} = p_{31}$, $p_{24} = p_{42}$ *etc*.

The final solution of the diffraction problem results in the following general intensity formula:

$$\begin{aligned}I(\mathbf{H}) = L(h,k)N\sum_\nu\{&A_\nu(\mathbf{H})(1-|\lambda_\nu|^2)\\ &\times[1-2|\lambda_\nu|\cos 2\pi(l-\varphi_\nu)+|\lambda_\nu|^2]^{-1}\\ &-2B_\nu(\mathbf{H})|\lambda_\nu|\sin 2\pi(l-\varphi_\nu)\\ &\times[1-2|\lambda_\nu|\cos 2\pi(l-\varphi_\nu)+|\lambda_\nu|^2]^{-1}\}.\end{aligned}\qquad(4.2.5.11)$$

Here A_ν and B_ν represent the real and imaginary part of the constants to be calculated with the aid of the boundary conditions of the problem. The first term in equation (4.2.5.11) determines the symmetrical part of a diffuse reflection with respect to the maximum and is completely responsible for the integrated intensity. The second term causes an antisymmetrical contribution to intensity profiles but does not influence the integrated intensities. These general relations enable a semiquantitative interpretation of the sharp and diffuse scattering in any case, without performing the time-consuming calculations of the constants, which may only be done in more complicated disorder problems with the aid of a computer program evaluating the boundary conditions of the problem.

This can be carried out with the aid of the characteristic values and a linear system of equations (Jagodzinski, 1949*a*,*b*,*c*), or with the aid of matrix formalism (Kakinoki & Komura, 1954; Takaki & Sakurai, 1976). As long as only the line profiles and positions of the reflections are required, these quantities may be determined experimentally and fitted to characteristic values of a matrix. The size of this matrix is given by the number of sharp and diffuse maxima observed, while $|\lambda_\nu|$ and $\exp\{2\pi i\varphi_\nu\}$ may be found by evaluating the line width and the position of diffuse reflections. Once this matrix has been found, a semiquantitative model of the disorder problem can be given. If a system of sharp reflections is available, the averaged structure can be solved as described in Section 4.2.3.2. The determination of the constants of the diffraction problem is greatly facilitated by considering the intensity modulation of diffuse scattering, which enables a phase determination of structure factors to be made under certain conditions.

The theory of close-packed structures with three equivalent translation vectors has been applied very frequently, even to

systems that do not obey the principle of close-packing. The first quantitative explanation was published by Halla *et al.* (1953). It was shown there that single crystals of $C_{18}H_{24}$ from the same synthesis may have a completely different degree of order. This was true even within the same crystal. Similar results were found for C, Si, CdI_2, CdS_2, mica and many other compounds. Quantitative treatments are less abundant [*e.g.* CdI_2 (Martorana *et al.*, 1986); MX_3 structures (Conradi & Müller, 1986)]. Special attention has been paid to the quantitative study of polytypic phase transformations in order to gain information about the thermodynamical stability or the mechanism of layer displacements, *e.g.* Co (Edwards & Lipson, 1942; Frey & Boysen, 1981), SiC (Jagodzinski, 1972; Pandey *et al.*, 1980*a*,*b*,*c*), ZnS (Müller, 1952; Mardix & Steinberger, 1970; Frey *et al.*, 1986) and others.

Certain laws may be derived for the reduced integrated intensities of diffuse reflections. 'Reduction' in this context means a division of the diffuse scattering along l by the structure factor, or the difference structure factor if $\langle F\rangle \neq 0$. This procedure is valuable if the number of stacking faults rather than a complete solution of the diffraction problem is required.

The discussion given above has been made under the assumption that the full symmetry of the layers is maintained in the statistics. Obviously, this is not necessarily true if external lower symmetries influence the disorder. An important example is the generation of stacking faults during plastic deformation. Problems of this kind need a complete reconsideration of symmetries. Furthermore, it should be pointed out that a treatment with the aid of an extended Ising model as described above is irrelevant in most cases. Simplified procedures describing the diffuse scattering of intrinsic, extrinsic, twin stacking faults and others have been described in the literature. Since their influence on *structure determination* can generally be neglected, the reader is referred to the literature for additional information.

A different approach to the analysis of planar disorder in close-packed structures is given by Varn *et al.* (2002). With simplifying assumptions, *e.g.* that spacings between identical defect-free layers are independent of local stacking arrangements, average correlations between them are extracted from experimental diffractograms *via* Fourier analysis. Spatial patterns of the layers are then constructed by a so-called epsilon machine, which reproduces the correlations with minimal states of the stacking process. The basic statistical description of the ensemble of spatial patterns produces the stacking distribution. With this technique, stacking sequences are generated which are compared with the correlation factors and the diffractograms. The authors report an improved matching of calculated and experimental data for ZnS.

4.2.5.3. Chain-like structures: two-dimensional disorder

In this section, disorder phenomena that are related to chain-like structural elements in crystals are considered. This topic includes the so-called '1D crystals', where translational symmetry (in direct space) exists in one direction only – crystals in which highly anisotropic binding forces are responsible for chain-like atomic groups, *e.g.* compounds that exhibit a well ordered 3D framework structure with tunnels in a unique direction in which atoms, ions or molecules are embedded. Examples are compounds with platinum, iodine or mercury chains, urea inclusion compounds with columnar structures (organic or inorganic), 1D ionic conductors, polymers *etc.* Diffuse-scattering studies of 1D conductors have been carried out in connection with investigations of stability/instability problems, incommensurate structures, phase transitions, dynamic precursor effects *etc.* These areas are not treated here. For general reading about diffuse scattering in connection with these topics see, *e.g.*, Comes & Shirane (1979) and references therein. Also excluded are specific problems related to polymers or liquid crystals (mesophases) (see Chapter 4.4) and magnetic structures with chain-like spin arrangements.

Trivial diffuse scattering occurs as 1D Bragg scattering (diffuse layers) by internally ordered chains. Diffuse phenomena in reciprocal space are due to 'longitudinal' disordering within the chains (along the unique direction) as well as to 'transverse' correlations between different chains over a restricted volume. Only static aspects are considered; diffuse scattering resulting from collective excitations or diffusion-like phenomena which are of inelastic or quasielastic origin are not treated here.

4.2.5.3.1. Randomly distributed collinear chains

As found in any elementary textbook of diffraction, the simplest result of scattering by a chain with period c,

$$l(\mathbf{r}) = l(z) = \sum_{n_3} \delta(z - n_3 c), \tag{4.2.5.12}$$

is described by one of the Laue equations:

$$G(L) = |L(L)|^2 = \sin^2 \pi NL / \sin^2 \pi L, \tag{4.2.5.13}$$

which gives broadened profiles for small N. In the context of phase transitions the Ornstein–Zernike correlation function is frequently used, *i.e.* (4.2.5.13) is replaced by a Lorentzian:

$$1/[\xi^2 + 4\pi^2 (L - l)^2], \tag{4.2.5.14}$$

where ξ denotes the correlation length.

In the limiting case $N \rightarrow \infty$, (4.2.5.13) becomes

$$\sum_l \delta(L - l). \tag{4.2.5.15}$$

The scattering by a real chain $a(\mathbf{r})$ consisting of molecules with structure factor F_M is therefore determined by

$$F_M(\mathbf{H}) = \sum_j f_j \exp\{2\pi i(Hx_j + Ky_j + Lz_j)\}. \tag{4.2.5.16}$$

The Patterson function is

$$\begin{aligned} P(\mathbf{r}) = {} & (1/c) \int\int |F_0(H, K)|^2 \cos 2\pi(Hx + Ky)\, \mathrm{d}H\, \mathrm{d}K \\ & + (2/c) \sum_l \int\int |F_l|^2 \exp\{2\pi i(Hx + Ky)\} \\ & \times \exp\{-2\pi i l z\}\, \mathrm{d}H\, \mathrm{d}K, \end{aligned} \tag{4.2.5.17}$$

where the index l denotes the only relevant position $L = l$ (the subscript M is omitted).

The intensity is concentrated in diffuse layers perpendicular to $\mathbf{c}^*$ from which the structural information may be extracted. Projections are:

$$\int a(\mathbf{r})\, \mathrm{d}z = \int\int F_0(H, K) \exp\{2\pi i(Hx + Ky)\}\, \mathrm{d}H\, \mathrm{d}K, \tag{4.2.5.18}$$

$$\int\int a(\mathbf{r})\, \mathrm{d}x\, \mathrm{d}y = (2/c) \sum_l F_l(00l) \exp\{-2\pi i l z\}. \tag{4.2.5.19}$$

Obviously the z parameters can be determined by scanning along a meridian $(00L)$ through the diffuse sheets (*e.g.* by a diffractometer recording). Owing to intersection of the Ewald sphere with the set of planes, the meridian cannot be recorded on *one* photograph; successive equi-inclination photographs are necessary. Only in the case of large c spacings is the meridian well approximated in one photograph.

There are many examples where a tendency to cylindrical symmetry exists: chains with p-fold rotational or screw symmetry around the preferred direction or assemblies of chains (or domains) with a statistical orientational distribution around the texture axis. In this context, it should be mentioned that symmetry operations with rotational parts belonging to the 1D rod groups actually occur, *i.e.* not only $p = 2, 3, 4, 6$.

In all these cases a treatment in the frame of cylindrical coordinates is advantageous (see, *e.g.*, Vainshtein, 1966):

Direct space	Reciprocal space
$x = r\cos\psi$	$H = H_r\cos\Psi$
$y = r\sin\psi$	$K = H_r\sin\Psi$
$z = z$	$L = L$

$$a(r,\psi,z) = \int\int\int F(\mathbf{H})\exp\{-2\pi i[H_r r\cos(\psi-\Psi)+Lz]\} \times H_r\,\mathrm{d}H_r\,\mathrm{d}\Psi\,\mathrm{d}L, \quad (4.2.5.20)$$

$$F(\mathbf{H}) = \int\int\int a(r,\psi,z)\exp\{2\pi i[H_r r\cos(\psi-\Psi)+Lz]\} \times r\,\mathrm{d}r\,\mathrm{d}\psi\,\mathrm{d}z. \quad (4.2.5.21)$$

The integrals may be evaluated by the use of Bessel functions:

$$J_n(u) = \tfrac{1}{2}\pi i^n\int\exp\{i(u\cos\varphi + n\varphi)\}\,\mathrm{d}\varphi$$

($u = 2\pi r H_r$; $\varphi = \psi - \Psi$).

The 2D problem $a = a(r,\psi)$ is treated first; an extension to the general case $a(r,\psi,z)$ is easily made afterwards.

Along the theory of Fourier series one has

$$a(r,\psi) = \sum_n a_n(r)\exp\{in\psi\},$$
$$a_n(r) = \frac{1}{2\pi}\int a(r,\psi)\exp\{-in\psi\}\,\mathrm{d}\psi, \quad (4.2.5.22)$$

or with

$$\alpha_n = \frac{1}{2\pi}\int a(r,\psi)\cos(n\psi)\,\mathrm{d}\psi,$$
$$\beta_n = \frac{1}{2\pi}\int a(r,\psi)\sin(n\psi)\,\mathrm{d}\psi,$$
$$a_n(r) = |a_n(r)|\exp\{-i\psi_n(r)\},$$
$$|a_n(r)| = \sqrt{a_n^2+\beta_n^2},$$
$$\psi_n(r) = \arctan\,\beta_n/\alpha_n.$$

If contributions to anomalous scattering are neglected $a(r,\psi)$ is a real function:

$$a(r,\psi) = \sum_n |a_n(r)|\cos[n\psi - \psi_n(r)]. \quad (4.2.5.23)$$

Analogously, one has

$$F(H_r,\Psi) = \sum_n |F_n(H_r)|\exp\{in\Psi\}. \quad (4.2.5.24)$$

$F(H_r,\Psi)$ is a complex function; $F_n(H_r)$ are the Fourier coefficients that are to be evaluated from the $a_n(r)$:

$$F_n(H_r) = \frac{1}{2\pi}\int F(H_r,\Psi)\exp\{-in\Psi\}\,\mathrm{d}\Psi$$
$$= \exp\{in\pi/2\}\int a_n(r)J_n(2\pi r H_r)2\pi r\,\mathrm{d}r,$$
$$F(H_r,\Psi) = \sum_n \exp\{in[\Psi+(\pi/2)]\} \times \int a_n(r)J_n(2\pi r H_r)2\pi r\,\mathrm{d}r, \quad (4.2.5.25)$$

$$a(r,\psi) = \sum_n \exp\{in[\Psi-(\pi/2)]\} \times \int F_n(H_r)J_n(2\pi r H_r)\,2\pi H_r\,\mathrm{d}H_r. \quad (4.2.5.26)$$

The formulae may be used for calculation of the diffuse intensity distribution within a diffuse sheet, in particular when the chain molecule is projected along the unique axis [*cf.* equation (4.2.5.18)].

Special cases are:

(1) *Complete cylinder symmetry*

$$F(H_r) = 2\pi\int a(r)J_0(2\pi r H_r)r\,\mathrm{d}r \quad (4.2.5.27),$$
$$a(r) = 2\pi\int F(H_r)J_n(2\pi r H_r)H_r\,\mathrm{d}H_r. \quad (4.2.5.28)$$

(2) *p-fold symmetry of the projected molecule*, where $a(r,\psi) = a[r,\psi+(2\pi/p)]$

$$F_p(H_r,\Psi) = \sum_n \exp\{inp[\Psi+(\pi/2)]\} \times \int a_{np}(r)J_{np}(2\pi r H_r)2\pi r\,\mathrm{d}r, \quad (4.2.5.29)$$

$$a_p(r,\psi) = \sum_n |a_{np}(r)|\cos[np\psi - \psi_{np}(r)]. \quad (4.2.5.30)$$

Only Bessel functions $J_0, J_p, J_{2p}, \ldots$ occur. In most cases J_{2p} and higher orders may be neglected.

(3) *Vertical mirror planes*

Only cosine terms occur, *i.e.* all $\beta_n = 0$ or $\psi_n(r) = 0$.

The *general 3D expressions* valid for extended chains with period c [equation (4.2.5.12)] are found in an analogous way,

$$a(r,\psi,z) = a_{\mathrm{M}}(r,\psi,z) * l(z),$$

$$F(\mathbf{H}) = F_l(H_r,\Psi,L) = F_{\mathrm{M}}(\mathbf{H})L(L) = \int\int\int a_{\mathrm{M}}(r,\psi,z)\exp\{2\pi i\,[H_r r\cos(\psi-\Psi)+Lz]\} \times 2\pi r\,\mathrm{d}r\,\mathrm{d}\psi\,\mathrm{d}z. \quad (4.2.5.31)$$

Using a series expansion analogous to (4.2.5.23) and (4.2.5.24),

$$a_{nl}(r) = \frac{1}{2\pi}\int\int a_{\mathrm{M}}\exp\{-i(n\psi - 2\pi lz)\}\,\mathrm{d}\psi\,\mathrm{d}z, \quad (4.2.5.32)$$

$$F_{nl}(H_r) = \exp\{in\pi/2\}\int a_{nl}(r)J_n(2\pi H_r r)2\pi r\,\mathrm{d}r, \quad (4.2.5.33)$$

one has

$$F_l(\mathbf{H}) = \sum_n \exp\{in[\Psi+(\pi/2)]\}\int a_{nl}(r)J_n(2\pi H_r r)2\pi r\,\mathrm{d}r. \quad (4.2.5.34)$$

In practice the integrals are often replaced by discrete summation of j atoms at positions $r = r_j$, $\psi = \psi_j$, $z = z_j$ ($0 \le z_j < c$):

$$F_l(\mathbf{H}) = \sum_j\sum_n f_j J_n(2\pi H_r r_j)\exp\{-in\psi_j\} \times \exp\{2\pi ilz_j\}\exp\{in[\Psi+(\pi/2)]\} \quad (4.2.5.35)$$

or

$$F_l(\mathbf{H}) = \sum_n(\alpha_n + i\beta_n)\exp\{in\Psi\},$$

$$\alpha_n = \sum_j f_j J_n(2\pi H_r r_j)\cos\{n[(\pi/2)-\psi_j] + 2\pi lz_j\},$$
$$\beta_n = \sum_j f_j J_n(2\pi H_r r_j)\sin\{n[(\pi/2)-\psi_j] + 2\pi lz_j\}.$$

Intensity in the lth diffuse layer is given by

$$I_l = \sum_n\sum_{n'}[(\alpha_n\alpha_{n'} + \beta_n\beta_{n'}) + i(\alpha_{n'}\beta_n - \alpha_n\beta_{n'})] \times \exp\{i(n-n')\Psi\}. \quad (4.2.5.36)$$

(*a*) *Cylinder symmetry* (free rotating molecules around the chain axis or statistical averaging with respect to ψ over an assembly of chains). Only component F_{0l} occurs:

$$F_{0l}(H_r, L) = 2\pi\int\int\langle a_{\mathrm{M}}\rangle J_0(2\pi H_r r)\exp\{2\pi ilz\}r\,\mathrm{d}r\,\mathrm{d}z$$

or

$$F_{0l}(H_r, L) = \sum_j f_j J_0(2\pi H_r r_j) \exp\{2\pi i l z_j\}.$$

In particular, $F_{00}(H_r)$ determines the radial component of the molecule projected along z:

$$F_{00}(H_r) = \sum_j f_j J_0(2\pi H_r r_j).$$

(*b*) *p-fold symmetry* of a plane molecule (or projected molecule) as outlined previously: only components *np* instead of *n* occur. Bessel functions J_0 and J_p are sufficient in most cases.

(*c*) *Vertical mirror plane*: see above.

(*d*) *Horizontal mirror plane* (perpendicular to the chain): Exponentials $\exp\{2\pi i l z\}$ in equation (4.2.5.32) may be replaced by $\cos 2\pi l z$.

(*e*) *Twofold symmetry axis* perpendicular to the chain axis (at positions $\psi = 0,\ 2\pi/p, \ldots$). Exponentials $\exp\{-i(np\psi - 2\pi l z)\}$ in equation (4.2.5.32) are replaced by the corresponding cosine term $\cos(np\psi + 2\pi l z)$.

Formulae concerning the reverse method (Fourier synthesis) are not given here (see, *e.g.*, Vainshtein, 1966). There is usually no practical use for this in diffuse-scattering work because it is very difficult to separate out a single component F_{nl}. *Every* diffuse layer is affected by *all* components F_{nl}. There is a chance of doing so only if *one* diffuse layer corresponds predominantly to *one* Bessel function.

4.2.5.3.2. Disorder within randomly distributed collinear chains

Deviations from strict periodicities in the z direction within one chain may be due to loss of translational symmetry of the centres of the molecules along z and/or due to varying orientations of the molecules with respect to different axes, such as azimuthal misorientation, tilting with respect to the z axis or combinations of both types. As in 3D crystals, there may or may not exist 1D structures in an averaged sense.

(1) *General treatment*

All formulae given in this section are only special cases of a 3D treatment (see, *e.g.*, Guinier, 1963). The 1D lattice (4.2.5.12) is replaced by a distribution:

$$\begin{aligned} d(z) &= \sum_\nu \delta(z - z_\nu), \\ D(L) &= \sum_\nu \exp\{2\pi i L z_\nu\}, \\ F(\mathbf{H}) &= F_{\rm M}(\mathbf{H}) D(L). \end{aligned} \tag{4.2.5.37}$$

The Patterson function is given by

$$P(\mathbf{r}) = [a_{\rm M}(\mathbf{r}) * a_{\rm M}(-\mathbf{r})] * [d(z) * d(-z)]. \tag{4.2.5.38}$$

Because the autocorrelation function $w = d * d$ is centrosymmetric,

$$w(z) = N\delta(z) + \sum_\nu \sum_\mu \delta[z - (z_\nu - z_\mu)] + \sum_\nu \sum_\mu \delta[z + (z_\nu - z_\mu)], \tag{4.2.5.39}$$

the interference function $W(L)$ $(= |D(L)|^2)$ is given by

$$W(L) = N + 2 \sum_\nu \sum_\mu \cos 2\pi [L(z_\nu - z_\mu)], \tag{4.2.5.40}$$

$$I(\mathbf{H}) = |F_{\rm M}(\mathbf{H})|^2 W(L). \tag{4.2.5.41}$$

Sometimes, *e.g.* in the following example of orientational disorder, there is an order only within domains. As shown in Section 4.2.3, this may be treated by a box or shape function $b(z) = 1$ for $z \le z_N$ and 0 elsewhere.

$$\begin{aligned} d(z) &= d_\infty b(z), \\ a(\mathbf{r}) &= a_{\rm M}(\mathbf{r}) * [d_\infty b(z)], \\ F(\mathbf{H}) &= F_{\rm M}(\mathbf{H})[D_\infty * B(L)], \end{aligned} \tag{4.2.5.42}$$

with

$$\begin{aligned} b(z) * b(-z) &\leftrightarrow |B(L)|^2, \\ I &= |F_{\rm M}(\mathbf{H})|^2 |D_\infty * B(L)|^2. \end{aligned} \tag{4.2.5.43}$$

If the order is perfect within one domain one has $D_\infty(L) \simeq \sum \delta(L - l)$; $(D_\infty * B) = \sum D(L - l)$; *i.e.* each reflection is affected by the shape function.

(2) *Orientational disorder*

A misorientation of the chain molecules with respect to one another is taken into account by different structure factors $F_{\rm M}$.

$$I(\mathbf{H}) = \sum_\nu \sum_\mu F_\nu(\mathbf{H}) F_\mu(\mathbf{H})^+ \exp\{2\pi i L(z_\nu - z_\mu)\}. \tag{4.2.5.44}$$

A further discussion follows the same arguments outlined in Section 4.2.3. For example, a very simple result is found in the case of uncorrelated orientations. Averaging over all pairs $F_\nu F_\mu^+$ yields

$$I(\mathbf{H}) = N(\langle |F|^2 \rangle - \langle |F| \rangle^2) + \langle |F| \rangle^2 L(L), \tag{4.2.5.44a}$$

where

$$\begin{aligned} \langle |F| \rangle^2 &= 1/N^2 \langle F_\nu F_\mu^+ \rangle \\ &= \sum_\nu \alpha_\nu F_\nu(\mathbf{H}) \sum_\mu \alpha_\mu F_\mu^+(\mathbf{H}), \quad (\nu \ne \mu) \\ \langle |F|^2 \rangle &= 1/N \langle F_\nu F_\nu^+ \rangle = \sum_\nu \alpha_\nu |F_\nu(\mathbf{H})|^2. \end{aligned}$$

Besides the diffuse layer system, there is a diffuse background modulated by the $\mathbf{H}$ dependence of $[\langle |F(\mathbf{H})|^2 \rangle - \langle |F(\mathbf{H})| \rangle^2]$.

(3) *Longitudinal disorder*

In this context, the structure factor of a chain molecule is neglected. Irregular distances between the molecules within a chain occur owing to the shape of the molecules, intrachain interactions and/or interaction forces *via* a surrounding matrix. A general discussion is given by Guinier (1963). It is convenient to reformulate the discrete Patterson function, *i.e.* the correlation function (4.2.5.39),

$$\begin{aligned} w(z) = N\delta(z) &+ \sum_\nu \delta[z \pm (z_\nu - z_{\nu+1})] \\ &+ \sum_\nu \delta[z \pm (z_\nu - z_{\nu+2})] + \ldots \end{aligned} \tag{4.2.5.39a}$$

in terms of continuous functions $a_\mu(z)$ that describe the probability of finding the μth neighbour within an arbitrary distance,

$$\begin{aligned} w'(z) = w(z)/N = \delta(z) &+ a_1(z) + a_{-1}(z) + \ldots \\ &+ a_\mu(z) + a_{-\mu}(z) + \ldots \end{aligned} \tag{4.2.5.45}$$

$[\int a_\mu(z)\,{\rm d}z = 1,\ a_\mu(z) = a_{-\mu}(-z)]$.

There are two principal ways to define $a_\mu(z)$. The first is the case of a well defined one-dimensional lattice with positional fluctuations of the molecules around the lattice points, *i.e.* long-range order is retained: $a_\mu(z) = \mu c_0 + z_\mu$, where z_μ denotes the displacement of the μth molecule in the chain. Gaussian distributions are frequently used:

$$c' \exp\{-(z - \mu c_0)^2 / 2\Delta^2\},$$

where c' is a normalizing constant and Δ is the standard deviation. Fourier transformation of equation (4.2.5.45) gives the well known result

$$I_D \simeq (1 - \exp\{-L^2\Delta^2\}),$$

i.e. a monotonically increasing intensity with L (any modulation due to a molecular structure factor is neglected). This result is quite analogous to the treatment of the scattering of independently vibrating atoms. If (short-range) correlations exist between the molecules, the Gaussian distribution is replaced by a multivariate normal distribution where correlation coefficients κ^μ $(0 < \kappa < 1)$ between a molecule and its μth neighbour are incorporated. κ^μ is defined by the second moment: $\langle z_0 z_\mu \rangle / \Delta^2$.

$$a_\mu(z) = c'' \exp\{-(z - \mu c_0)^2 / 2\Delta^2(1 - \kappa^\mu)\}.$$

Obviously, the variance increases if the correlation diminishes and reaches an upper bound of twice the single-site variance. Fourier transformation gives an expression for the diffuse intensity (Welberry, 1985):

$$I_D(L) \simeq \exp\{-L^2\Delta^2\} \sum_j (-L^2\Delta^2)^j / j! \times (1 - \kappa^{2j})/(1 + \kappa^{2j} - 2\kappa^j \cos 2\pi L c_0). \quad (4.2.5.46)$$

For small Δ, terms with $j > 1$ are mostly neglected. The terms become increasingly important with higher values of L. On the other hand, κ^j becomes smaller with increasing j, each additional term in equation (4.2.5.46) becomes broader and, as a consequence, the diffuse planes in reciprocal space become broader with higher L.

In a different way – in the paracrystal method – the position of the second and subsequent molecules with respect to some reference zero point depends on the *actual* position of the predecessor. The variance of the position of the μth molecule relative to the first becomes unlimited. There is a continuous transition to a fluid-like behaviour of the chain molecules. This 1D paracrystal (these are sometimes called distortions of the second kind) is only a special case of the 3D paracrystal concept (see Hosemann & Bagchi, 1962; Wilke, 1983). Despite some difficulties with this concept (Brämer, 1975; Brämer & Ruland, 1976), it is widely used as a theoretical model for describing diffraction by highly distorted lattices. One essential development is to limit the size of a paracrystalline grain so that fluctuations never become too large (Hosemann, 1975).

If this concept is used for the 1D case, $a_\mu(z)$ is defined by convolution products of $a_1(z)$. For example, the probability of finding the next-nearest molecule is given by

$$a_2(z) = \int a_1(z')\, a_1(z - z')\, \mathrm{d}z' = a_1(z) * a_1(z)$$

and, generally,

$$a_\mu(z) = a_1(z) * a_1(z) * a_1(z) * \ldots * a_1(z)$$

(μ-fold convolution).

The mean distance between next-nearest neighbours is

$$\langle c \rangle = \int z' a_1(z')\, \mathrm{d}z'$$

and between neighbours of the μth order it is $\mu\langle c \rangle$. The average value of $a_\mu = 1/\langle c \rangle$, which is also the value of $w(z)$ for $z > z_k$, where the distribution function is completely smeared out. The general expression for the interference function $G(L)$ is

$$G(L) = 1 + \sum_\mu \{F^\mu + F^{+\mu}\} = \mathrm{Re}\{(1 + F)/(1 - F)\} \quad (4.2.5.47)$$

with $F(L) \leftrightarrow a_1(z)$, $F^\mu(L) \leftrightarrow a_\mu(z)$.

With $F = |F| \exp\{i\chi\}$ $(\chi = L\langle c \rangle)$, equation (4.2.5.47) is written

$$G(L) = [1 - |F(L)|^2]/[1 - 2|F(L)| \cos\chi + |F(L)|^2]. \quad (4.2.5.47a)$$

[Note the close similarity to the diffuse part of equation (4.2.5.5), which is valid for 1D disorder problems.]

This function has maxima of height $(1 + |F|)/(1 - |F|)$ and minima of height $(1 - |F|)/(1 + |F|)$ at positions lc^* and $(l + \frac{1}{2})c^*$, respectively. With decreasing $|F|$ the oscillations vanish; a critical L value (corresponding to z_k) may be defined by $G_{max}/G_{min} \lesssim 1.2$. Actual values depend strongly on $F(\mathbf{H})$.

The paracrystal method is substantiated by the choice $a_1(z)$, *i.e.* the disorder model. Again, a Gaussian distribution is frequently used:

$$a_1(z) = (1/\sqrt{2\pi}\Delta) \exp\{-(z - \langle c \rangle)^2 / 2\Delta^2\}$$
$$a_\mu(z) = (1/\sqrt{\mu})(1/\sqrt{2\pi}\Delta) \exp\{-(z - \mu\langle c \rangle)^2 / 2\mu\Delta^2\} \quad (4.2.5.48)$$

with the two parameters $\langle c \rangle$, Δ.

There are peaks of height $1/[\pi^2 L^2 (\Delta/\langle c \rangle)^2]$ which obviously decrease with L^2 and $(\Delta/\langle c \rangle)^2$. The oscillations vanish for $|F| \simeq 0.1$, *i.e.* $1/\langle c \rangle \simeq 0.25/\Delta$. The width of the mth peak is $\Delta_m = \sqrt{m}\Delta$. The integral reflectivity is approximately $1/\langle c \rangle [1 - \pi^2 L^2 (\Delta/\langle c \rangle)^2]$ and the integral width (defined by integral reflectivity divided by peak reflectivity) (background subtracted!) is $1/\langle c \rangle \pi^2 L^2 (\Delta/\langle c \rangle)^2$ which, therefore, increases with L^2. In principle, the same results are given by Zernike & Prins (1927). In practice, a single Gaussian distribution is not fully adequate and modified functions must be used (Rosshirt *et al.*, 1985).

Our final remark concerns the normalization [equation (4.2.5.39)]. Going from (4.2.5.39) to (4.2.5.45) it is assumed that N is a large number so that the correct normalization factors $(N - |\mu|)$ for each $a_\mu(z)$ may be approximated by a uniform N. If this is not true then

$$G(L) = N + \sum_\mu (N - |\mu|)(F^\mu + F^{+\mu}) = N\,\mathrm{Re}\{(1 + |F|)/(1 - |F|)\} - 2\,\mathrm{Re}\{|F|(1 - |F|^N)/(1 - |F|^2)\}. \quad (4.2.5.49)$$

The correction term may be important in the case of relatively small (1D) domains. As mentioned above, the structure factor of a chain molecule was neglected. The $\mathbf{H}$ dependence of F_M, of course, obscures the intensity variation of the diffuse layers as described by (4.2.5.47*a*).

The matrix method developed for the case of planar disorder was adapted to 2D disorder by Scaringe & Ibers (1979). Other models and corresponding expressions for diffuse scattering are developed from specific microscopic models (potentials), *e.g.* in the case of $Hg_{3-\delta}AsF_6$ (Emery & Axe, 1978; Radons *et al.*, 1983), hollandites (Beyeler *et al.*, 1980; Ishii, 1983), iodine chain compounds (Endres *et al.*, 1982) or urea inclusion compounds (Forst *et al.*, 1987; Weber *et al.*, 2000).

4.2.5.3.3. Correlations between almost collinear chains

In real cases there are quite strong correlations between different chains, at least within small domains. Deviations from a strict (3D) order of chain-like structural elements are due to several reasons: the shape and structure of the chains, varying binding forces, and thermodynamical or kinetic considerations.

Many types of disorder occur. (1) Relative shifts parallel to the common axis while projections along this axis give a perfect 2D ordered net ('axial disorder'). (2) Relative fluctuations of the distances between the chains (perpendicular to the unique axis) with short-range order along the transverse **a** and/or **b** directions. The net of projected chains down to the *ab* plane is distorted ('net distortions'). Disorder of types (1) and (2) is sometimes correlated owing to nonuniform cross sections of the chains. (3) Turns, twists and torsions of chains or parts of chains. This azimuthal type of disorder may be treated in a similar way to the case of

azimuthal disorder of single-chain molecules. Correlations between axial shifts and torsions produce 'screw shifts' (helical structures). Torsion of chain parts may be of dynamic origin (such as rotational vibrations). (4) Tilting or bending of the chains in a uniform or nonuniform way ('conforming/nonconforming' disorder). Many of these types and a variety of combinations between them are found in polymer and liquid crystals, and are therefore treated separately. Only some simple basic ideas are discussed here in brief.

For the sake of simplicity, the paracrystal concept in combination with Gaussians is used again. Distribution functions are given by convolution products of next-nearest-neighbour distribution functions. As long as averaged lattice directions and lattice constants in a plane perpendicular to the chain axis exist, only two functions, $a_{100} = a_1(xyz)$ and $a_{010} = a_2(xyz)$, are needed to describe the arrangement of next-nearest chains. Longitudinal disorder is treated as before by a third distribution function $a_{001} = a_3(xyz)$. The phenomena of chain bending or tilting may be incorporated by an x and y dependence of a_3. Any general fluctuation in the spatial arrangement of chains is given by

$$a_{mpq} = a_1 * \ldots * a_1 * a_2 * \ldots * a_2 * a_3 * \ldots * a_3. \qquad (4.2.5.50)$$

(m-fold, p-fold, q-fold self-convolution of a_1, a_2, a_3, respectively.)

$$w(\mathbf{r}) = \delta(\mathbf{r}) \sum_m \sum_p \sum_q [a_{mpq}(\mathbf{r}) + a_{-mpq}(\mathbf{r})]. \qquad (4.2.5.51)$$

a_ν ($\nu = 1, 2, 3$) are called fundamental functions. If an averaged lattice cannot be defined, more fundamental functions a_ν are needed to account for correlations between them.

By Fourier transformations, the interference function is given by

$$G(\mathbf{H})\, G_\nu = \mathrm{Re}\{(1 + |F_\nu|)/(1 - |F_\nu|)\}. \qquad (4.2.5.52)$$

If Gaussian functions are assumed, simple pictures are derived. For example

$$a_1(\mathbf{r} + \langle \mathbf{a} \rangle) = [1/(2\pi)^{3/2}][1/(\Delta_{11}\Delta_{12}\Delta_{13})] \times \exp\left\{-\tfrac{1}{2}[(x^2/\Delta_{11}^2) + (y^2/\Delta_{12}^2) + (z^2/\Delta_{13}^2)]\right\} \qquad (4.2.5.53)$$

describes the distribution of neighbours in the x direction (with a mean distance $\langle a \rangle$). Parameters Δ_{13}, Δ_{11} and Δ_{12} concern axial, radial and tangential fluctuations, respectively. Pure axial distribution along **c** is given by projection of a_1 on the z axis; pure net distortions are given by projection on the xy plane. If the chain-like structure is neglected, the interference function

$$G_1(\mathbf{H}) = \exp\{-2\pi^2(\Delta_{11}^2 H^2 + \Delta_{12}^2 K^2 + \Delta_{13}^2 L^2)\} \qquad (4.2.5.54)$$

describes a set of diffuse planes perpendicular to $\mathbf{a}^*$ with a mean distance of $1/\langle a \rangle$. These diffuse layers broaden along H with $m\Delta_{11}$ and decrease in intensity along K and L monotonically. There is an ellipsoid-shaped region in reciprocal space defined by main axes of length $1/\Delta_{11}, 1/\Delta_{12}, 1/\Delta_{13}$ with a limiting surface given by $|F| \simeq 0.1$, beyond which the diffuse intensity is completely smeared out. The influence of a_2 may be discussed in an analogous way.

If the chain-like arrangement parallel to **c** [equation (4.2.5.12)] is taken into consideration,

$$l(z) = \sum_{n_3} \delta(z - n_3 c),$$

the set of planes perpendicular to $\mathbf{a}^*$ (and/or $\mathbf{b}^*$) is subdivided in the L direction by a set of planes located at $l(1/c)$ [equation (4.2.5.15)].

Longitudinal disorder is given by $a_3(z)$ [equation (4.2.5.48), $\Delta_{33} = \Delta$] and leads to two intersecting sets of broadened diffuse layer systems.

Particular cases like pure axial distributions ($\Delta_{11}, \Delta_{12} \simeq 0$), pure tangential distributions (net distortions: $\Delta_{11}, \Delta_{13} \simeq 0$), uniform bending of chains or combinations of these effects are discussed in the monograph by Vainshtein (1966).

4.2.5.4. Defects, short-range ordering, clustering: three-dimensional disorder

4.2.5.4.1. General formulation (elastic diffuse scattering)

In this section general formulae for diffuse scattering will be derived that may best be applied to crystals with a well ordered average structure, characterized by (almost) sharp Bragg peaks. Textbooks and review articles concerning defects and local ordering are by Krivoglaz (1969, 1996*a*,*b*), Dederichs (1973), Peisl (1975), Schwartz & Cohen (1977), Schmatz (1973, 1983), Bauer (1979), Kitaigorodsky (1984) and Schweika (1998). A series of interesting papers on local order is given by Young (1975) and also by Cowley *et al.* (1979). Expressions for polycrystalline samples are given by Warren (1969) and Fender (1973).

Two general methods may be applied: (*a*) the average difference cluster method, where a representative cluster of scattering differences between the average structure and the cluster is used; and (*b*) the method of short-range-order correlation functions, where formal parameters are introduced.

The two methods are equivalent in principle. The cluster method is generally more convenient in cases where a single average cluster is a good approximation. This holds for small concentrations of clusters. In the literature this problem is treated in terms of fluctuations of the distribution functions as will be discussed below (Section 4.2.5.4.6). The most convenient way to derive the distribution function correctly from experimental data is the use of low-angle scattering, which generally shows one or more clear maxima caused by partly periodic properties of the distribution function. For the deconvolution of the distribution function, achieved by Fourier transformation of the corrected diffuse low-angle scattering, the reader is referred to the relevant literature. However, deconvolutions are not unique and some reasonable assumptions are necessary for a final solution.

The method of short-range-order parameters is optimal in cases where isolated clusters are not realized and the correlations do not extend to long distances. Otherwise periodic solutions are more convenient in most cases.

In any case, the first step towards the solution of the diffraction problem is the accurate determination of the average structure. As described in Section 4.2.4, important information on fractional occupations, interstitials and displacements of atoms (shown by unusual thermal parameters) may be derived. Unfortunately, all defects contribute to diffuse scattering; hence one has to start with the assumption that the disorder to be interpreted is predominant. Fractional occupancy of certain lattice sites by two or more kinds of atoms plays an important role in the literature, especially in metallic or ionic structures. Since vacancies may be treated as atoms with zero scattering amplitude, structures containing vacancies may be formally treated as multicomponent systems.

Since the solution of the diffraction problem should not be restricted to metallic systems with a simple (primitive) structure, we have to consider the structure of the unit cell – as given by the average structure – and the propagation of order according to the translation group separately. In simple metallic systems this difference is immaterial. It is well known that the thermodynamic problem of propagation of order in a three-dimensional crystal can hardly ever be solved analytically in a general way. Some solutions have been published with the aid of the Ising model using next-nearest-neighbour interactions. They are excellent for

an understanding of the principles of order–disorder phenomena, but they can rarely be applied quantitatively in practical problems. Hence, methods have been developed to derive the propagation of order from the diffraction pattern by means of Fourier transformation. This method has been described qualitatively in Section 4.2.3.1 and will be used here for a quantitative application. In a first approximation, the assumption of a small number of different configurations of the unit cell is made, represented by the corresponding number of structure factors. Displacements of atoms caused by the configurations of the neighbouring cells are excluded. This problem will be treated subsequently.

The finite number of structures of the unit cell in the disordered crystal is given by

$$F_\nu(\mathbf{r}) = \sum_j \sum_\mu \pi^\nu_{j\mu} f_\mu(\mathbf{r} - \mathbf{r}_j). \tag{4.2.5.55}$$

Note that $F_\nu(\mathbf{r})$ is defined in real space and $\mathbf{r}_j$ gives the position vector of site j; $\pi^\nu_{j\mu} = 1$ if in the νth structure factor the site j is occupied by an atom of kind μ, and 0 elsewhere.

In order to apply the laws of Fourier transformation adequately, it is useful to introduce the distribution function of F_ν,

$$\pi_\nu(\mathbf{r}) = \sum_{\mathbf{n}} \pi_{\mathbf{n}\nu} \delta(\mathbf{r} - \mathbf{n}), \tag{4.2.5.56}$$

with $\pi_{\mathbf{n}\nu} = 1$ if the cell $\mathbf{n} = n_1\mathbf{a} + n_2\mathbf{b} + n_3\mathbf{c}$ has the F_ν structure and $\pi_{\mathbf{n}\nu} = 0$ elsewhere.

In the definitions given above $\pi_{\mathbf{n}\nu}$ are numbers (scalars) assigned to the cell. Since all these are occupied we have

$$\sum_\nu \pi_\nu(\mathbf{r}) = l(\mathbf{r})$$

where $l(\mathbf{r})$ is the lattice in real space.

The structure of the disordered crystal is given by

$$\sum_\nu \pi_\nu(\mathbf{r}) * F_\nu(\mathbf{r}). \tag{4.2.5.57}$$

$\pi_\nu(\mathbf{r})$ consists of $\alpha_\nu N$ points, where $N = N_1N_2N_3$ is the total (large) number of unit cells and α_ν denotes the *a priori* probability (concentration) of the νth cell occupation.

It is now useful to introduce

$$\Delta\pi_\nu(\mathbf{r}) = \pi_\nu(\mathbf{r}) - \alpha_\nu l(\mathbf{r}) \tag{4.2.5.58}$$

with

$$\sum_\nu \Delta\pi_\nu(\mathbf{r}) = \sum_\nu \pi_\nu(\mathbf{r}) - l(\mathbf{r}) \sum_\nu \alpha_\nu = l(\mathbf{r}) - l(\mathbf{r}) = 0.$$

Introducing (4.2.5.58) into (4.2.5.57) gives

$$\begin{aligned}\sum_\nu \pi_\nu(\mathbf{r}) * F_\nu(\mathbf{r}) &= \sum_\nu \Delta\pi_\nu(\mathbf{r}) * F_\nu(\mathbf{r}) + l(\mathbf{r}) \sum_\nu \alpha_\nu F_\nu(\mathbf{r}) \\ &= \sum_\nu \Delta\pi_\nu(\mathbf{r}) * F_\nu(\mathbf{r}) + l(\mathbf{r})\langle F(\mathbf{r})\rangle.\end{aligned} \tag{4.2.5.59}$$

Similarly

$$\begin{aligned}\Delta F_\nu(\mathbf{r}) &= F_\nu(\mathbf{r}) - \langle F(\mathbf{r})\rangle, \\ \sum_\nu \alpha_\nu \Delta F_\nu(\mathbf{r}) &= \sum_\nu \alpha_\nu F_\nu(\mathbf{r}) - \sum_\nu \alpha_\nu \langle F(\mathbf{r})\rangle = 0.\end{aligned} \tag{4.2.5.60}$$

Using (4.2.5.60) it follows from (4.2.5.58) that

$$\begin{aligned}\sum_\nu \pi_\nu(\mathbf{r}) * F_\nu(\mathbf{r}) &= \sum_\nu \Delta\pi_\nu(\mathbf{r}) * \Delta F_\nu(\mathbf{r}) \\ &\quad + \sum_\nu \Delta\pi_\nu(\mathbf{r}) * \langle F(\mathbf{r})\rangle + l(\mathbf{r}) * \langle F(\mathbf{r})\rangle \\ &= \sum_\nu \Delta\pi_\nu(\mathbf{r}) * \Delta F_\nu(\mathbf{r}) + l(\mathbf{r}) * \langle F(\mathbf{r})\rangle.\end{aligned} \tag{4.2.5.61}$$

Comparison with (4.2.5.59) yields

$$\sum_\nu \Delta\pi_\nu(\mathbf{r}) * F_\nu(\mathbf{r}) = \sum_\nu \Delta\pi_\nu(\mathbf{r}) * \Delta F_\nu(\mathbf{r}).$$

Fourier transformation of (4.2.5.61) gives

$$\sum_\nu \Pi_\nu(\mathbf{H}) F_\nu(\mathbf{H}) = \sum_\nu \Delta\Pi_\nu(\mathbf{H}) \Delta F_\nu(\mathbf{H}) + L(\mathbf{H})\langle F(\mathbf{H})\rangle$$

with

$$\sum_\nu \Delta\Pi_\nu(\mathbf{H}) = 0, \quad \sum_\nu \Delta F_\nu(\mathbf{H}) = 0.$$

The expression for the scattered intensity is therefore

$$\begin{aligned}I(\mathbf{H}) &= \left|\sum_\nu \Delta\Pi_\nu(\mathbf{H}) \Delta F_\nu(\mathbf{H})\right|^2 + |L(\mathbf{H})\langle F(\mathbf{H})\rangle|^2 \\ &\quad + L(\mathbf{H})\Bigg\{\langle F^+(\mathbf{H})\rangle \sum_\nu \Delta\Pi_\nu(\mathbf{H}) F_\nu(\mathbf{H}) \\ &\quad + \langle F^+(\mathbf{H})\rangle \sum_\nu \Delta\Pi^+_\nu(\mathbf{H}) F^+_\nu(\mathbf{H})\Bigg\}.\end{aligned} \tag{4.2.5.62}$$

Because of the multiplication by $L(\mathbf{H})$, the third term in (4.2.5.62) contributes to sharp reflections only. Since they are correctly given by the second term in (4.2.5.62), the third term vanishes. Hence the diffuse part is given by

$$I_{\rm D}(\mathbf{H}) = \left|\sum_\nu \Delta\Pi_\nu(\mathbf{H}) \Delta F_\nu(\mathbf{H})\right|^2. \tag{4.2.5.63}$$

For a better understanding of the behaviour of diffuse scattering it is useful to return to real space:

$$\begin{aligned}i_{\rm D}(\mathbf{r}) &= \sum_\nu \Delta\pi_\nu(\mathbf{r}) * \Delta F_\nu(\mathbf{r}) * \sum_{\nu'} \Delta\pi_{\nu'}(-\mathbf{r}) * \Delta F_{\nu'}(-\mathbf{r}) \\ &= \sum_\nu \sum_{\nu'} \Delta\pi_\nu(\mathbf{r}) * \Delta\pi_{\nu'}(-\mathbf{r}) * \Delta F_\nu(\mathbf{r}) * \Delta F_{\nu'}(-\mathbf{r})\end{aligned} \tag{4.2.5.64}$$

and with (4.2.5.58):

$$\begin{aligned}i_{\rm D}(\mathbf{r}) &= \sum_\nu \sum_{\nu'} [\pi_\nu(\mathbf{r}) - \alpha_\nu l(\mathbf{r})] * [\pi_{\nu'}(-\mathbf{r}) - \alpha_{\nu'} l(\mathbf{r})] \\ &\quad * \Delta F_\nu(\mathbf{r}) * \Delta F_{\nu'}(-\mathbf{r}).\end{aligned} \tag{4.2.5.65}$$

Evaluation of this equation for a single term yields

$$\begin{aligned}&[\pi_\nu(\mathbf{r}) * \pi_{\nu'}(-\mathbf{r}) - \alpha_\nu l(\mathbf{r}) * \pi_{\nu'}(-\mathbf{r}) \\ &\quad - \alpha_{\nu'} l(\mathbf{r}) * \pi_\nu(\mathbf{r}) + \alpha_\nu \alpha_{\nu'} l(\mathbf{r}) * l(\mathbf{r})] \\ &\quad * \Delta F_\nu(\mathbf{r}) * \Delta F_{\nu'}(\mathbf{r}).\end{aligned} \tag{4.2.5.66}$$

Since $l(\mathbf{r})$ is a periodic function of points, all convolution products with $l(\mathbf{r})$ are also periodic. For the final evaluation the decrease of the number of overlapping points (maximum N) in the convolution products with increasing displacements of the functions is neglected (it is assumed that there is no particle-size effect). Then (4.2.5.66) becomes

$$[\pi_\nu(\mathbf{r}) * \pi_{\nu'}(-\mathbf{r}) - N\alpha_\nu\alpha_{\nu'}l(\mathbf{r}) - N\alpha_\nu\alpha_{\nu'}l(\mathbf{r}) + N\alpha_\nu\alpha_{\nu'}l(\mathbf{r})]$$
$$* \Delta F_\nu(\mathbf{r}) * \Delta F_{\nu'}(-\mathbf{r})$$
$$= [\pi_\nu(\mathbf{r}) * \pi_{\nu'}(-\mathbf{r}) - N\alpha_\nu\alpha_{\nu'}l(\mathbf{r})]$$
$$* \Delta F_\nu(\mathbf{r}) * \Delta F_{\nu'}(-\mathbf{r}). \quad (4.2.5.67)$$

If the first term in (4.2.5.67) is considered, the convolution of the two functions for a given distance $\mathbf{n}$ counts the number of coincidences of the function $\pi_\nu(\mathbf{r})$ with $\pi_{\nu'}(-\mathbf{r})$. This quantity is given by $Nl(\mathbf{r})\alpha_\nu p_{\nu\nu'}(-\mathbf{r})$, where $\alpha_\nu p_{\nu\nu'}(\mathbf{r})$ is the probability of a pair occupation in the $\mathbf{r}$ direction.

Equation (4.2.5.67) then reads

$$[Nl(\mathbf{r})\alpha_\nu p_{\nu\nu'}(-\mathbf{r}) - N\alpha_\nu\alpha_{\nu'}l(\mathbf{r})]$$
$$* \Delta F_\nu(\mathbf{r}) * \Delta F_{\nu'}(-\mathbf{r})$$
$$= N\alpha_\nu[p'_{\nu\nu'}(-\mathbf{r})l(\mathbf{r})]$$
$$* [\Delta F_\nu(\mathbf{r}) * \Delta F_{\nu'}(-\mathbf{r})] \quad (4.2.5.68)$$

with $p'_{\nu\nu'}(\mathbf{r}) = p_{\nu\nu'}(\mathbf{r}) - \alpha_{\nu'}$. The function $\alpha_\nu p'_{\nu\nu'}(\mathbf{r})$ is usually called the pair-correlation function $g \leftrightarrow \alpha_{\nu\nu'|\mathbf{nn}'}$ in physics.

The following relations hold:

$$\sum_\nu \alpha_\nu = 1; \quad (4.2.5.69a)$$
$$\sum_{\nu'} \alpha_\nu p_{\nu\nu'}(\mathbf{r}) = \alpha_{\nu'}; \quad \sum_{\nu'} \alpha_\nu p'_{\nu\nu'}(\mathbf{r}) = 0 \quad (4.2.5.69b)$$
$$\sum_\nu \alpha_\nu p_{\nu\nu'}(\mathbf{r}) = \alpha_{\nu'}; \quad \sum_\nu \alpha_\nu p'_{\nu\nu'}(\mathbf{r}) = 0 \quad (4.2.5.69c)$$
$$\alpha_\nu p_{\nu\nu'}(\mathbf{r}) = \alpha_{\nu'} p_{\nu'\nu}(-\mathbf{r}). \quad (4.2.5.69d)$$

Functions normalized to unity are also in use. Obviously the following relation is valid: $p'_{\nu\nu'}(0) = \delta_{\nu\nu'} - \alpha_{\nu'}$.

Hence

$$\alpha_{\nu\nu'|\mathbf{nn}'} = \alpha_{\nu'} p'_{\nu\nu'}(\mathbf{r})/(\delta_{\nu\nu'} - \alpha_{\nu'})$$

is unity for $\mathbf{r} = 0\,(\mathbf{n} = \mathbf{n}')$. This property is especially convenient in binary systems.

With (4.2.5.68), equation (4.2.5.64) becomes

$$i_{\mathrm{D}}(\mathbf{r}) = N \sum_\nu \sum_{\nu'} [\alpha_\nu p'_{\nu\nu'}(-\mathbf{r})l(\mathbf{r})] * [\Delta F_\nu(\mathbf{r}) * \Delta F_{\nu'}(-\mathbf{r})] \quad (4.2.5.70)$$

and Fourier transformation yields

$$I_{\mathrm{D}}(\mathbf{H}) = N \sum_\nu \sum_{\nu'} [\alpha_\nu P'_{\nu\nu'}(-\mathbf{H}) * L(\mathbf{H})] \Delta F_\nu(\mathbf{H}) \Delta F^+_{\nu'}(\mathbf{H}). \quad (4.2.5.71)$$

It may be concluded from equations (4.2.5.69) that all functions $p'_{\nu\nu'}(\mathbf{r})$ may be expressed by $p'_{11}(\mathbf{r})$ in the case of two structure factors F_1, F_2. Then all $p'_{\nu\nu'}(\mathbf{r})$ are symmetric in $\mathbf{r}$; the same is true for the $P'_{\nu\nu'}(\mathbf{H})$. Consequently, the diffuse reflections described by (4.2.5.71) are all symmetric. The position of the diffuse peak depends strongly on the behaviour of $p'_{\nu\nu'}(\mathbf{r})$; in the case of cluster formation Bragg peaks and diffuse peaks coincide. Diffuse superstructure reflections are observed if the $p'_{\nu\nu'}(\mathbf{r})$ show some damped periodicities.

It should be emphasized that the condition $p'_{\nu\nu'}(\mathbf{r}) = p'_{\nu\nu'}(-\mathbf{r})$ may be violated for $\nu \neq \nu'$ if more than two cell occupations are involved. As shown below, the possibly asymmetric functions may be split into symmetric and antisymmetric parts. From equation (4.2.3.8) it follows that the Fourier transform of the antisymmetric part of $p'_{\nu\nu'}(\mathbf{r})$ is also antisymmetric. Hence, the convolution in the two terms in square brackets in (4.2.5.71) yields an antisymmetric contribution to each diffuse peak, generated by the convolution with the reciprocal lattice $L(\mathbf{h})$.

Obviously, equation (4.2.5.71) may also be applied to primitive lattices occupied by two or more kinds of atoms. Then the structure factors F_ν are merely replaced by the atomic scattering factors f_ν and the α_ν are equivalent to the concentrations of atoms c_ν. In terms of the $\alpha_{\nu\nu'|\mathbf{nn}'}$ (Warren short-range-order parameters) equation (4.2.5.71) reads

$$I_{\mathrm{D}}(\mathbf{H}) = N(\overline{f^2} - \bar{f}^2) \sum_{\mathbf{n}} \sum_{\mathbf{n}'} \alpha_{\nu\nu'|\mathbf{nn}'} \exp\{2\pi i \mathbf{H} \cdot (\mathbf{n} - \mathbf{n}')\}. \quad (4.2.5.71a)$$

In the simplest case of a binary system A, B,

$$\alpha_{\mathbf{nn}'} = (1 - p_{AB|\mathbf{nn}'})/c_B = (1 - p_{BA|\mathbf{nn}'})/c_A;$$
$$c_A p_{AB} = c_B p_{BA}; \quad p_{AA} = 1 - p_{AB};$$

$$I_{\mathrm{D}}(\mathbf{H}) = N c_A c_B (f_A - f_B)^2 \sum_{\mathbf{n}} \sum_{\mathbf{n}'} \alpha_{\mathbf{nn}'} \exp\{2\pi i \mathbf{H} \cdot (\mathbf{n} - \mathbf{n}')\}. \quad (4.2.5.71b)$$

[The exponential in (4.2.5.71*b*) may even be replaced by a cosine term owing to the centrosymmetry of this particular case.]

It should be mentioned that the formulations of the problem in terms of pair probabilities, pair-correlation functions, short-range-order parameters or concentration waves (Krivoglaz, 1969, 1996*a*,*b*) are equivalent. The Patterson function may also be used when using continuous electron (or nuclear) density functions where site occupancies are implied (Cowley, 1981).

4.2.5.4.2. Random distribution of defects

As shown above in the case of random distributions, all $p'_{\nu\nu'}(\mathbf{r})$ are zero except for $\mathbf{r} = 0$. Consequently, $p'_{\nu\nu'}(\mathbf{r})l(\mathbf{r})$ may be replaced by

$$\alpha_\nu p'_{\nu\nu'}(\mathbf{r}) = \alpha_\nu \delta_{\nu\nu'} - \alpha_\nu\alpha_{\nu'}. \quad (4.2.5.72)$$

According to (4.2.5.59) and (4.2.5.61), the diffuse scattering can be given by the Fourier transformation of

$$\sum_\nu \sum_{\nu'} \Delta\pi_\nu(\mathbf{r}) * \Delta\pi_{\nu'}(-\mathbf{r}) * F_\nu(\mathbf{r}) * F_\nu(-\mathbf{r})$$
$$= \sum_\nu \sum_{\nu'} p'_{\nu\nu'}(\mathbf{r}) * F_\nu(\mathbf{r}) * F_{\nu'}(-\mathbf{r})$$

or with (4.2.5.72)

$$i_{\mathrm{D}}(\mathbf{r}) = N \sum_\nu \sum_{\nu'} [\alpha_\nu \delta_{\nu\nu'} - \alpha_\nu\alpha_{\nu'}] * F_\nu(\mathbf{r}) * F_{\nu'}(-\mathbf{r}).$$

Fourier transformation gives

$$I_{\mathrm{D}}(\mathbf{H}) = N\left\{\sum_\nu \alpha_\nu |F_\nu(\mathbf{H})|^2 - \sum_\nu \alpha_\nu F_\nu(\mathbf{H}) \sum_{\nu'} \alpha_{\nu'} F^+_{\nu'}(\mathbf{H})\right\}$$
$$= N\{\langle |F(\mathbf{H})|^2 \rangle - |\langle F(\mathbf{H}) \rangle|^2\}. \quad (4.2.5.73)$$

This is the most general form of any diffuse scattering by systems ordered randomly ('Laue scattering'). Occasionally it is called 'incoherent scattering' (see Section 4.2.2).

4.2.5.4.3. Short-range order in multicomponent systems

The diffuse scattering of a disordered binary system without displacements of the atoms has already been discussed in Section 4.2.5.4.1. It could be shown that all distribution functions $p'_{\nu\nu'}(\mathbf{r})$ are mutually dependent and may be replaced by a single function [*cf.* (4.2.5.69)]. In that case $p'_{\nu\nu'}(\mathbf{r}) = p'_{\nu\nu'}(-\mathbf{r})$ was valid for all. This condition, however, may be violated in multicomponent systems. If a tendency towards an $F_1F_2F_3$ order in a ternary system is assumed, for example, $p_{12}(\mathbf{r})$ is apparently different from $p_{12}(-\mathbf{r})$. In this particular case it is useful to introduce

$$\langle p'_{\nu\nu'}(\mathbf{r})\rangle = \tfrac{1}{2}[p'_{\nu\nu'}(\mathbf{r}) + p'_{\nu\nu'}(-\mathbf{r})],$$
$$\Delta p'_{\nu\nu'}(\mathbf{r}) = \tfrac{1}{2}[p'_{\nu\nu'}(\mathbf{r}) - p'_{\nu\nu'}(-\mathbf{r})]$$

and their Fourier transforms $\langle P'_{\nu\nu'}(\mathbf{H})\rangle$, $\Delta P'_{\nu\nu'}(\mathbf{H})$, respectively.

The asymmetric correlation functions are therefore expressed by

$$p'_{\nu\nu'}(\mathbf{r}) = \langle p'_{\nu\nu'}(\mathbf{r})\rangle + \Delta p'_{\nu\nu'}(\mathbf{r});$$
$$p'_{\nu\nu'}(-\mathbf{r}) = \langle p'_{\nu\nu'}(\mathbf{r})\rangle - \Delta p'_{\nu\nu'}(\mathbf{r});$$
$$\Delta p'_{\nu\nu}(\mathbf{r}) = 0.$$

Consequently, $i_{\mathrm{D}}(\mathbf{r})$ (4.2.5.70) and $I_{\mathrm{D}}(\mathbf{H})$ (4.2.5.71) may be separated according to the symmetric and antisymmetric contributions. The final result is

$$\begin{aligned} I_{\mathrm{D}}(\mathbf{H}) = N\Big\{ & \sum_{\nu} \alpha_\nu [P'_{\nu\nu}(\mathbf{H}) * L(\mathbf{H})] |F_\nu(\mathbf{H})|^2 \\ & + \sum_{\nu>\nu'} \alpha_\nu [\langle P'_{\nu\nu'}(\mathbf{H})\rangle * L(\mathbf{H})] \\ & \times [\Delta F_\nu(\mathbf{H}) \Delta F^+_{\nu'}(\mathbf{H}) + \Delta F^+_\nu(\mathbf{H}) \Delta F_{\nu'}(\mathbf{H})] \\ & + \sum_{\nu>\nu'} \alpha_\nu [\Delta P'_{\nu\nu'}(-\mathbf{H}) * L(\mathbf{H})] \\ & \times [\Delta F_\nu(\mathbf{H}) \Delta F^+_{\nu'}(\mathbf{H}) - \Delta F^+_\nu(\mathbf{H}) \Delta F_{\nu'}(\mathbf{H})] \Big\}. \end{aligned} \tag{4.2.5.74}$$

Obviously, antisymmetric contributions to line profiles will only occur if structure factors of acentric cell occupations are involved. This important property may be used to draw conclusions with respect to the structure factors involved in the statistics. It should be mentioned here that the Fourier transform of the antisymmetric function $\Delta p'_{\nu\nu'}(\mathbf{r})$ is imaginary and antisymmetric. Since the last term in (4.2.5.74) is also imaginary, the product of the two factors in brackets is real, as it should be.

4.2.5.4.4. Displacements: general remarks

Even small displacements may have an important influence on the problem of propagation of order. Therefore, no structural treatments other than the introduction of formal parameters (*e.g.* Landau's theory) have been published in the literature. Most of the examples with really reliable results refer to binary systems and even these represent very crude approximations, as will be shown below. For this reason we shall restrict ourselves here to binary systems, although general formulae where displacements are included may be developed in a formal way.

Two kinds of atoms, $f_1(\mathbf{r})$ and $f_2(\mathbf{r})$, are considered. Obviously, the position of any given atom is determined by its surroundings. Their extension depends on the forces acting on the atom under consideration. These may be very weak in the case of metals (repulsive forces, the 'size effect'), but long-range effects have to be expected in ionic crystals. For the development of formulae authors have assumed that small displacements $\Delta\mathbf{r}_{\nu\nu'}$ may be assigned to the pair-correlation functions $p'_{\nu\nu'}(\mathbf{r})$ by adding a phase factor $\exp\{2\pi i\mathbf{H}\cdot\Delta\mathbf{r}_{\nu\nu'}\}$, which is then expanded in the usual way:

$$\exp\{2\pi i\mathbf{H}\cdot\Delta\mathbf{r}_{\nu\nu'}\} \simeq 1 + 2\pi i\mathbf{H}\cdot\Delta\mathbf{r}_{\nu\nu'} - 2[\pi\mathbf{H}\cdot\Delta\mathbf{r}_{\nu\nu'}]^2. \tag{4.2.5.75}$$

The displacements and correlation probabilities are separable if the change of atomic scattering factors in the angular range considered may be neglected. The formulae in use are given in the next section. As shown below, this method represents nothing other than a kind of average over certain sets of displacements. For this purpose, the correct solution of the problem has to be discussed. In the simplest model the displacements are due to next-nearest neighbours only. It is further assumed that the configurations rather than the displacements determine the position of the central atom and a general displacement of the centre of the first shell does not occur (there is no influence of a strain field). Obviously, the formal correlation function of pairs is not independent of displacements. This difficulty may be avoided either by assuming that the pair-correlation function has already been separated from the diffraction data, or by theoretical calculations of the correlation function (the mean-field method) (Moss, 1966; de Fontaine, 1972, 1973). The validity of this procedure is subject to the condition that the displacements have no influence on the correlation functions themselves.

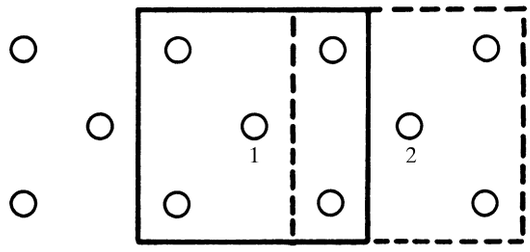

Fig. 4.2.5.1. Construction of the correlation function in the method of overlapping clusters.

The observation of a periodic average structure justifies the definition of a periodic array of origins, which normally depends on the degree of order. Local deviations of origins may be due to fluctuations in the degree of order and due to the surrounding atoms of a given site. For example, a b.c.c. lattice with eight nearest neighbours is considered. It is assumed that only these have an influence on the position of the central atom owing to different forces of the various configurations. With two kinds of atoms, there are $2^9 = 512$ possible configurations of the cluster (the central atom plus 8 neighbours). Symmetry considerations reduce this number to 28. Each is characterized by a displacement vector. Hence their *a priori* probabilities and the propagation of 28 different configurations have to be determined. Since each atom has to be considered as the centre once, this problem may be treated by introducing 28 different atomic scattering factors as determined from the displacements: $f_\nu(\mathbf{r})\exp\{2\pi i\mathbf{H}\cdot\Delta\mathbf{r}_{\nu\nu'}\}$. The diffraction problem has to be solved with the aid of the propagation of order of overlapping clusters. This is demonstrated by a two-dimensional model with four nearest neighbours (Fig. 4.2.5.1). Here the central and the neighbouring cluster (full and broken lines) overlap with two sites in, for example, the x direction. Hence only neighbouring clusters with the same overlapping pairs are admitted. These restrictions introduce severe difficulties into the problem of propagation of cluster ordering which determines the displacement field. Since it was assumed that the problem of pair correlation had been solved, the cluster probabilities may be derived by calculating

$$\alpha_\nu l(\mathbf{r}) \prod_{\mathbf{n}\neq 0} p'_{\nu\nu'}(\mathbf{r}-\mathbf{n}). \tag{4.2.5.76}$$

Only next-nearest neighbours have to be included in the product. This must be performed for the central cluster ($\mathbf{r} = 0$) *and* for the reference cluster at $\mathbf{r} = n_1\mathbf{a} + n_2\mathbf{b} + n_3\mathbf{c}$, because all are characterized by different displacements. So far, possible displacement of the centre has not been considered; this may also be influenced by the problem of propagation of cluster ordering. These displacement factors should best be attached to the function describing the propagation of order which determines, in principle, the local fluctuations of the lattice constants (the strain field *etc.*). This may be understood by considering a binary system with a high degree of order but with atoms of different size. Large fluctuations of lattice constants are involved in the case of

exsolution of the two components because of their different lattice parameters, but they become small in the case of superstructure formation where a description in terms of antiphase domains is reasonable (with equal lattice constants). This example demonstrates the mutual dependence of ordering and displacements, which is mostly neglected in the literature.

The method of assigning phase factors to the pair-correlation function is now discussed. Pair-correlation functions average over all pairs of clusters having the same central atom. An analogous argument holds for displacements: using pair correlations for the determination of displacements means nothing other than averaging over all displacements caused by various clusters around the same central atom. There remains the general strain field due to the propagation of order, whereas actual displacements of atoms are realized by fluctuations of configurations. Since large fluctuations of this type occur in highly disordered crystals, the displacements become increasingly irrelevant. Hence the formal addition of displacement factors to the pair-correlation function does not yield much information about the structural basis of the displacements. This situation corresponds exactly to the relationship between a Patterson function and a real structure: the structure has to be found which explains the quite complicated function completely, and its unique solution is rather difficult. We state these points here because in most publications related to this subject these considerations are not taken into account adequately. Displacements usually give rise to antisymmetric contributions to diffuse reflections. As pointed out above, the influence of displacements has to be considered as phase factors which may be attached either to the structure factors or to the Fourier transforms $P'_{\nu\nu'}(\mathbf{H})$ of the correlation functions in equation (4.2.5.71). As has been mentioned in the context of equation (4.2.5.74), antisymmetric contributions will occur if acentric structure factors are involved. Apparently, this condition is met by the phase factors of displacements. In consequence, antisymmetric contributions to diffuse reflections may also originate from the displacements. This fact can also be demonstrated if the assignment of phase factors to the Fourier transforms of the correlation functions is advantageous. In this case, equations (4.2.5.69*a*,*b*) are no longer valid because the functions $p'_{\nu\nu'}(\mathbf{r})$ become complex. The most important change is the relation corresponding to (4.2.5.69):

$$\alpha_\nu p'_{\nu\nu'}(\mathbf{r}) = \alpha_{\nu'} p'^{+}_{\nu\nu'}(-\mathbf{r}) \leftrightarrow \alpha_\nu P'_{\nu\nu'}(\mathbf{H}) = \alpha_{\nu'} P'^{+}_{\nu'}(\mathbf{H}). \quad (4.2.5.77)$$

Strictly speaking, we have to replace the *a priori* probabilities α_ν by complex numbers $\alpha_\nu \exp\{2\pi i \Delta\mathbf{r}_\nu \cdot \mathbf{H}\}$, which are determined by the position of the central atom. In this way, all correlations between displacements may be included with the aid of the clusters mentioned above. To a rough approximation it may be assumed that no correlations of this kind exist. In this case, the complex factors may be assigned to the structure factors involved. Averaging over all displacements results in diffraction effects that are very similar to a static Debye–Waller factor for all structure factors. On the other hand, the thermal motion of atoms is treated similarly. Obviously, both factors affect the sharp Bragg peaks. Hence this factor can easily be determined by the average structure, which contains a Debye–Waller factor including static and thermal displacements. It should be pointed out, however, that these static displacements cause elastic diffuse scattering, which cannot be separated by inelastic neutron-scattering techniques.

A careful study of the real and imaginary parts of

$$\langle p'_{\nu\nu'}(\mathbf{r})\rangle = \langle p'_{\nu\nu'}(\mathbf{r})\rangle_{\mathrm{R}} + \langle p'_{\nu\nu'}(\mathbf{r})\rangle_{\mathrm{I}}$$

and

$$\Delta p'_{\nu\nu'}(\mathbf{r}) = \Delta p'_{\nu\nu'}(\mathbf{r})_{\mathrm{R}} + \Delta p'_{\nu\nu'}(\mathbf{r})_{\mathrm{I}}$$

and their Fourier transforms results, after some calculations, in the following relation for diffuse scattering:

$$\begin{aligned} I_{\mathrm{D}} \simeq\ & N \sum_\nu \alpha_\nu |\Delta F_\nu(\mathbf{H})|^2 \{[\langle P'_{\nu\nu}(\mathbf{H})\rangle - \Delta P'_{\nu\nu}(\mathbf{H})] * L(\mathbf{H})\} \\ & + 2N \sum_{\nu>\nu'} \alpha_\nu (\Delta F_\nu \Delta F^{+}_{\nu'})_{\mathrm{R}} \\ & \times \{[\langle P'_{\nu\nu'}(\mathbf{H})\rangle_{\mathrm{R}} - \Delta P'_{\nu\nu'}(\mathbf{H})_{\mathrm{I}}] * L(\mathbf{H})\} \\ & + 2N \sum_{\nu>\nu'} \alpha_\nu (\Delta F_\nu \Delta F^{+}_{\nu'})_{\mathrm{I}} \\ & \times \{[\langle P'_{\nu\nu'}(\mathbf{H})\rangle_{\mathrm{I}} - \Delta P'_{\nu\nu'}(\mathbf{H})_{\mathrm{R}}] * L(\mathbf{H})\}. \end{aligned} \quad (4.2.5.78)$$

It should be noted that all contributions are real. This follows from the properties of Fourier transforms of symmetric and antisymmetric functions. All $\Delta P_{\nu\nu'}(\mathbf{H})$ are antisymmetric; hence they generate antisymmetric contributions to the line profiles. In contrast to equation (4.2.5.75), the real *and* the imaginary parts of the structure factors contribute to the asymmetry of the line profiles.

4.2.5.4.5. Distortions in binary systems

In substitutional binary systems (with a primitive cell with only one sublattice) the Borie–Sparks method is widely used (Sparks & Borie, 1966; Borie & Sparks, 1971). The method is formulated in the short-range-order-parameter formalism. The diffuse scattering may be separated into two parts (*a*) owing to short-range order and (*b*) owing to static displacements.

Corresponding to the expansion (4.2.5.75), $I_{\mathrm{D}} = I_{\mathrm{sro}} + I_2 + I_3$, where I_{sro} is given by equation (4.2.5.71*b*) and the correction terms I_2 and I_3 relate to the linear and the quadratic term in (4.2.5.75). The intensity expression will be split into terms of A–A, A–B, ... pairs. More explicitly $\Delta\mathbf{r}_{\nu\nu'} = \mathbf{u}_{\mathbf{n}\nu} - \mathbf{u}_{\mathbf{n}'\nu'}$ and with the following abbreviations

$$\begin{aligned} \delta_{\mathbf{nn}'|AA} &= \mathbf{u}_{\mathbf{n}|A} - \mathbf{u}_{\mathbf{n}'|A} = x_{\mathbf{nn}'|AA}\mathbf{a} + y_{\mathbf{nn}'|AA}\mathbf{b} + z_{\mathbf{nn}'|AA}\mathbf{c} \\ \delta_{\mathbf{nn}'|AB} &= \mathbf{u}_{\mathbf{n}|A} - \mathbf{u}_{\mathbf{n}'|B} = \ldots \\ F_{\mathbf{nn}'|AA} &= [f_A^2/(f_A - f_B)^2][(c_A/c_B) + \alpha_{\mathbf{nn}'}] \\ F_{\mathbf{nn}'|BB} &= [f_B^2/(f_A - f_B)^2][(c_B/c_A) + \alpha_{\mathbf{nn}'}] \\ F_{\mathbf{nn}'|AB} &= [2f_A f_B/(f_A - f_B)^2](1 - \alpha_{\mathbf{nn}'}) = F_{\mathbf{nn}'|BA} \end{aligned}$$

one finds (where the short-hand notation is self-explanatory):

$$\begin{aligned} I_2 = 2\pi i c_A c_B (f_A - f_B)^2 \sum_{\mathbf{n}} \sum_{\mathbf{n}'} \{ & H[F_{\mathbf{nn}'|AA}\langle x_{\mathbf{nn}'|AA}\rangle \\ & + F_{\mathbf{nn}'|BB}\langle x_{\mathbf{nn}'|BB}\rangle + F_{\mathbf{nn}'|AB}\langle x_{\mathbf{nn}'|AB}\rangle] + K[\text{`}y\text{'}] \\ & + L[\text{`}z\text{'}]\} \exp\{2\pi i \mathbf{H}\cdot(\mathbf{n} - \mathbf{n}')\}, \end{aligned} \quad (4.2.5.79)$$

$$\begin{aligned} I_3 = c_A c_B (f_A - f_B)^2 (-2\pi)^2 \sum_{\mathbf{n}} \sum_{\mathbf{n}'} \{ & H^2[F_{\mathbf{nn}'}\langle x^2_{\mathbf{nn}'|AA}\rangle \\ & + F_{\mathbf{nn}'|BB}\langle x^2_{\mathbf{nn}'|BB}\rangle + F_{\mathbf{nn}'|AB}\langle x^2_{\mathbf{nn}'|AB}\rangle] \\ & + K^2[\text{`}y^2\text{'}] + L^2[\text{`}z^2\text{'}] \\ & + HK[F_{\mathbf{nn}'|AA}\langle (xy)_{\mathbf{nn}'|AA}\rangle + F_{\mathbf{nn}'|BB}\langle (xy)_{\mathbf{nn}'|BB}\rangle \\ & + F_{\mathbf{nn}'|AB}\langle (xy)_{\mathbf{nn}'|AB}\rangle] \\ & + KL[\text{`}(yz)\text{'}] + LH[\text{`}(zx)\text{'}]\} \\ & \times \exp\{2\pi i \mathbf{H}\cdot(\mathbf{n} - \mathbf{n}')\}. \end{aligned} \quad (4.2.5.80)$$

With further abbreviations

$$\gamma_{\mathbf{nn}'|x} = 2\pi(F_{\mathbf{nn}'|AA}\langle x_{\mathbf{nn}'|AA}\rangle + F_{\mathbf{nn}'|BB}\langle x_{\mathbf{nn}'|BB}\rangle + F_{\mathbf{nn}'|AB}\langle x_{\mathbf{nn}'|AB}\rangle)$$
$$\gamma_{\mathbf{nn}'|y} = \ldots$$
$$\gamma_{\mathbf{nn}'|z} = \ldots$$
$$\delta_{\mathbf{nn}'|x} = (-2\pi^2)(F_{\mathbf{nn}'|AA}\langle x^2_{\mathbf{nn}'|AA}\rangle + F_{\mathbf{nn}'|BB}\langle x^2_{\mathbf{nn}'|BB}\rangle + F_{\mathbf{nn}'|AB}\langle x^2_{\mathbf{nn}'|AB}\rangle)$$
$$\delta_{\mathbf{nn}'|y} = \ldots$$
$$\delta_{\mathbf{nn}'|z} = \ldots$$
$$\varepsilon_{\mathbf{nn}'|xy} = (-4\pi^2)(F_{\mathbf{nn}'|AA}\langle (xy)_{\mathbf{nn}'|AA}\rangle + F_{\mathbf{nn}'|BB}\langle (xy)_{\mathbf{nn}'|BB}\rangle + F_{\mathbf{nn}'|AB}\langle (xy)_{\mathbf{nn}'|AB}\rangle)$$
$$\varepsilon_{\mathbf{nn}'|yz} = \ldots$$
$$\varepsilon_{\mathbf{nn}'|zx} = \ldots$$
$$I_2 = c_A c_B (f_A - f_B)^2 \sum_{\mathbf{n}} \sum_{\mathbf{n}'} i(\gamma_{\mathbf{nn}'|x} + \gamma_{\mathbf{nn}'|y} + \gamma_{\mathbf{nn}'|z}) \times \exp\{2\pi i \mathbf{H}\cdot(\mathbf{n}-\mathbf{n}')\}$$
$$I_3 = c_A c_B (f_A - f_B)^2 \sum_{\mathbf{n}} \sum_{\mathbf{n}'} (\delta_{\mathbf{nn}'|x}H^2 + \delta_{\mathbf{nn}'|y}K^2 + \delta_{\mathbf{nn}'|z}L^2 + \varepsilon_{\mathbf{nn}'|xy}HK + \varepsilon_{\mathbf{nn}'|yz}KL + \varepsilon_{\mathbf{nn}'|zx}LH)\exp\{2\pi i \mathbf{H}\cdot(\mathbf{n}-\mathbf{n}')\}.$$

If the $F_{\mathbf{nn}'|AA}, \ldots$ are independent of $|\mathbf{H}|$ in a range of measurement which is better fulfilled with neutrons than with X-rays (see below), γ, δ, ε are the coefficients of the Fourier series:

$$Q_x = \sum_{\mathbf{n}} \sum_{\mathbf{n}'} i\gamma_{\mathbf{nn}'|x} \exp\{2\pi i \mathbf{H}\cdot(\mathbf{n}-\mathbf{n}')\};$$
$$Q_y = \ldots; \qquad Q_z = \ldots;$$
$$R_x = \sum_{\mathbf{n}} \sum_{\mathbf{n}'} \delta_{\mathbf{nn}'|x} \exp\{2\pi i \mathbf{H}\cdot(\mathbf{n}-\mathbf{n}')\};$$
$$R_y = \ldots; \qquad R_z = \ldots;$$
$$S_{xy} = \sum_{\mathbf{n}} \sum_{\mathbf{n}'} \varepsilon_{\mathbf{nn}'|xy} \exp\{2\pi i \mathbf{H}\cdot(\mathbf{n}-\mathbf{n}')\};$$
$$S_{yz} = \ldots; \qquad S_{zx} = \ldots.$$

The functions Q, R, S are then periodic in reciprocal space.

The double sums over $\mathbf{n}$, $\mathbf{n}'$ may be replaced by $N\sum_{m,n,p}$ where m, n, p are the coordinates of the interatomic vectors $(\mathbf{n}-\mathbf{n}')$ and I_2 becomes

$$I_2 = -Nc_A c_B (f_A - f_B)^2 \sum_m \sum_n \sum_p (H\gamma_{lmn|x} + \ldots + \ldots) \times \sin 2\pi(Hm + Kn + Lp). \qquad (4.2.5.81)$$

The intensity is therefore modulated sinusoidally and increases with scattering angle. The modulation gives rise to an asymmetry in the intensity around a Bragg peak. Similar considerations for I_3 reveal an intensity contribution h_i^2 times a sum over cosine terms which is symmetric around the Bragg peaks ($i = 1, 2, 3$ with $h_1 = h$, $h_2 = k$, $h_3 = l$). This term shows a quite analogous influence of local static displacements and thermal movements: an increase of diffuse intensity around the Bragg peaks and a reduction of Bragg intensities, which is not discussed here. The second contribution I_2 has no analogue owing to the nonvanishing average displacement. The various diffuse intensity contributions may be separated by symmetry considerations. Once they are separated, the single coefficients may be determined by Fourier inversion. Owing to the symmetry constraints, there are relations between the displacements $\langle x \ldots \rangle$ and, in turn, between the γ and Q components. The same is true for the δ, ε and R, S components. Consequently, there are symmetry conditions for the individual contributions of the diffuse intensity which may be used to distinguish them. In general, the total diffuse intensity may be split into only a few independent terms. The single components of Q, R, S may be expressed separately by combinations of diffuse intensities that are measured in definite selected volumes in reciprocal space. Only a minimum volume must be explored in order to reveal the behaviour over the whole reciprocal space. This minimum repeat volume is different for the single components: I_{sro}, Q, R, S or combinations of them.

The Borie–Sparks method has been applied very frequently to binary and even ternary systems; some improvements have been communicated by Bardhan & Cohen (1976). The diffuse scattering of the historically important metallic compound Cu_3Au was been studied by Cowley (1950*a*,*b*) and the pair-correlation parameters could be determined. The typical fourfold splitting was found by Moss (1966) and explained in terms of atomic displacements. The same splitting has been found for many similar compounds such as Cu_3Pd (Ohshima *et al.*, 1976), Au_3Cu (Bessière *et al.*, 1983) and $Ag_{1-x}Mg_x$ (x = 0.15–0.20) (Ohshima & Harada, 1986). Similar pair-correlation functions have been determined. In order to demonstrate the disorder parameters in terms of structural models, computer programs were used (*e.g.* Gehlen & Cohen, 1965). A similar microdomain model was proposed by Hashimoto (1974, 1981, 1983, 1987). According to approximations made in the theoretical derivation, the evaluation of diffuse scattering is generally restricted to an area in reciprocal space where the influence of displacements is of the same order of magnitude as that of the pair-correlation function. The agreement between calculation and measurement is fairly good, but it should be remembered that the amount and quality of the experimental information used is low. No residual factors are so far available; these would give an idea of the reliability of the results.

The more general case of a multicomponent system with several atoms per lattice point was treated similarly by Hayakawa & Cohen (1975). Sources of error in the determination of the short-range-order coefficients are discussed by Gragg *et al.* (1973). In general, the assumption of constant $F_{\mathbf{nn}'|AA}, \ldots$ produces an incomplete separation of the order- and displacement-dependent components of diffuse scattering. By an alternative method, by separation of the form factors from the Q, R, S functions and solving a large array of linear relationships by least-squares methods, the accuracy of the separation of the various contributions is improved (Tibbals, 1975; Georgopoulos & Cohen, 1977; Wu *et al.*, 1983). The method does not work for neutron diffraction. The case of planar short-range order with corresponding diffuse intensity along rods in reciprocal space may also be treated along the Borie & Sparks method (Ohshima & Moss, 1983).

Multiwavelength methods taking advantage of the variation of the structure factor near an absorption edge (anomalous dispersion) are discussed by Cenedese *et al.* (1984). The same authors show that in some cases the neutron method allows contrast variation by using samples with different isotope substitution.

In general, X-ray and neutron methods are complementary. The neutron method is helpful in the cases of hydrides, oxides, carbides, Al–Mg distributions *etc.* In favourable cases it is possible to suppress (nuclear) Bragg scattering of neutrons when isotopes are used so that $\sum_\nu c_\nu f_\nu = 0$ for all equivalent positions. Another way to separate Bragg peaks is to record the diffuse intensity, if possible, at low $|\mathbf{H}|$ values. This can be achieved either by measurement at low angles or by using long wavelengths. For reasons of absorption the latter are the domain of neutron scattering. Bragg scattering is ruled out by exceeding the Bragg cut-off. In this way, 'diffuse' background owing to multiple Bragg scattering is avoided. Other diffuse-scattering contributions that increase with the $|\mathbf{H}|$ value [thermal diffuse scattering (TDS) and scattering due to long-range static displacements] are thus also minimized. Neutrons are preferable in cases where X-rays show only a small scattering contrast: (heavy) metal lattice distortions,

Huang scattering and so on should be measured at large values of $|\mathbf{H}|$. TDS can be separated by purely elastic neutron methods within the limits given by the energy resolution of an instrument. This technique is of particular importance at higher temperatures where TDS becomes remarkably strong. Neutron scattering is a good tool only in cases where (isotope/spin-) incoherent scattering is not too strong. In the case of magnetic materials, confusion with paramagnetic diffuse scattering could occur. This is also important when electrons are trapped by defects which themselves act as paramagnetic centres.

4.2.5.4.6. Comparison with the cluster method

In the general formula for diffuse scattering from random distributions equation (4.2.3.23*a*,*b*) may be used. Here $|\langle F(\mathbf{H})\rangle|^2$ describes the sharp Bragg maxima, while $|\Delta F(\mathbf{H})|^2 = \langle|F(\mathbf{H})|^2\rangle - |\langle F(\mathbf{H})\rangle|^2$ represents the contribution to diffuse scattering. Correlation effects can also be taken into account by using clusters of sufficient size if their distribution may be considered as random to a good approximation. The diffuse intensity is then given by

$$I_{\rm D}(\mathbf{H}) = \sum_\nu p_\nu |F_\nu(\mathbf{H})|^2 - \Big|\sum_\nu p_\nu F_\nu(\mathbf{H})\Big|^2, \qquad (4.2.5.82)$$

where $F_\nu(\mathbf{H})$ represents the difference structure factor of the νth cluster and p_ν is its *a priori* probability. Obviously equation (4.2.5.82) is of some use in only two cases. (1) The number of clusters is sufficiently small and meets the condition of a nearly random distribution. In principle, the structure may then be determined with the aid of refinement methods according to equation (4.2.5.82). Since the second term is assumed to be known from the average structure, the first term may be evaluated by introducing as many parameters as there are clusters involved. A special computer program for incoherent refinement has to be used if more than one representative cluster has to be introduced. In the case of more clusters constraints are necessary. (2) The number of clusters with similar structures is not limited. It may be assumed that their size distribution may be expressed by fluctuations using well known analytical expressions, *e.g.* Gaussians or Lorentzians. The distribution is still assumed to be random.

An early application of the cluster method was the calculation of the diffuse intensity of Guinier–Preston zones, where a single cluster is sufficient (see, *e.g.*, Gerold, 1954; Bubeck & Gerold, 1984). Unfortunately, no refinements of cluster structures have so far been published. The full theory of the cluster method was outlined by Jagodzinski & Haefner (1967).

A different approach to analysing extended defects in crystals is simply to construct analytically disorder models that include chemical substitution and atomic displacements around an atomic defect as consequence of the surrounding local distortions. This method works if the number of 'shells' of the first, second, ... neighbours is limited and if short- or long-range correlations between different clusters are neglected. After subtracting the underlying average structure and the calculation of the Fourier transform of the difference structure ΔF, the intensities can be fitted to the observed diffuse diffraction pattern and the parameters of the disorder model (occupancies and displacements) can be determined. For examples of this method see Neder *et al.* (1990) or Kaiser-Bischoff *et al.* (2005). Short-range correlations may simply be included by approximating the distribution function by summing over a finite number of defects (clusters) (Goff *et al.*, 1999).

4.2.5.5. Molecular crystals: orientational disorder

Molecular crystals show in principle disorder phenomena similar to those discussed in previous sections (*i.e.* substitutional or displacement disorder). Here we have to replace the structure factors $F_\nu(\mathbf{H})$ used in the previous sections by the molecular structure factors in their various orientations. These are usually rapidly varying functions in reciprocal space which may obscure the disorder diffuse scattering. Disorder in molecular crystals is treated by Guinier (1963), Amorós & Amorós (1968), Flack (1970), Epstein *et al.* (1982), Welberry & Siripitayananon (1986, 1987) and others.

A particular type of disorder is very common in molecular and also in ionic crystals: the centres of masses of molecules or ionic complexes form a perfect 3D lattice but their orientations are disordered. Sometimes these solids are called plastic crystals. In comparison, the liquid-crystalline state is characterized by an orientational order in the absence of long-range positional order of the centres of the molecules. A clear-cut separation is not possible in cases where translational symmetry occurs in a low dimension, *e.g.* in sheets or parallel to a few directions in crystal space. For discussion of these mesophases see Chapter 4.4.

An orientationally disordered crystal may be pictured by freezing molecules in different sites in one of several orientations. Local correlations between neighbouring molecules and correlations between position and orientation may be responsible for orientational short-range order. Thermal reorientations of the molecules are often related to an orientationally disordered crystal. Thermal vibrations of the centres of masses of the molecules, librational or rotational excitations around one or more axes of the molecules, jumps between different equilibrium positions or diffusion-like phenomena are responsible for diffuse scattering of dynamic origin. As mentioned above, the complexity of molecular structures and the associated large number of thermal modes complicate a separation from static disorder effects.

In general, high Debye–Waller factors are typical for scattering by orientationally disordered crystals. Consequently only a few Bragg reflections are observable. A large amount of structural information is stored in the diffuse background. It has to be analysed with respect to an incoherent and coherent part, elastic, quasielastic or inelastic nature, short-range correlations within one and the same molecule and between orientations of different molecules, and cross correlations between positional and orientational disorder scattering. Combined X-ray and neutron methods are therefore highly recommended.

(1) *General expressions*

On the assumption of a well ordered 3D lattice, a general expression for the scattering by an orientationally disordered crystal with one molecule per unit cell may be given. This is a very common situation. Moreover, orientational disorder is frequently related to molecules with an overall 'globular' shape and consequently to crystals of high (in particular, averaged) spherical symmetry. In the following, the relevant equations are given for this situation; these are discussed in some detail in a review article by Fouret (1979). The orientation of a molecule is characterized by a parameter ω_l, *e.g.* the set of Eulerian angles of three molecular axes with respect to the crystal axes: $l = 1, \ldots, D$ (for D possible different orientations). The equilibrium position of the centre of mass of a molecule in orientation ω_l is given by $\mathbf{r}_l$, the equilibrium position of atom k within a molecule l in orientation ω_l by $\mathbf{r}_{lk}$ and a displacement from this equilibrium position by $\mathbf{u}_{lk}$. Averaging over a long time, *i.e.* supposing that the lifetime of a discrete configuration is long compared with the period of atomic vibrations, the observed intensity may be deduced from the intensity expression corresponding to a given configuration at time t:

$$I(\mathbf{H}, t) = \sum_l \sum_{l'} F_l(\mathbf{H}, t) F_{l'}^+(\mathbf{H}, t) \times \exp\{2\pi i \mathbf{H}\cdot(\mathbf{r}_l - \mathbf{r}_{l'})\}, \qquad (4.2.5.83)$$

$$F_l(\mathbf{H}, t) = \sum_k f_k \exp\{2\pi i \mathbf{H}\cdot(\mathbf{r}_{lk} + \mathbf{u}_{lk})\}. \qquad (4.2.5.84)$$

Averaging procedures must be carried out with respect to the thermal vibrations (denoted by an overbar) and over all configurations (symbol $\langle\,\rangle$). The centre-of-mass translational vibrations and librations of the molecules are most important in this context. (Internal vibrations of the molecules are assumed to be decoupled and remain unconsidered.)

$$I(\mathbf{H},t)=\sum_l\sum_{l'}\langle\overline{F_l(\mathbf{H},t)F_{l'}^{+}(\mathbf{H},t)}\rangle \times\exp\{2\pi i\mathbf{H}\cdot(\mathbf{r}_l-\mathbf{r}_{l'})\}. \quad (4.2.5.83a)$$

Thermal averaging gives (*cf.* Chapter 4.1)

$$I=\sum_l\sum_{l'}\overline{F_lF_{l'}^{+}}\exp\{2\pi i\mathbf{H}\cdot(\mathbf{r}_l-\mathbf{r}_{l'})\},$$
$$\overline{F_lF_{l'}^{+}}=\sum_k\sum_{k'}f_kf_{k'}\exp\{2\pi i\mathbf{H}\cdot(\mathbf{r}_{lk}-\mathbf{r}_{l'k'})\} \times\overline{\exp\{2\pi i\mathbf{H}\cdot(\mathbf{u}_{lk}-\mathbf{u}_{l'k'})\}}. \quad (4.2.5.85)$$

In the harmonic approximation $\exp\{\overline{2\pi i\mathbf{H}\cdot\Delta\mathbf{u}}\}$ is replaced by $\exp\{\frac{1}{2}|2\pi\mathbf{H}\cdot\Delta\mathbf{u}|^2\}$. This is, however, a rather crude approximation because strongly anharmonic vibrations are quite common in an orientationally disordered crystal. In this approximation $\overline{F_lF_{l'}^{+}}$ becomes

$$\overline{F_lF_{l'}^{+}}=\sum_k\sum_{k'}f_kf_{k'}\exp\{-B_k(\omega_l)\} \times\exp\{-B_{k'}(\omega_{l'})\}\exp\{D_{lk;\,l'k'}\}. \quad (4.2.5.86)$$

B_k is equal to $\frac{1}{2}\overline{(2\pi\mathbf{H}\cdot\mathbf{u}_{lk})^2}$ (the Debye–Waller factor) and depends on the specific configuration ω_l. $D_{lk;\,l'k'}=\overline{(2\pi\mathbf{H}\cdot\mathbf{u}_{lk})(2\pi\mathbf{H}\cdot\mathbf{u}_{l'k'})}$ includes all the correlations between positions, orientations and vibrations of the molecules.

Averaging over different configurations demands a knowledge of the orientational probabilities. The probability of finding molecule l in orientation ω_l is given by $p(\omega_l)$. The double probability $p(\omega_l,\omega_{l'})$ gives the probability of finding two molecules l, l' in different orientations ω_l and $\omega_{l'}$, respectively. In the absence of correlations between the orientations we have $p(\omega_l,\omega_{l'})=p(\omega_l)p(\omega_{l'})$. If correlations exist, $p(\omega_l,\omega_{l'})=p(\omega_l)p'(\omega_l|\omega_{l'})$, where $p'(\omega_l|\omega_{l'})$ defines the conditional probability that molecule l' has the orientation ω_l *if* molecule l has the orientation $\omega_{l'}$. For long distances between l and l' $p'(\omega_l|\omega_{l'})$ tends to $p(\omega_{l'})$.

The difference $\Delta(\omega_l|\omega_{l'})=p'(\omega_l|\omega_{l'})-p(\omega_{l'})$ characterizes, therefore, the degree of short-range orientational correlation. Note that this formalism corresponds fully to the $p_\mu, p_{\mu\mu'}$ used in the context of translational disorder.

The average structure factor, sometimes called averaged form factor, of the molecule is given by

$$\langle F_l\rangle=\sum_{\omega_l}p(\omega_l)F_l(\omega_l). \quad (4.2.5.87)$$

(*a*) Negligible correlations between vibrations of different molecules (Einstein model):

$$D_{lk;\,l'k'}=0 \text{ for } l\neq l'.$$

From (4.2.5.86) it follows that (the prime symbol takes the Debye–Waller factor into account)

$$\overline{\langle I\rangle}=N^2|\langle F'\rangle|^2L(\mathbf{G}) + N\Big\{\sum_k\sum_{k'}\sum_{\omega_l}p(\omega_l)f_kf_{k'}\exp\{2\pi i\mathbf{H}\cdot(\mathbf{r}_{lk}-\mathbf{r}_{lk'})\} \times\exp\{D_{lk;\,lk'}\}-|\langle F'\rangle|^2\Big\} + N\sum_{\Delta l\neq0}\sum_{\omega_l}\sum_{\omega_{l'}}p(\omega_l)\Delta(\omega_l|\omega_{l'}) \times F_l'(\omega_l)F_{l'}^{+}(\omega_{l'}) \times\exp\{2\pi i\mathbf{H}\cdot(\mathbf{r}_l-\mathbf{r}_{l'})\}. \quad (4.2.5.88)$$

$L(\mathbf{G})$ is the reciprocal lattice of the well defined ordered lattice. The first term describes Bragg scattering from an averaged structure. The second term governs the diffuse scattering in the absence of short-range orientational correlations. The last term takes the correlation between the orientations into account.

If rigid molecules with centre-of-mass translational displacements and negligible librations are assumed, which is a first approximation only, $|\langle F\rangle|^2$ is no longer affected by a Debye–Waller factor.

In this approximation the diffuse scattering may therefore be separated into two parts:

$$N(\langle F^2\rangle-|\langle F'\rangle|^2)=N(F^2-|\langle F\rangle|^2)+N(|\langle F\rangle|^2-|\langle F'\rangle|^2) \quad (4.2.5.89)$$

with

$$\langle F^2\rangle=\sum_{\omega_l}\sum_{\omega_{l'}}\sum_k\sum_{k'}f_k(\omega_l)f_{k'}(\omega_{l'})p(\omega_l) \times\exp\{2\pi i\mathbf{H}\cdot(\mathbf{r}_{lk}-\mathbf{r}_{l'k'})\}. \quad (4.2.5.90)$$

The first term in (4.2.5.89) gives the scattering from equilibrium fluctuations in the scattering from individual molecules (diffuse scattering without correlations), the second gives the contribution from the centre-of-mass thermal vibrations of the molecules.

(*b*) If intermolecular correlations between the molecules cannot be neglected, the final intensity expression for diffuse scattering is very complicated. In many cases these correlations are caused by dynamical processes (see Chapter 4.1). A simplified treatment assumes the molecule to be a rigid body with a centre-of-mass displacement $\mathbf{u}_l$ and neglects vibrational–librational and librational–librational correlations: $D_{l;\,l'}=\overline{(2\pi\mathbf{H}\cdot\mathbf{u}_l)(2\pi\mathbf{H}\cdot\mathbf{u}_{l'})}$ $(l\neq l')$. The following expression approximately holds:

$$\overline{\langle I\rangle}=N^2|\langle F'\rangle|^2L(\mathbf{G}) + \Big\langle\sum_l\sum_{l'}F_l'(\omega_l)F_{l'}^{'+}(\omega_{l'})\exp\{D_{l;\,l'}\}\Big\rangle\{2\pi i\mathbf{H}\cdot(\mathbf{r}_l-\mathbf{r}_{l'})\} + N\Big[\sum_{\omega_l}\sum_{k,\,k'}p(\omega_l)f_kf_{k'}\exp\{2\pi i\mathbf{H}\cdot(\mathbf{r}_{lk}-\mathbf{r}_{l'k'})\} \times\exp\{D_{lk;\,l'k'}\}-\sum_{\omega_l}\sum_{\omega_{l'}}\sum_k\sum_{k'}p(\omega_l)p(\omega_{l'})f_kf_{k'} \times\exp\{2\pi i\mathbf{H}\cdot(\mathbf{r}_{lk}-\mathbf{r}_{l'k'})\} \times\exp\{D_{lk;\,l'k'}\}\Big]+\sum_{l\neq l'}\sum_{\omega_l}\sum_{\omega_l}p(\omega_l)\Delta(\omega_l|\omega_{l'}) \times F_l'(\omega_l)F_{l'}^{'+}(\omega_{l'}) \times\exp\{2\pi i\mathbf{H}\cdot(\mathbf{r}_l-\mathbf{r}_{l'})\}\exp\{D_{l;\,l'}\}. \quad (4.2.5.91)$$

Again, the first term describes Bragg scattering and the second corresponds to the average thermal diffuse scattering in the disordered crystal. Because just one molecule belongs to one unit cell only acoustic waves contribute to this part. To an approximation, the result for an ordered crystal may be used by replacing F by $\langle F'\rangle$ [Chapter 4.1, equation (4.1.3.4)]. The third term corresponds to random-disorder diffuse scattering. If librations are neglected this term may be replaced by $N(\langle F^2\rangle-\langle F\rangle^2)$. The

last term in (4.2.5.91) describes space correlations. Omission of $\exp\{D_{l;\,l'}\}$ or expansion to $\sim(1 + D_{l;\,l'})$ are further simplifying approximations.

In either (4.2.5.88) or (4.2.5.91) the diffuse-scattering part depends on a knowledge of the conditional probability $\Delta(\omega_l|\omega_{l'})$ and the orientational probability $p(\omega_l)$. The latter may be found, at least in principle, from the average structure factor.

(2) *Rotational structure (form) factor*

In certain cases and with simplifying assumptions, $\langle F\rangle$ [equation (4.2.5.87)] and $\langle \Delta F^2\rangle$ [equation (4.2.5.90)] may be calculated. Assuming only one molecule per unit cell and treating the molecule as a rigid body, one derives from the structure factor of an ordered crystal F_l

$$\langle F\rangle = \sum_k f_k \langle \exp\{2\pi i \mathbf{H}\cdot\mathbf{r}_{lk}\}\rangle \tag{4.2.5.92}$$

and

$$\langle \Delta F^2\rangle = \sum_k \sum_{k'} f_k f_{k'} [\langle \exp\{2\pi i \mathbf{H}\cdot(\mathbf{r}_{lk} - \mathbf{r}_{l'k'})\}\rangle - \langle \exp\{2\pi i \mathbf{H}\cdot\mathbf{r}_{lk}\}\rangle\langle \exp\{2\pi i \mathbf{H}\cdot\mathbf{r}_{l'k'}\}\rangle]. \tag{4.2.5.93}$$

If the molecules have random orientation in space the following expressions hold [see, *e.g.*, Dolling *et al.* (1979)]:

$$\langle F\rangle = \sum_k f_k j_0(\mathbf{H}\cdot\mathbf{r}_k) \tag{4.2.5.94}$$

$$\langle |\Delta F|^2\rangle = \sum_k \sum_{k'} f_k f_{k'} \{ j_0[\mathbf{H}\cdot(\mathbf{r}_k - \mathbf{r}_{k'})] - j_0(\mathbf{H}\cdot\mathbf{r}_k) j_0(\mathbf{H}\cdot\mathbf{r}_{k'})\}. \tag{4.2.5.95}$$

$j_0(z)$ is the zeroth order of the spherical Bessel functions and describes an atom k uniformly distributed over a shell of radius r_k.

In practice the molecules perform finite librations about the main orientation. The structure factor may then be found by the method of symmetry-adapted functions [see, *e.g.*, Press (1973), Press & Hüller (1973), Dolling *et al.* (1979), Prandl (1981, and references therein)].

$$\langle F\rangle = \sum_k f_k 4\pi \sum_\nu \sum_{\mu=-\nu}^{+\nu} i^\nu j_\nu(\mathbf{H}\cdot\mathbf{r}_k) C_{\nu\mu}^{(k)} Y_{\nu\mu}(\theta,\varphi). \tag{4.2.5.96}$$

$j_\nu(z)$ is the νth order of spherical Bessel functions, the coefficients $C_{\nu\mu}^{(k)}$ characterize the angular distribution of $\mathbf{r}_k$ and $Y(\theta,\varphi)$ are the spherical harmonics where $|\mathbf{H}|, \theta, \varphi$ denote polar coordinates of $\mathbf{H}$.

The general case of an arbitrary crystal, site and molecular symmetry and the case of several symmetrically equivalent orientationally disordered molecules per unit cell are treated by Prandl (1981); an example is given by Hohlwein *et al.* (1986). As mentioned above, cubic plastic crystals are common and therefore mostly studied up to now. The expression for $\langle F\rangle$ may then be formulated as an expansion in cubic harmonics $K_{\nu\mu}(\theta,\varphi)$:

$$\langle F\rangle = \sum_k f_k 4\pi \sum_\nu \sum_\mu i^\nu j_\nu(\mathbf{H}\cdot\mathbf{r}_k) C_{\nu\mu}^{\prime(k)} K_{\nu\mu}(\theta,\varphi), \tag{4.2.5.97}$$

where $C'_{\nu\mu}$ are modified expansion coefficients.

Taking into account isotropic centre-of-mass translational displacements, which are not correlated with the librations, we obtain

$$\langle F'\rangle = \langle F\rangle \exp\{-\tfrac{1}{6}H^2\langle U^2\rangle\}. \tag{4.2.5.98}$$

U is the mean-square translational displacement of the molecule. Correlations between translational and vibrational displacements are treated by Press *et al.* (1979).

Equivalent expressions for crystals with symmetry other than cubic may be found from the same concept of symmetry-adapted functions [tables are given by Bradley & Cracknell (1972)].

(3) *Short-range correlations*

The final terms in equations (4.2.5.88) and (4.2.5.91) concern correlations between the orientations of different molecules. Detailed evaluations need knowledge of a particular model. Examples are compounds with nitrate groups (Wong *et al.*, 1984; Lefebvre *et al.*, 1984), CBr_4 (More *et al.*, 1980, 1984) and many others (see Sherwood, 1979). The situation is even more complicated when a modulation wave with respect to the occupation of different molecular orientations is superimposed. A limiting case would be a box-like function describing a pattern of domains. Within one domain all molecules have the same orientation. This situation is common in ferroelectrics where molecules exhibit a permanent dipole moment. The modulation may occur in one or more directions in space. The observed intensity in this type of orientationally disordered crystal is characterized by a system of more or less diffuse satellite reflections. The general scattering theory of a crystal with occupational modulation waves follows the same lines as outlined in Section 4.2.3.5.1.

4.2.6. Disorder diffuse scattering from aperiodic crystals

The preceding sections of this chapter have either been related to disorder phenomena in conventional crystals defined by the presence of 3D translational symmetry, *i.e.* by a 3D lattice function, at least in the averaged sense, or to solids with crystalline order in only lower (2 or 1) dimensions where the ordering principle along 'nonperiodic' directions shows a gradual transition from long- to short-range order, in particular to a liquid-like behaviour and, finally, to an (almost) random ordering behaviour of structural units. So-called aperiodic crystals do not fit this treatment because aperiodicity denotes a different type of order, which is nonperiodic in 3D space but where translational order may be restored in higher-dimensional ($n > 3$) direct space. Three types of solids are commonly included in the class of aperiodic structures: (i) incommensurately modulated structures (IMSs), where structural parameters of any kind (coordinates, occupancies, orientations of extended molecules or subunits in a structure, atomic displacement parameters) deviate periodically from the average ('basic') structure and where the modulation period is incommensurate compared to that of the basic structure; (ii) composite structures (CSs), which consist of two (or more) intergrown incommensurate substructures with mutual interactions giving rise to mutual (incommensurate) modulations; and (iii) quasicrystals (QCs), which might simply be viewed as made up by n (≥ 2) different tiles – analogous to the elementary cell in crystals – which are arranged according to specific matching rules and which are decorated by atoms or atomic clusters. Most common are icosahedral (i-type) quasicrystals with 3D aperiodic order (3D 'tiles') and decagonal quasicrystals (d-phases) with 2D aperiodicity and one unique axis along which the QC is periodically ordered. The basic 'crystallography' of aperiodic crystals is given in Chapter 4.6 of this volume; see also the review articles by Janssen & Janner (1987) and van Smaalen (2004) (and further references therein). We only point out some of the aspects here to provide the background for a short discussion about disorder diffuse scattering in aperiodic crystals.

As outlined in Section 4.6.1, a d-dimensional (dD) ideal aperiodic crystal can be defined as a dD irrational section of an nD ('hyper'-)crystal with nD crystal symmetry. Corresponding to the section of the nD hypercrystal with the dD ($d = 1, 2, 3$) direct physical (= 'external' or 'parallel') space we have a projection of the (weighted) nD reciprocal hyperlattice onto the dD reciprocal physical space. The occurrence of Bragg reflections as a signature

of an ordered (in at least an averaged sense) aperiodic crystal form a countable dense pattern of the projected reciprocal (hyper-)lattice vectors. Disorder phenomena, *i.e.* deviations from the periodicity in higher-dimensional direct (hyper-)space, are thus related to diffuse phenomena in reciprocal (hyper-)space projected down to the reciprocal physical space. Therefore only fluctuations from the aperiodic order infer diffuse scattering in its true sense, which might be hard to discern in a dense pattern of discrete (Bragg) reflections. As a consequence, in the higher-dimensional description of aperiodic crystals the atoms must be replaced by 'hyperatoms' or 'atomic surfaces', which are extended along $(n - d)$ dimensions. If, for example, an IMS exhibits a modulation in only one direction (1D IMS), we have $n = 2$ and a 1D atomic surface (which is a continuous modulation function extended along the 1D 'internal' or 'perpendicular' subspace). The physical subspace is spanned by 1 (and +2 'unaffected') dimensions. In a second example, a decagonal QC with aperiodic order in two dimensions is described by $n = 4$ (plus the remaining coordinate along the unaffected periodic direction) and $d = 2$, *i.e.* by 2D atomic surfaces. The atomic surfaces are, as shown in Chapter 4.6, continuous n-dimensional objects for IMSs and CSs, and discrete ones in the case of QCs. In addition to the 'hyperlattice' fluctuations within the physical (parallel) subspace we have therefore an additional quality of disorder phenomena related to positions and shape and size fluctuations of the atomic surfaces within the perpendicular subspace. Therefore, one has to consider disordering effects in aperiodic crystals related to fluctuations in the (external) physical subspace as well as in the internal subspace, but one should bear in mind that the two types are often coupled. Disordering due to displacements along directions within the physical subspace are – in the context of aperiodic crystals – commonly termed 'phonon-like', in contrast to 'phason-like' disorder related to displacements parallel to directions within the internal subspace. The term phason originates from a particular type of (dynamical) fluctuations of an IMS (see below).

4.2.6.1. Incommensurately modulated structures

Quite generally, small domains with periodic or aperiodic structures give rise to broadening of reflections. Diffuse satellite scattering is due to the limited coherence length of a modulation wave within a crystal or due to short-range order of twin or nanodomains (with an 'internal' modulated structure) embedded in a periodic matrix structure. This type of diffuse scattering can be treated by the rules outlined in Section 4.2.3.5. Structural fluctuations with limited correlation lengths are, for example, responsible for diffuse scattering in 1D organic conductors (Pouget, 2004). In some cases, modulated structures are intermediate phases within a limited temperature range between a high- and low-temperature phase (*e.g.* quartz) where the structural change is driven by a dynamical instability (a soft mode). In addition to (inelastic) soft-mode diffuse scattering, dynamic fluctuations of phase and amplitude of the modulation wave give rise to diffuse intensity. In particular, the phase fluctuations, *phasons*, give rise to low-frequency scattering which might be observable as an additional diffuse contribution around condensing reflections.

4.2.6.2. Composite structures

In the case of CSs, diffuse scattering relates to interactions between the component substructures which are responsible for mutual modulations: each substructure becomes modulated with the period of the other. If one of the substructures is low-dimensional, for example chain-like structural elements embedded in tubes of a host structure, one observes diffuse planes if direct interchain correlations are mostly absent. The diffuse planes are, however, not only due to the included subsystem, but also due to corresponding modulations of the matrix structure. On the other hand, maxima superimposed on the diffuse planes reflect the influence of the matrix structure on the chain system. The thickness of the diffuse planes depends on the degree of short- or long-range order along the unique direction (*cf.* Section 4.2.5.3). This might be either a consequence of faults in the surrounding matrix which interrupt the (longitudinal) coherence of the chains (Rosshirt *et al.*, 1991) or, intrinsically, due to the degree of misfit between the periods of the mutually incommensurate structures of the host and guest structures. If this misfit becomes large, *e.g.* as a consequence of different thermal expansion coefficients of the two substructures, the modulation is only preserved within small domains and one observes a series of diffuse satellite planes (Weber *et al.*, 2000). Equivalent considerations relate to composite systems made up from stacks of planar molecules (*e.g.* van Smaalen *et al.*, 1998) or an intergrowth of layer-like substructures where the modulation is mainly due to a one-dimensional stacking along the normal to the layers. Correspondingly, quite extended diffuse streaks occur at positions of the satellites in reciprocal space.

A further discussion of the more complicated disorder diffuse scattering of higher- (than one-) dimensionally modulated IMSs and CSs and the corresponding diffuse patterns in reciprocal space is beyond the scope of this chapter. We refer to Section 4.6.3 and the references cited therein. For examples, see also Petricek *et al.* (1991).

4.2.6.3. Quasicrystals

As in the case of conventional crystals, there is no unique theory of diffuse scattering by quasicrystals. Chemical disorder, phonon- and phason-like displacive disorder, topological glass-like disorder and domain disorder exist. The term domain covers those with an aperiodic structure as well as periodic approximant domains, which are also known as approximant phases (*cf.* Section 4.6.3). Approximant phases exhibit local atomic clusters which do not differ significantly from those of related aperiodic QCs. In d-phases, disorder diffuse scattering occurs which is related to the periodic direction. Reviews of disorder diffuse scattering from quasicrystals are given, *e.g.*, by Steurer & Frey (1998) and Estermann & Steurer (1998).

Chemical disorder. Many of the quasicrystals are ternary intermetallic phases consisting of atomic clusters where two components are transition metals (TMs) with only a small difference in Z (the number of electrons). Most of them exhibit a certain amount of substitutional (chemical) disorder, in particular with respect to the distribution of the TMs. This behaviour is equally true in the approximant phases. Chemical short-range order between the TMs, if any, is largely uninvestigated because conventional X-ray diffraction and electron-microscopy methods are not sensitive enough to provide significant contrast between the TMs. If the X-ray form-factor difference Δf is small, X-ray patterns do not show diffuse scattering, whereas an analogous neutron pattern could reveal a diffuse component due to the different scattering contrast Δb of the TMs (where the b's are the neutron scattering lengths). In practice, the chemical disorder phenomena might be more complex as the compositional stability of the QCs is often rather extended and the atomic distribution in a sample is not always structurally homogeneous. Depending on the crystal-growth process, microstructures may occur with locally coexisting small QC domains with fluctuating chemical content and, moreover, coexisting QC and approximant domains. Chemical disorder might also be caused by phasonic disorder.

Phonon-type (static or dynamic) displacements, fluctuations or straining relate to the physical subspace coordinates giving rise to continuous local distortions of the atomic structure. Phason-type disorder describes, as indicated above, discontinuous atomic jumps between different sites in an aperiodic structure. Qualitatively, dominant phonon- or phason-related scattering may be separated by analysing the dependence of the diffracted inten-

sities on the components of the scattering vector in the external and the internal subspace, H_e (Q_e) and H_i (Q_i), respectively (*cf.* above and also Section 4.6.3). There are different kinds of phason-like disorder, including random phason fluctuations, phason-type modulations and phason straining, and also shape and size fluctuations of the hyperatomic surfaces. If displacing an atomic surface (hyperatom) parallel to an internal space component by any kind of phason fluctuation which is equivalent to an infinitesimal rotation of the external (physical) space, it might happen that the hyperatom no longer intersects the physical space. Then an empty site is created, which is compensated by a (real) atom 'appearing' at a different position in physical space. In addition, there might even be a change of atomic species as a hyperatom may be chemically different at different sites of the atomic surface. Randomly distributed phason strains are responsible for Bragg-peak broadening and Huang-type diffuse scattering close to Bragg peaks. There are well developed theories based on the elastic theory of icosahedral (*e.g.* Jaric & Nelson, 1988) or decagonal (Lei *et al.*, 1999) quasicrystals that also include phonon–phason coupling. An example of the quantitative analysis of diffuse scattering by an i-phase (Al–Pd–Mn) is given by de Boissieu *et al.* (1995) and by a d-phase (Al–Ni–Fe) by Weidner *et al.* (2004). Dislocations in quasicrystals have partly phonon- and partly phason-like character; a discussion of the specific dislocation-related diffuse scattering will not be given here (*cf.* Section 4.6.3). Arcs and rings of localized diffuse scattering are observed in various i-phases and could be modelled in terms of some short-range 'glass-like' ordering of icosahedral clusters (Goldman *et al.*, 1988; Gibbons & Kelton, 1993). Phason-related diffuse scattering phenomena are discussed in more detail in Section 4.6.3. Depending on the exact stoichiometry and the growth conditions, d-phases very often show intergrown domain structures where the internal atomic structure of an individual domain varies between a (periodic) approximant structure, more or less strained aperiodic domains, or transient aperiodic variants (Frey & Weidner, 2002). Apart from finite size effects of domains of any kind which cause peak broadening, there are complex diffraction patterns of satellite reflections, diffuse maxima and diffuse streaking in d-Al–Ni–Co and other d-phases (Weidner *et al.*, 2001). In various d-phases one also observes, in addition to the Bragg layers, prominent diffuse layers perpendicular to the unique 'periodic' axis. They correspond to n-fold (n = 2, 4, 8) superperiods along this direction. In different d-phases there is a gradual change from almost completely diffuse planes to layers of superstructure reflections (satellites). The picture of a kind of stacking disorder of aperiodic layers does not match such observations. An explanation is rather due to 1D columns of atomic icosahedral clusters along the unique direction (Steurer & Frey, 1998). The temperature behaviour of these diffuse layers was studied by *in situ* neutron diffraction (Frey & Weidner, 2003), which shed some light on the complicated order/disorder phase transitions in d-Al–Ni–Co.

4.2.7. Computer simulations and modelling

4.2.7.1. Introduction

The various analytical expressions given in Section 4.2.5 are mostly rather complex, so their application is often restricted to relatively simple systems. Even in these cases analytical solutions are often not available. For larger displacements the approximations that use an expansion of the exponentials [*e.g.* equation (4.2.3.27)] are no longer valid. Hence there is a need for alternative approaches to tackling more complicated disorder models. In the past, optical transforms (*e.g.* Harburn *et al.*, 1974, 1975) and the videographic method (Rahman, 1993) were developed for this purpose. In the first method, a 2D mask with holes with sizes that represent the scattering power of the atoms is generated, which is then subjected to coherent light (from a laser) to produce a diffraction image. Problems arise for strong scatterers requiring very large holes. These problems were overcome in the second method, where the mask is replaced by a computer image with intensities proportional to the scattering power for each pixel. With the advent of more and more powerful computers these methods are now replaced by complete computer simulations, both to set up the disorder model and to calculate the diffraction pattern.

4.2.7.2. Simulation programs

Having established a disordered crystal with the types and positions of all atoms involved (a configuration), *e.g.* by using one of the methods described below, computer programs employing fast-Fourier-transform techniques can be used to calculate the diffraction pattern, which may be compared with the observation. It has to be borne in mind, however, that there is still a large gap between a real crystal with its ~10^{23} atoms and the one simulated by the computer with only several thousand atoms. This means that very long range correlations can not be included and have to be treated in an average manner. Furthermore, the limited size of the simulated crystal leads to termination effects, giving rise to considerable noise in the calculated diffraction pattern. Butler & Welberry (1992) have introduced a technique to avoid this problem in their program *DIFFUSE* by dividing the simulated crystal into smaller 'lots'. For each lot the intensity is calculated and then the intensities of all lots are summed up incoherently, which finally results in a smooth intensity distribution. Note, however, that in this case long-range correlations are restricted to even smaller values. To overcome this problem Boysen (1997) has proposed a method for suppressing the subsidiary maxima by multiplying the scattering density of the model crystal by a suitably designed weighting function simulating the effect of the instrumental resolution function.

A very versatile computer program, *DISCUS*, which allows not only the calculation of the scattering intensities but also allows the model structures to be built up in various ways, has been designed by Proffen & Neder (1999). It contains modules for reverse Monte Carlo (RMC, see below) simulation, the calculation of powder patterns, RMC-type refinement of pair-distribution functions (PDFs, see below) and many other useful tools for analysing disorder diffuse scattering.

Other computer programs have been developed to calculate diffuse scattering, some for specific tasks, such as *SERENA* (Micu & Smith, 1995), which uses a collection of atomic configurations calculated from a molecular dynamics simulation of molecular crystals.

4.2.7.3. Modelling procedures

Several well established methods can be used to create the simulated crystal on the computer. With such a crystal at hand, it is possible to calculate various thermodynamical properties and study the effect of specific parameters of the underlying model. By Fourier transformation, one obtains the diffraction pattern of the total scattering, *i.e.* the diffuse intensities and the Bragg peaks. The latter may lead to difficulties due to the termination effects mentioned in Section 4.2.7.2. These may be circumvented by excluding regions around the Bragg peaks (note, however, that in this case valuable information about the disorder may be lost), by subtracting the average structure or by using the approximation of Boysen (1997) mentioned above. A major advantage of such modelling procedures is that realistic physical models are introduced at the beginning, providing further insight into the pair interactions of the system, which can only be obtained *a posteriori* from the correlation parameters or fluctuation wave amplitudes derived from one of the methods described in Section 4.2.5.

4.2.7.3.1. Molecular dynamics

Molecular dynamics (MD) techniques have been developed to study the dynamics of a system. They may also be used to study static disorder problems (by taking time averages or snapshots), but they are particularly useful in the case of dynamic disorder, *e.g.* diffusing atoms in superionic conductors. The principle is to set up a certain configuration of atoms with assumed interatomic potentials $\Phi_{ij}(r_{ij})$ and subject them to Newton's equation of motion,

$$F_i(t) = m_i \frac{\mathrm{d}^2 r_i(t)}{\mathrm{d}t^2}, \qquad (4.2.7.1)$$

where the force $F_i(t)$ is calculated from the gradient of Φ. The equations are solved approximately by replacing the differential $\mathrm{d}t$ by a small but finite time step Δt to find new positions $r_i(t + \Delta t)$. This is repeated until an equilibrium configuration is found. MD techniques are quite useful if only short-range interactions are effective, even allowing the transfer of potential parameters between different systems, but are less reliable in the presence of significant long-range interactions.

4.2.7.3.2. Monte Carlo calculations

Monte Carlo (MC) methods appear to be more suited to the study of static disorder and many examples of their application can be found in the literature. Different variants allowing simulations and refinements have been applied:

(1) *Direct MC simulation*. In this method, introduced by Metropolis *et al.* (1953), a starting configuration is again set up in accordance with the known average structure and other crystal, chemical and physical information if available, and an appropriate interaction potential is chosen. The choice of this potential can be a quite delicate task. On the one hand, it should be as simple as possible to allow as large a simulation box size as can reasonably be handled by the computer's capacity. On the other hand, it must be detailed enough to include all the relevant interaction parameters of the system. Frequently used interaction potentials are a pseudo spin Ising Hamiltonian, where the 'spins' can either be binary (*e.g.* atom types or molecular orientations) or continuous (displacements), and harmonic springs for the displacements.

Having set up the starting configuration and defined the Hamiltonian, one proceeds by choosing a specific site at random and changing its parameters (occupancies and positions) by a random amount (a 'move'). The energy of this new configuration is calculated and compared with the old one. If the difference ΔE is negative, the move is accepted. If it is positive it is accepted with a probability

$$P = \exp\{-\Delta E/k_\mathrm{B}T\}/[1 + \exp\{-\Delta E/k_\mathrm{B}T\}], \qquad (4.2.7.2)$$

where T is a temperature and k_B is Boltzmann's constant. Then another site is chosen at random and the process is repeated again and again until an equilibrium configuration is found, *i.e.* until the energies fluctuate around some average value. After this, the corresponding intensity distribution is calculated and compared with the observed one. The parameters of the Hamiltonian may then be modified to improve the agreement between the calculated and observed diffraction patterns. This rather cumbersome trial-and-error method may be used to study the influence of the various parameters of the model. Further details of this method together with some illustrative examples may be found in Welberry & Butler (1994).

In an attempt to automate the adjustment of the model parameters, Welberry *et al.* (1998) have used a least-squares procedure to minimize

$$\chi^2 = \sum w(\Delta I)^2, \qquad (4.2.7.3)$$

where ΔI are the differences between the observed and calculated intensities and w are the appropriate weights. The problem with this approach is that the necessary differentials $\delta\Delta I/\delta p_i$ must be calculated numerically by performing full MC simulations with parameters p_i and $p_i + \delta p_i$ at each iteration step, which presents a formidable task even for the fastest modern computers.

(2) *Reverse MC calculations*. Application of the direct MC method may be very time consuming, as many MC simulations are necessary to arrive at a final configuration. To overcome this problem, the so-called reverse Monte Carlo (RMC) method has been developed, originally for liquids and glasses (McGreevy & Pusztai, 1988) and later for disordered single crystals (Nield *et al.*, 1995).

RMC is a model-free approach, *i.e.* without the need to define a proper interaction Hamiltonian. Otherwise it proceeds in a very similar way to direct MC analysis. A starting configuration is set up and random 'moves' of the atoms are carried out. The only difference is that acceptance or non-acceptance of a move is based on the agreement between observed and calculated diffraction intensities, *i.e.* equation (4.2.7.2) is replaced by

$$P = \exp\{-\Delta\chi^2/2\}, \qquad (4.2.7.4)$$

where χ^2 is defined in equation (4.2.7.3) and $\Delta\chi^2 = \chi^2_\mathrm{new} - \chi^2_\mathrm{old}$. Usually only a single MC run is necessary to arrive at a configuration with a diffraction pattern consistent with the observation. A drawback of the RMC technique is that usually only one configuration is found satisfying the observed diffraction pattern. In fact, it is possible that different configurations may produce the same or very similar intensity distributions (see *e.g.* Welberry & Butler, 1994). In this context, it has to be borne in mind that the diffuse scattering contains information about two-body correlations only, while the physical reason for a particular disordered structure may also be influenced by three- and many-body correlations. Such many-body correlations can easily be incorporated in the direct MC method. Moreover, RMC is susceptible to fitting artefacts (noise) in the diffraction pattern. To avoid unreasonable atomic configurations, restrictions such as a limiting nearest-neighbour approach can be built in. Weak constraints, *e.g.* ranges of interatomic distances or bond angles (*i.e.* three-body correlations) can be introduced by adding further terms in the definition of χ^2 [equation (4.2.7.3)]. In the same way, multiple data sets (*e.g.* neutron and X-ray data, EXAFS measurements *etc.*) may be incorporated. For more details and critical reviews of this method see *e.g.* McGreevy (2001) and Welberry & Proffen (1998). Many applications of this method can be found in the literature, mainly for powder diffraction, but also for single-crystal data.

(3) *Simulated annealing and evolutionary algorithms*. A general problem with MC methods is that they may easily converge to some local minima without having found the global one. One way to reduce such risks is to start with a high probability in (4.2.7.2) by using a large 'temperature' T, *i.e.* initially allowing many 'false' moves before gradually reducing T during the course of the simulation cycles. This is called 'simulated annealing', although it has nothing to do with real annealing. In the RMC method one may introduce a weighting parameter similar to T in (4.2.7.2).

Another effective way to find the global minimum and also to accelerate the optimization of the energy parameters of a given MC model is by using the principles of evolutionary theory: selection, recombination and mutation. Two such evolutionary (or genetic) algorithms have been proposed: the differential evolution (DE) algorithm (Weber & Bürgi, 2002) and the cooperative evolution (CE) algorithm (Weber, 2005). A single parameter of the model is called a gene and a set of genes is called a chromosome, p being the genotype of an individual. First a population consisting of several individuals is built up and the corresponding diffraction patterns are calculated and compared

with the observation. The fitness of each individual is quantified by χ^2. Children are then created by choosing one parent individual and calculating the second one from three randomly chosen individuals according to

$$p'_c = p_c + f_m(p_a - p_b), \qquad (4.2.7.5)$$

where f_m governs the mutations. The chromosome of the child is obtained by combining the genes of the two parents governed by a crossover (or recombination) constant f_r. If its fitness is higher than that of the parent, it replaces it. This procedure is repeated until some convergence criterion is reached. This DE method is still rather time-consuming on the computer. Therefore, the CE technique was introduced, where only one crystal is built up during the refinement. Here a large population is created spanning a large but reasonable parameter space. Individuals are selected at random to decide upon acceptance or rejection of an MC move *via* their own energy criteria. Then χ^2 is calculated and according to its positive or negative change a gratification or penalty weight is given to that individual. It may live as long as this weight is positive, otherwise it is replaced by a new individual calculated from (4.2.7.5). This way, useful individuals live longer to act on the same crystal, while unsuccessful ones are eliminated early. Note that the recombination operation is not used in this technique.

(4) *The PDF method*. The pair-distribution function (PDF) has long been used for the analysis of liquids, glasses and amorphous substances (Warren, 1969), but has recently regained considerable interest for the analysis of crystalline substances as well (Egami, 1990; Billinge & Egami, 1993; Egami, 2004). The PDF is obtained by a Fourier transformation of the total (Bragg plus diffuse) scattering in a powder pattern,

$$\rho_0 G(r) = \rho_0 + \tfrac{1}{2}\int H[S(H) - 1]\sin(2\pi H)\ \mathrm{d}H. \qquad (4.2.7.6)$$

This is nothing other than the van Hove correlation function (4.2.2.2) or the related Patterson function (4.2.2.5) averaged spherically and taken at $t = 0$ (a snapshot) and is given by

$$G^{\mathrm{PDF}}(r) = 4\pi r[\rho(r) - \rho_0] = \left(\sum c_i b_i\right)^{-2} 4\pi r \rho_0 G(r), \qquad (4.2.7.7)$$

where ρ_0 is the average number density and

$$\rho(r) = (1/N)\sum (b_i b_{i'}/\langle b\rangle^2)\delta(r - r_{ii'}). \qquad (4.2.7.8)$$

The δ functions are then convoluted with a normalized Gaussian to account for (harmonic) thermal motion. Parameter refinement proceeds in a similar way to the RMC technique. First a model is built, initially within just one unit cell and with periodic boundary conditions, then its PDF is calculated, compared with the observed one and further improved using, for example, MC simulated annealing. The model is then enlarged to include longer-range correlations. Owing to the small size of the models, this technique is much faster than the RMC method. It is essential, however, that data are measured up to very high H values to minimize truncation errors in (4.2.7.6).

4.2.7.3.3. General remarks

All of the different modelling techniques mentioned in this section have their specific merits and limitations and have contributed much to our understanding of disorder in crystalline materials following the interpretation of the corresponding diffuse scattering. It should be borne in mind, however, that application of these methods is still far from being routine work and it requires a lot of intuition to ensure that the final model is physically and chemically reasonable. In particular, it must always be ensured that the average structure remains consistent with that derived from the Bragg reflections alone. This may be done by keeping the Bragg reflections, *i.e.* by analysing the total scattering, or by designing special algorithms, *e.g.* by swapping two atoms at the same time (Proffen & Welberry, 1997). Moreover, possible traps and corrections like local minima, termination errors, instrumental resolution, statistical noise, inelasticity *etc*. must be carefully considered. All this means that the analytical methods outlined in Section 4.2.5 keep their value and should be preferred wherever possible.

The newly emerging technique of using full quantum-mechanical *ab initio* calculations for structure predictions along with MD simulations may also be applied to disordered systems. The limited currently available computer power, however, restricts this possibility to rather simple systems and small simulation box sizes, but, with the expected further increase of computer capacities, this may open up new perspectives for the future.

4.2.8. Experimental techniques and data evaluation

Single-crystal and powder diffractometry are used in diffuse scattering work. Conventional and more sophisticated special techniques and instruments are now available at synchrotron facilities and modern neutron reactor and spallation sources. The full merit of the dedicated machines may be assessed by inspecting the corresponding handbooks, which are available upon request from the facilities. In the following, some common important aspects that should be considered when planning and performing a diffuse-scattering experiment are summarized and a short overview of the techniques is given. Methodological aspects of diffuse scattering at low angles, *i.e.* small-angle-scattering techniques, and high-resolution single-crystal diffractometers are excluded. Instruments of the latter type are used when diffuse intensities beneath Bragg reflections or reflection profiles and tails must be analysed to study long-range distortion fields around single defects or small defect aggregates. In the case of small defect concentrations, the crystal structure remains almost perfect and the dynamical theory of diffraction is more appropriate. This topic is beyond the scope of this chapter.

4.2.8.1. Single-crystal techniques

In general, diffuse scattering is weak in comparison with Bragg scattering, and is anisotropically and inhomogeneously distributed in reciprocal space. The origin may be a static phenomenon or a dynamic process, giving rise to elastic or inelastic (quasi-elastic) diffuse scattering, respectively. If the disorder problem relates to more than one structural element, different parts of the diffuse scattering may show different behaviour in reciprocal space and/or on an energy scale. Therefore, before starting an experiment, some principal aspects should be considered: Is there need for X-ray and/or neutron methods? What is the optimum wavelength or energy (band), or does a 'white' technique offer advantages? Can focusing techniques be used without too strong a loss of resolution and what are the best scanning procedures? How can the background be minimized? Has the detector a low intrinsic noise and a high dynamic range?

On undertaking an investigation of a disorder problem by an analysis of the diffuse scattering, an overall picture should first be recorded by X-ray diffraction. Several sections through reciprocal space help to define the problem. For this purpose 'old-fashioned' film methods may be used, where the classical film is now commonly replaced by an imaging plate (IP) or a charge-coupled device (CCD) camera (see below). Clearly, short crystal-to-detector distances provide larger sections and avoid long exposure times, but suffer from spatial resolution. Distorted sections through the reciprocal lattice, such as produced by the Weissenberg method, may be transformed into a form suitable for easy interpretation (Welberry, 1983). The transformation of diffuse data measured using an IP or CCD requires suitable

software for the specific type of detector and is not always routinely available (Estermann & Steurer, 1998).

Standing-crystal techniques in combination with monochromatic radiation, usually called monochromatic Laue techniques (see, *e.g.*, Flack, 1970), save exposure time, which is particularly interesting for 'in-house' laboratory diffuse X-ray work. The Noromosic technique (Jagodzinski & Korekawa, 1973) is characterized by a convergent monochromatic beam which simulates an oscillation photograph over a small angular range. Heavily overexposed images, with respect to Bragg scattering, allow for sampling of diffuse intensity if a crystal is oriented in such a way that there is a well defined section between the Ewald sphere and the diffuse phenomenon under consideration. By combining single Noromosic photographs, Weissenberg patterns can be simulated. This relatively tedious method is often unavoidable because the heavily overexposed Bragg peaks obscure weak diffuse phenomena. Furthermore, standing pictures at distinct crystal settings in comparison with conventional continuous recording are frequently sufficient in diffuse scattering work and save time. Long-exposure Weissenberg photographs are therefore not equivalent to a smaller set of standing photographs. In this context it should be mentioned that a layer-line screen has not only the simple function of a selecting diaphragm, but the gap width determines the resolution volume within which diffuse intensity is collected (Welberry, 1983). For further discussion of questions of resolution see below. A comparison of Weissenberg and diffractometer methods for the measurement of diffuse scattering is given by Welberry & Glazer (1985). It should be pointed out, however, that diffractometer methods at synchrotron sources become more widely used if only very small (micrometre-sized) single-crystal specimens have to be used to study a disorder problem.

The basic arguments for using neutron-diffraction methods were given in Section 4.2.2.2: (i) the different interactions of X-rays and neutrons with matter; (ii) the lower absorption of neutrons, in particular when using longer (> 0.15 nm) wavelengths; and (iii) the matching of the energy of thermal neutrons with that of the phonons that contribute to the TDS background, and, in consequence, to separate it by a 'purely' elastic measurement. A comparative consideration of synchrotron- and neutron-related diffuse work on disordered alloys is given by Schweika (1998). Specific aspects of neutron diffraction and instruments are discussed at the end of this section.

Intensities: As mentioned above, diffuse intensities are usually weaker by several orders of magnitude than Bragg data. Therefore intense radiation sources are needed. Even a modern X-ray tube is a stronger source, defined by the flux density from the anode (number of photons $\mathrm{cm}^{-2}\,\mathrm{s}^{-1}$), than modern neutron sources. For this reason most experimental work which can be performed with X-rays should be. In home laboratories the intense characteristic spectrum of an X-ray tube is commonly used. At synchrotron storage rings any wavelength from a certain range can be selected. The extremely high brilliance (number of quanta cm^{-2}, sr^{-1}, s^{-1} and wavelength interval) of modern synchrotron sources is, however, unnecessary in the case of slowly varying diffuse phenomena. In these cases, an experimental setup at a laboratory rotating anode is competitive and often even superior if specimens with sufficient size are available. Various aspects of diffuse X-ray work at a synchrotron facility are discussed by Matsubara & Georgopoulos (1985), Oshima & Harada (1986) and Ohshima *et al.* (1986). Diffuse neutron-diffraction work can only be performed on a high-flux reactor or on a powerful spallation source. Highly efficient monochromator systems are needed when using a crystal diffractometer. Time-of-flight (TOF) neutron diffractometers at pulsed (spallation) neutron sources are equivalent to conventional diffractometers at reactors (Windsor, 1982). The merits of diffuse neutron work at pulsed sources have been discussed by Nield & Keen (2001).

Wavelength: The choice of an optimum wavelength is important with respect to the problem to be solved. For example, point defects cause diffuse scattering to fall off with increasing scattering vector; short-range ordering between clusters causes broad peaks corresponding to large d spacings; lattice-relaxation processes induce a broadening of the interferences; static modulation waves with long periods give rise to satellite scattering close to Bragg peaks. In all these cases, a long wavelength is preferable due to the higher resolution. The use of a long wavelength is also profitable when the main diffuse contributions can be recorded within an Ewald sphere as small as the Bragg cutoff of the sample at $H \simeq 1/(2d_{\max})$. 'Contamination' by Bragg scattering can thus be avoided. This is also advantageous from a different point of view: because the contribution of thermal diffuse scattering increases with increasing scattering vector $\mathbf{H}$, the relative amount of this component becomes negligibly small within the first reciprocal cell. However, one has to take care with the absorption of long-wavelength neutrons.

On the other hand, short wavelengths are needed where atomic displacements play the dominant role. If diffuse peaks in large portions of the reciprocal space, or diffuse streaks or planes, have to be recorded up to high values of the scattering vector in order to decide between different structural disorder models, hard X-rays or hot neutrons are needed. For example, high-energy X-rays (65 keV) provided at a synchrotron source were used by Welberry *et al.* (2003) to study diffuse diffraction from ceramic materials and allowed studies with better d resolution.

The λ^3 dependence of the scattered intensity, in the framework of the kinematical theory, is a crucial point for exposure or data-acquisition times. Moreover, the accuracy with which an experiment can be carried out suffers from a short wavelength: generally, momentum as well as energy resolution are lower. For a quantitative estimate detailed considerations of resolution in reciprocal space (and energy) are needed.

A specific wavelength aspect concerns the method of (X-ray) anomalous dispersion, which may also be used in diffuse-scattering work. It allows the contrast and identification of certain elements in a disordered structure. Even small concentrations of impurity atoms or defects as low as 10^{-6} can be determined by this method if the impurity atoms are located at specific sites, *e.g.* in domain boundaries, or if certain other defect structures exist with characteristic diffuse scattering in reciprocal space. The (weak) diffuse scattering can then be contrasted by tuning the wavelength across an absorption edge of the particular atomic species. To avoid strong fluorescence background scattering such an experiment is usually performed at different wavelengths (energies) at the 'low absorption side' close to an edge. The merit of this method was demonstrated by Berthold & Jagodzinski (1990), who analysed diffuse streaks due to boundaries between lamellar domains in an albite feldspar. Similar element contrast can be achieved in neutron diffuse work if using specimens with different isotopes, *e.g.* H–D exchange.

Monochromacy: In classical crystal diffractometry, monochromatic radiation is used in order to eliminate broadening effects due to the wavelength distribution. Focusing monochromators and other focusing devices (guides, mirrors) help to overcome the lack of luminosity. A focusing technique is very helpful for deciding between geometrical broadening and 'true' diffuseness. In a method that is used with some success, the sample is placed in a monochromatic divergent beam with its selected axis lying in the scattering plane of the monochromator (Jagodzinski, 1968). The specimen is fully embedded in the incident beam, which is focused onto a 2D detector. Using this procedure the influence of the sample size is suppressed in one dimension. In white-beam (neutron) time-of-flight diffractometry the time resolution is the counterpart to the wavelength resolution. This is discussed in some detail in the textbook of Keen & Nield (2004).

Detectors: Valuable developments with a view to diffuse-scattering work are multidetectors (see, *e.g.*, Haubold, 1975) and position-sensitive detectors for X-rays (Arndt, 1986*a*,*b*) and neutrons (Convert & Forsyth, 1983). A classical '2D area detector' is the photographic film – nowadays of less importance – which has to be 'read out' by microdensitometer scanning. Important progress in recording diffuse X-ray data has been made by the availability of multiwire detectors, IPs and CCD cameras (Estermann & Steurer, 1998). For 2D position-sensitive (proportional) counters problems may arise from inhomogeneities of the wire array as well as the limited dynamic range when a Bragg reflection is accidentally recorded. IP systems have the major advantage of a larger dynamic range, 10^5–10^6, compared to 10^2–10^3 for an X-ray film. IPs can also be used in diffuse experiments carried out with hard (65 keV) X-rays (Welberry *et al.*, 2003). IPs are also available for neutron work, where the necessary transformation of the detected neutrons into light signals is provided by special neutron-absorbing converter foils (Niimura *et al.*, 2003). The problem of an intrinsic sensitivity to gamma radiation may be overcome by protection with a thin sheet of lead. IPs allow data collection either in plane geometry or in simple rotation or Weissenberg geometry, both in combination with low- and high-temperature devices. CCD detectors are well suited for X-ray diffuse scattering, and when used in combination with converter foils they can also be used for the detection of neutrons. A basic prerequisite is a low intrinsic noise, which can be achieved by cooling the CCD with liquid nitrogen. With these detectors, extended diffuse data sets can be collected by rotating the sample in distinct narrow steps around a spindle axis over several χ settings and subsequent oscillations over a small angular range. Thus large parts of the reciprocal space can be recorded. An example is given by Campbell *et al.* (2004), who studied subtle defect structures in the microporous framework material mordenite. Linear position-sensitive detectors are mainly used in powder work, but can also be used for recording diffuse scattering by single crystals. By combining a linear position-sensitive detector and the TOF method, a whole area in reciprocal space is accessible simultaneously (Niimura *et al.*, 1982; Niimura, 1986).

Diffuse data recorded with IPs or CCDs are commonly evaluated by commercial software supplied by the manufacturer. These software packages include corrections for extracted Bragg data, but no special software tools for treating extended (diffuse) data are commonly available. One particular problem relates to the background definition for diffuse IP data. Even after subtraction of electronic noise, there remains considerable uncertainty about the amount of true background scattering from the sample as recorded by an IP scanner. The definitions of errors and error maps remain doubtful as long as the true conversion rate between the captured neutron or photon *versus* the recorded optical signal is unknown.

Absorption: Special attention must be paid to absorption phenomena, in particular when (in the X-ray case) an absorption edge of an element of the sample is close to the wavelength. Then strong fluorescence scattering may completely obscure weak diffuse-scattering phenomena. In comparison with X-rays, the generally lower absorption coefficients of neutrons make absolute measurements easier. This also allows the use of larger sample volumes, which is not true in the X-ray case. Moreover, the question of sample environment is less serious in the neutron case than in the X-ray case. However, the availability of hard X-rays at a synchrotron source (Butler *et al.*, 2000; Welberry *et al.*, 2003) makes the X-ray absorption problem less serious: irregularly shaped specimens without special surface treatment could be used. There is also no need for complicated absorption corrections and the separation of fluorescence background is rather simple.

Extinction: An extinction problem does not generally exist in diffuse-scattering work.

Background: An essential prerequisite for a diffuse-scattering experiment is the careful suppression of background scattering. Incoherent X-ray scattering by a sample gives continuous blackening in the case of fluorescence, or scattering at high 2θ angles owing to Compton scattering or 'incoherent' inelastic effects. Protecting the image plate with a thin Al or Ni foil is of some help against fluorescence, but also attenuates the diffuse intensity. Obviously, energy-dispersive counter methods are highly efficient in this case (see below). Air scattering produces a background at low 2θ angles which may easily be avoided by special slit systems and evacuation of the camera.

In X-ray or neutron diffractometer measurements, incoherent and multiple scattering contribute to a background which varies only slowly with 2θ and can be subtracted by linear interpolation or fitting a smooth curve, or can even be calculated quantitatively and then subtracted. In neutron diffraction there are rare cases when monoisotopic and 'zero-nuclear-spin' samples are available and, consequently, the corresponding incoherent scattering part vanishes completely. In some cases, a separation of coherent and incoherent neutron scattering is possible by polarization analysis (Gerlach *et al.*, 1982). An 'empty' scan can take care of instrumental background contributions. Evacuation or controlled-atmosphere studies need a chamber, which may give rise to spurious scattering. This can be avoided if no part of the vacuum chamber is hit by the primary beam. The problem is less serious in neutron work. The mounting of the specimen, *e.g.*, on a silica fibre with cement, poorly aligned collimators and beam catchers are further sources. Sometimes a specimen has to be enclosed in a capillary, which will always be hit by the incident beam. Careful and tedious experimental work is necessary in the case of low- and high-temperature (or -pressure) investigations, which have to be carried out in many disorder problems. While the experimental situation is again less serious in neutron scattering, there are problems with scattering from walls and containers in X-ray work. Because TDS dominates at high temperatures and in the presence of a static disorder problem, a quantitative separation can rarely be carried out in the case of high experimental background. Calculation and subtraction of the TDS is possible in principle, but difficult in practice. If the disorder problem in which one is interested in does not change with temperature, a low-temperature experiment can be carried out. Another way to get rid off TDS, at least partly, is by using a neutron diffractometer with an additional analyser set to zero-energy transfer.

Resolution: A quantitative analysis of diffuse-scattering data is essential for reaching a definite decision about a disorder model, but – in many cases – it is cumbersome. By comparing the calculated and corrected experimental data the magnitudes of the parameters of the structural disorder model may be derived. A careful analysis of the data requires, therefore, after separation of the background (see above), corrections for polarization (in the X-ray case), absorption (in conventional X-ray work) and resolution. Detailed considerations of instrumental resolution are necessary; the resolution depends, in addition to other factors, on the scattering angle and implies intensity corrections analogous to the Lorentz factor used in structure analysis from sharp Bragg reflections.

Resolution is conveniently described by the function $R(\mathbf{H}-\mathbf{H}_0)$, which is defined as the probability of detecting a photon or neutron with momentum transfer $h\mathbf{H} = h(\mathbf{k}-\mathbf{k}_0)$ when the instrument is set to measure $\mathbf{H}_0$. This function R depends on the instrumental parameters (such as the collimations, the mosaic spread of monochromator and the scattering angle) and the spectral width of the source. Fig. 4.2.8.1 shows a schematic sketch of a diffractometer setting. Detailed considerations of resolution volume in X-ray and neutron diffractometry are given by Sparks & Borie (1966) and by Cooper & Nathans (1968*a*,*b*), respectively. If a triple-axis (neutron) instrument is used, for example in a purely elastic configuration, the set of instrumental parameters includes the mosaicity of the analyser

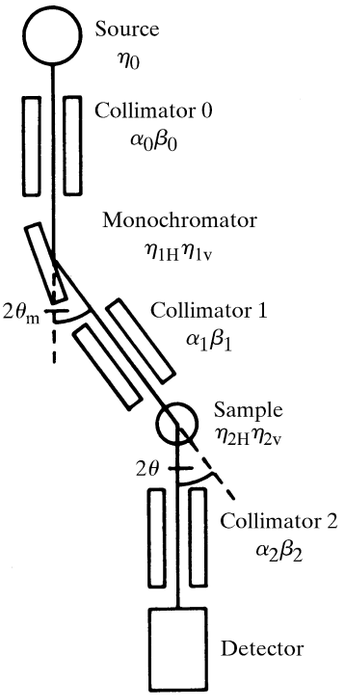

Fig. 4.2.8.1. Schematic sketch of a diffractometer setting.

and the collimations between the analyser and detector. In general, Gaussians are assumed to parameterize the mosaic distributions and transmission functions. Sophisticated resolution-correction programs are usually provided at any standard instrument for carrying out experiments at synchrotron and neutron facilities.

The general assumption of Gaussians is not too serious in the X-ray case (Iizumi, 1973). Restrictions are due to absorption, which makes the profiles asymmetric. Box-like functions are considered to be better for the spectral distribution or for large apertures (Boysen & Adlhart, 1987). These questions are treated in some detail by Klug & Alexander (1954). The main features, however, may also be derived by the Gaussian approximation. In practice, the function R may be obtained either by calculation from the known instrumental parameters or by measuring Bragg peaks from a perfect unstrained crystal. In the latter case, the intensity profile is given solely by the resolution function. Normalization with the Bragg intensities is also useful in order to place the diffuse-scattering intensity on an absolute scale.

In conventional single-crystal diffractometry the measured intensity is given by the convolution product of $\mathrm{d}\sigma/\mathrm{d}\Omega$ with R,

$$I(\mathbf{H}_0) = \int \frac{\mathrm{d}\sigma}{\mathrm{d}\Omega}(\mathbf{H})[R(\mathbf{H}-\mathbf{H}_0)]\,\mathrm{d}\mathbf{H}, \tag{4.2.8.1}$$

where $\mathrm{d}\sigma/\mathrm{d}\Omega$ describes the scattering cross section for the disorder problem. In a more accurate form the mosaicity of the sample has to be included:

$$\begin{aligned} I(\mathbf{H}_0) &= \int \frac{\mathrm{d}\sigma}{\mathrm{d}\Omega}(\mathbf{H}-\Delta\mathbf{K})[\eta(\Delta\mathbf{K})R(\mathbf{H}-\mathbf{H}_0)]\,\mathrm{d}\mathbf{H}\,\mathrm{d}(\Delta\mathbf{K}) \\ &= \int \frac{\mathrm{d}\sigma}{\mathrm{d}\Omega}(\mathbf{H}')[R'(\mathbf{H}'-\mathbf{H}_0)]\,\mathrm{d}\mathbf{H}'. \end{aligned} \tag{4.2.8.1a}$$

$R'(\mathbf{H}'-\mathbf{H}_0) = \int \eta(\Delta\mathbf{K})R(\mathbf{H}'+\Delta\mathbf{K}-\mathbf{H}_0)\,\mathrm{d}(\Delta\mathbf{K})$. The mosaic block distribution around a most probable vector $\mathbf{K}_0$ is described by $\eta(\Delta\mathbf{K})$: $\Delta\mathbf{K} = \mathbf{K}-\mathbf{K}_0$; $\mathbf{H}' = \mathbf{H}-\Delta\mathbf{K}$.

In (4.2.8.1) all factors independent of 2θ are neglected. All intensity expressions have to be calculated from equations (4.2.8.1) or (4.2.8.1a).

The intensity variation of diffuse peaks with 2θ measured with a single detector was studied in detail by Yessik *et al.* (1973). In principle, all special cases are included there. In practice, however, some important simplifications can be made if $\mathrm{d}\sigma/\mathrm{d}\Omega$ is either very broad or very sharp compared with R, *i.e.* for Bragg peaks, sharp streaks, 'thin' diffuse layers or extended 3D diffuse peaks (Boysen & Adlhart, 1987).

In the latter case, the cross section $\mathrm{d}\sigma/\mathrm{d}\Omega$ may be treated as nearly constant over the resolution volume so that the corresponding 'Lorentz' factor is independent of 2θ:

$$L_{3\mathrm{D}} = 1. \tag{4.2.8.2}$$

For a diffuse plane within the scattering plane with very small thickness and slowly varying cross section within the plane, one derives for a point measurement in the plane

$$L_{2\mathrm{D},\parallel} = (\beta_1'^2 + \beta_2^2 + 4\eta_{2\mathrm{v}}^2\sin^2\theta)^{-1/2}, \tag{4.2.8.3}$$

exhibiting an explicit dependence on θ (β_1', β_2 and $\eta_{2\mathrm{v}}$ determine an effective vertical divergence before the sample, the divergence before the detector and the vertical mosaic spread of the sample, respectively).

In the case of *relaxed* vertical collimations $\beta_1', \beta_2 \gg \eta_{2\mathrm{v}}$

$$L_{2\mathrm{D},\parallel} = (\beta_1'^2 + \beta_2^2)^{-1/2}, \tag{4.2.8.3a}$$

i.e. again independent of θ.

Scanning across the diffuse layer in a direction perpendicular to it one obtains an integrated intensity which is also independent of 2θ. This is even true if approximations other than Gaussians are used.

If, on the other hand, an equivalent diffuse plane is positioned perpendicular to the scattering plane, the equivalent expression for $L_{2\mathrm{D},\perp}$ of a point measurement is given by

$$\begin{aligned} L_{2\mathrm{D},\perp} \simeq [&4\eta_{2\mathrm{H}}^2\sin^2\theta\cos^2\psi + \alpha_2^2\sin^2(\psi-\theta) \\ &+ \alpha_1'^2\sin^2(\psi+\theta) + 4\eta_0'\sin^2\theta\sin^2\psi \\ &- 4\alpha_1''\sin\theta\sin\psi\sin(\theta+\psi)], \end{aligned} \tag{4.2.8.4}$$

where ψ gives the angle between the vector $\mathbf{H}_0$ and the line of intersection between the diffuse plane and the scattering plane. The coefficients $\eta_{2\mathrm{H}}$, α_2, α_1', α_1'' and η are either instrumental parameters or functions of them, defining horizontal collimations and mosaic spreads. In the case of a sharp X-ray line (produced, for example, by filtering) the last two terms in equation (4.2.8.4) vanish.

The use of integrated intensities from individual scans perpendicular to the diffuse plane, now carried out within the scattering plane, again gives a Lorentz factor independent of 2θ.

In the third fundamental special case, diffuse streaking along one reciprocal direction within the scattering plane (with a narrow cross section and slowly varying intensity along the streak), the Lorentz factor for a point measurement may be expressed by the product

$$L_{1\mathrm{D},\parallel} \simeq L_{2\mathrm{D},\parallel}L_{2\mathrm{D},\perp}, \tag{4.2.8.5}$$

where ψ now defines the angle between the streak and $\mathbf{H}_0$. The integrated intensity taken from an H scan perpendicular to the streak has to be corrected by a Lorentz factor which is equal to $L_{2\mathrm{D},\parallel}$ [equation (4.2.8.3)]. In the case of a diffuse streak perpendicular to the scattering plane, a relatively complicated equation holds for the corresponding Lorentz factor (Boysen & Adlhart, 1987). Again, simpler expressions hold for integrated intensities from H scans perpendicular to the streaks. Such scans may be performed in the radial direction (corresponding to a θ–2θ scan),

$$L_{1\mathrm{D},\perp,\mathrm{rad}} = (4\eta_{2\mathrm{H}}^2 + \alpha_2^2 + \alpha_1'^2)^{-1/2}(1/\sin\theta), \tag{4.2.8.6}$$

or perpendicular to the radial direction (within the scattering plane) (corresponding to an ω scan),

$$L_{1\mathrm{D},\perp,\mathrm{per}} = (\alpha_2^2 + \alpha_1^2 + 4\eta_0' \tan^2\theta - 4\alpha_1'' \tan\theta)^{-1/2}(1/\cos\theta). \quad (4.2.8.7)$$

Note that only the radial scan yields a simple θ dependence ($\sim 1/\sin\theta$).

From these considerations it is recommended that integrated intensities from scans perpendicular to a diffuse plane or a diffuse streak should be used in order to extract the disorder cross sections. For other scan directions, which make an angle α with the intersection line (diffuse plane) or with a streak, the L factors are simply $L_{2\mathrm{D},\perp}/\sin\alpha$ and $L_{1\mathrm{D},\perp}/\sin\alpha$, respectively.

One point should be emphasized: since in a usual experiment with a single counter the integration is performed over an angle $\Delta\omega$ *via* a general $\delta\omega{:}(g\delta 2\theta)$ scan, an additional correction factor arises:

$$\Delta\omega/\Delta\mathbf{H}_\beta = \sin(\beta+\theta)/(\mathbf{k}_0 \sin 2\theta). \quad (4.2.8.8)$$

β is the angle between $\mathbf{H}_0$ and the scan direction $\mathbf{H}_\beta$, and $g = (\tan\beta + \tan\theta)/(2\tan\theta)$ defines the coupling ratio between the rotation of the crystal around a vertical axis and the rotation of the detector shaft. The so-called 1:2 and ω-scan techniques are most frequently used, where $\beta = 0$ and 90°, respectively.

White-beam techniques: Techniques for the measurement of diffuse scattering using a *white* spectrum are common in neutron diffraction. Owing to the relatively low velocity of thermal or cold neutrons, TOF methods in combination with time-resolving detector systems placed at a fixed angle 2θ allow for a simultaneous recording along a radial direction through the origin of reciprocal space (see, *e.g.*, Turberfield, 1970; Bauer *et al.*, 1975). The scan range is limited by the Ewald spheres corresponding to $\lambda_{\max}$ and $\lambda_{\min}$, respectively. With several such detector systems placed at different angles or a 2D detector several scans may be carried out simultaneously during one neutron pulse.

An analogue of neutron TOF diffractometry in the X-ray case is a combination of a white source of X-rays and an energy-dispersive detector. This technique, which has been known in principle for a long time, suffered from relatively weak white sources. With the development of high-power X-ray generators and synchrotron sources this method has now become highly interesting. Its use in diffuse-scattering work (in particular, the effects on resolution) is discussed by Harada *et al.* (1984).

Some examples of neutron instruments dedicated to diffuse scattering are the diffractometers D7 at the Institut Laue–Langevin (ILL, Grenoble), DNS at the Forschungsneutronenquelle Heinz Maier-Leibnitz (FRM-II, Munich), G4-4 at the Laboratoire Léon Brillouin (LLB, Saclay) or SXD at ISIS, Rutherford Appleton Laboratory (RAL, UK). The instrument DNS uses a polarization analysis for diffuse scattering (Schweika & Böni, 2001; Schweika, 2003) and the SXD diffractometer is a TOF instrument using a (pulsed) white beam (Keen & Nield, 2004). All these instruments are equipped with banks of detectors. The single-crystal diffractometer D19 at the ILL, equipped with a multiwire area detector, is also suitable for collecting diffuse data. The flat-cone machine E2 at the Hahn–Meitner Institut (HMI, Berlin) is equipped with a bank of area detectors, has an option to record higher-order layers and can also be operated in an 'elastic' mode with a multicrystal analyser. The instrument D10 at the ILL is a versatile instrument which can be operated as a low-background two-axis or three-axis diffractometer with several further options. Neutron diffractometers that have recently become operational are BIX-3 at the Japan Atomic Energy Research Institute (JAERI, Japan), LADI at the ILL, where neutron-sensitive IPs are used for macromolecular work (for a comparison see Niimura *et al.*, 2003), and RESI at the Forschungsneutronenquelle Heinz Maier-Leibnitz (FRM-II, Munich) for common solid-state investigations. Information about all these instruments can be found in the respective handbooks or on the websites of the facilities.

4.2.8.2. Powders and polycrystals

The diffuse background in powder diagrams also contains valuable information about disorder. Only in very simple cases can a model be deduced from a powder pattern alone, but a refinement of a known disorder model can favourably be carried out, *e.g.* the temperature dependence may be studied. On account of the intensity integration, the ratio of diffuse intensity to Bragg intensity is enhanced in a powder pattern. Moreover, a powder pattern contains, in principle, all the information about the sample and might thus reveal more than single-crystal work. However, in powder-diffractometer experiments preferred orientations and textures could lead to a complete misidentification of the problem. Single-crystal experiments are generally preferable in this respect. Nevertheless, high-resolution powder investigations may give quick supporting information, *e.g.* about superlattice peaks, split reflections, lattice strains, domain-size effects, lattice-constant changes related to a disorder effect *etc*.

Evaluation of diffuse-scattering data from powder diffraction follows the same theoretical formulae developed for the determination of the radial distribution function for glasses and liquids. The final formula for random distributions may be given as (Fender, 1973)

$$I_D^p = \{\langle|F(\mathbf{H})|^2\rangle - |\langle F(\mathbf{H})\rangle|^2\} \sum_i s_i \sin(2\pi H r_i)/(2\pi H r_i). \quad (4.2.8.9)$$

s_i represents the number of atoms at distance r_i from the origin. An equivalent expression for a substitutional binary alloy is

$$I_D^p = \alpha(1-\alpha)\{|f_2(\mathbf{H}) - f_2(\mathbf{H})|^2\} \sum_i s_i \sin(2\pi H r_i)/(2\pi H r_i). \quad (4.2.8.10)$$

A quantitative calculation of a diffuse background is also helpful in combination with Rietveld's method (1969) for refining an averaged structure by fitting Bragg data. In particular, for highly anisotropic diffuse phenomena characteristic asymmetric line shapes occur.

The calculation of these line shapes is treated in the literature, mostly neglecting the instrumental resolution (see, *e.g.*, Warren, 1941; Wilson, 1949; Jones, 1949; and de Courville-Brenasin *et al.*, 1981). This is not justified if the variation of the diffuse intensity becomes comparable with that of the resolution function, as is often the case in neutron diffraction. The instrumental resolution may be incorporated using the resolution function of a powder instrument (Caglioti *et al.*, 1958). A detailed analysis of diffuse peaks is given by Yessik *et al.* (1973) and the equivalent considerations for diffuse planes and streaks are discussed by Boysen (1985). The case of 3D random disorder (incoherent neutron scattering, monotonous Laue scattering, averaged TDS, multiple scattering or short-range-order modulations) is treated by Sabine & Clarke (1977).

In polycrystalline samples the cross section has to be averaged over all orientations:

$$\frac{\mathrm{d}\sigma_\mathrm{p}}{\mathrm{d}\Omega}(\mathbf{H}') = \frac{n_\mathrm{c}}{H^2}\int \frac{\mathrm{d}\sigma}{\mathrm{d}\Omega}(\mathbf{H}') R'(|\mathbf{H}'| - |\mathbf{H}_0|)\,\mathrm{d}\mathbf{H}', \quad (4.2.8.11)$$

where n_c is number of crystallites in the sample; this averaged cross section enters the relevant expressions for the convolution product with the resolution function.

A general intensity expression may be written as (Boysen, 1985)

$$I_n(H_0) = P \sum_T m(T) A_n \Phi_n(H_0, T). \quad (4.2.8.12)$$

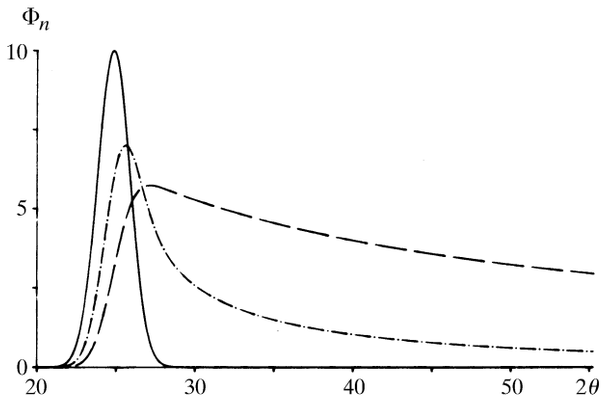

Fig. 4.2.8.2. Line profiles in powder diffraction for diffuse peaks (full line), continuous streaks (dot–dash lines) and continuous planes (broken lines). For explanation see text.

P denotes a scaling factor that depends on the instrumental luminosity, T is the shortest distance to the origin of the reciprocal lattice, $m(T)$ is the corresponding symmetry-induced multiplicity, A_n contains the structure factor of the structural units and the type of disorder, and Φ_n describes the characteristic modulation of the diffuse phenomenon of dimension n in the powder pattern. These expressions are given below with the assumption of Gaussian line shapes of width D for the narrow extension(s). The formulae depend on a factor $M = A_{1/2}(4k_1^2 - H_0^2)/(32\ln 2)$, where $A_{1/2}$ describes the dependence of the Bragg peaks on the instrumental parameters U, V and W (see Caglioti *et al.*, 1958),

$$A_{1/2}^2 = U\tan^2\theta + V\tan\theta + W, \qquad (4.2.8.13)$$

and $k_1 = 1/\lambda$.

(*a*) *Isotropic diffuse peak around T*

$$\Phi_0 = [2\pi(M^2 + D^2)]^{-1/2}(1/T^2) \times \exp\{-(H_0 - T)^2/2(M^2 + D^2)\}. \qquad (4.2.8.14)$$

The moduli $|\mathbf{H}_0|$ and T enter the exponential, *i.e.* the variation of $d\sigma/d\Omega$ along $|\mathbf{H}_0|$ is essential. For broad diffuse peaks ($M \ll D$) the angular dependence is due to $1/T^2$, *i.e.* proportional to $1/\sin^2\theta$. This result is valid for diffuse peaks of any shape.

(*b*) *Diffuse streak*

$$\Phi_1 = [2\pi(M^2 + D^2)]^{-1/2} \int_{-\infty}^{\infty} (T^2 + H^2)^{-1/2} \times \exp\{-H_0 - (T^2 + H^2)^{1/2}/2(M^2 + D^2)\}\,dH. \qquad (4.2.8.15)$$

The integral has to be evaluated numerically. If $(M^2 + D^2)$ is not too large, the term $1/(T^2 + H^2)$ varies only slowly compared to the exponential term and may be kept outside the integral, setting it approximately to $1/H_0^2$.

(*c*) *Diffuse plane (with $R^2 = H_x^2 + H_y^2$)*

$$\Phi_2 = (M^2 + D^2)^{-1/2} \int R^2/(T^2 + R^2) \times \exp\{-H_0 - (T^2 + R^2)^{1/2}/2(M^2 + D^2)\}\,dR. \qquad (4.2.8.16)$$

With the same approximation as in (*b*) the expression may be simplified to

$$\Phi_2 = \pi/H_0[1 - \mathrm{erf}\{(T - H_0)/[2(M^2 + D^2)]^{1/2}\} + 1/H_0^2[2\pi(M^2 + D^2)]^{1/2} \times \exp\{-(H_0 - T)^2/2(M^2 + D^2)\}]. \qquad (4.2.8.17)$$

(*d*) *Slowly varying diffuse scattering in three dimensions*

Φ_3 = constant. Consequently, the intensity is directly proportional to the cross section. The characteristic functions Φ_0, Φ_1 and Φ_2 are shown in Fig. 4.2.8.2 for equal values of T and D. Note the relative peak shifts and the high-angle tail.

4.2.8.3. Total diffraction pattern

As mentioned in Section 4.2.7.3.2, the atomic pair-distribution function (PDF), which is classically used for the analysis of the atomic distributions in liquids, melts or amorphous samples, can also be used to gain an understanding of disorder in crystals. The PDF is the Fourier transform of the total scattering. The measurement of total scattering is basically similar to recording X-ray or neutron powder patterns. The success of the method depends, however, decisively on various factors: (i) The availability of a large data set, *i.e.* reliable intensities up to high H values, in order to get rid of truncation ripples, which heavily influence the interpretation. Currently, values of $H_{\max}$ of more than 7 Å^{-1} can be achieved either with synchrotron X-rays [at the European Synchrotron Radiation Facility (ESRF) or Cornell High Energy Synchrotron Source (CHESS)] or with neutrons from reactors (*e.g.* instrument D4 at the ILL) and spallation sources [at ISIS or at LANSCE (instrument NPDF)]. (ii) High H resolution. (iii) High intensities, in particular at high H values. (iv) Low background of any kind which does not originate from the sample. High-quality intensities are therefore to be extracted from the raw data by taking care of an adequate absorption correction, correction of multiple-scattering effects, separation of inelastically scattered radiation (*e.g.* Compton scattering) and careful subtraction of 'diffuse' background which is not the 'true' diffuse scattering from the sample. These conditions are in practice rather demanding. A further detailed discussion is beyond the scope of this chapter, but a more thorough discussion is given, *e.g.*, by Egami (2004), and some examples are given by Egami & Billinge (2003).

References

Adlhart, W. (1981). *Diffraction by crystals with planar domains*. *Acta Cryst.* A**37**, 794–801.

Amorós, J. L. & Amorós, M. (1968). *Molecular Crystals: Their Transforms and Diffuse Scattering*. New York: John Wiley.

Arndt, U. W. (1986*a*). *X-ray position sensitive detectors*. *J. Appl. Cryst.* **19**, 145–163.

Arndt, U. W. (1986*b*). *The collection of single crystal diffraction data with area detectors*. *J. Phys. (Paris) Colloq.* **47**(C5), 1–6.

Aroyo, M. I., Boysen, H. & Perez-Mato, J. M. (2002). *Inelastic neutron scattering selection rules for phonons: application to leucite phase transitions*. *Appl. Phys. A*, **74**, S1043–S1048.

Axe, J. D. (1980). *Debye–Waller factors for incommensurate structures*. *Phys. Rev. B*, **21**, 4181–4190.

Bardhan, P. & Cohen, J. B. (1976). *X-ray diffraction study of short-range-order structure in a disordered Au_3Cu alloy*. *Acta Cryst.* A**32**, 597–614.

Bauer, G., Seitz, E. & Just, W. (1975). *Elastic diffuse scattering of neutrons as a tool for investigation of non-magnetic point defects*. *J. Appl. Cryst.* **8**, 162–175.

Bauer, G. S. (1979). *Diffuse elastic neutron scattering from nonmagnetic materials*. In *Treatise on Materials Science and Technology*, Vol. 15, edited by G. Kostorz, pp. 291–336. New York: Academic Press.

Berthold, T. & Jagodzinski, H. (1990). *Analysis of the distribution of impurities in crystals by anomalous X-ray scattering*. *Z. Kristallogr.* **193**, 85–100.

Bessière, M., Lefebvre, S. & Calvayrac, Y. (1983). *X-ray diffraction study of short-range order in a disordered Au_3Cu alloy*. *Acta Cryst.* B**39**, 145–153.

Beyeler, H. U., Pietronero, L. & Strässler, S. (1980). *Configurational model for a one-dimensional ionic conductor*. *Phys. Rev. B*, **22**, 2988–3000.

Billinge, S. J. L. & Egami, T. (1993). *Short-range atomic structure of $Nd_{2-x}Ce_xCuO_{4-y}$ determined by real-space refinement of neutron-powder-diffraction data. Phys. Rev B*, **47**, 14386–14406.

Billinge, S. J. L. & Thorpe, M. F. (1998). *Local Structure from Diffraction*. New York: Plenum Press.

Boissieu, M. de, Boudard, M., Hennion, M., Bellissent, R., Kycia, S., Goldman, A., Janot, C. & Audier, M. (1995). *Diffuse scattering and phason elasticity in the AlPdMn icosahedral phase. Phys. Rev. Lett.* **75**, 89–92.

Borie, B. & Sparks, C. J. (1971). *The interpretation of intensity distributions from disordered binary alloys. Acta Cryst.* A**27**, 198–201.

Boysen, H. (1985). *Analysis of diffuse scattering in neutron powder diagrams. Applications to glassy carbon. J. Appl. Cryst.* **18**, 320–325.

Boysen, H. (1995). *Diffuse scattering by domains and domain walls*. *Phase Transit.* **55**, 1–16.

Boysen, H. (1997). *Suppression of subsidiary maxima in computer simulations of diffraction intensities*. *Z. Kristallogr*. **212**, 634–636.

Boysen, H. (2007). *Coherence effects in the scattering from domain structures*. *J. Phys. Condens. Matter*, **19**, 270526–270537.

Boysen, H. & Adlhart, W. (1987). *Resolution corrections in diffuse scattering experiments. J. Appl. Cryst.* **20**, 200–209.

Boysen, H. & Frey, F. (1998). *Diffuse scattering: X-rays vs. neutrons. Phase Transit.* **67**, 197–217.

Boysen, H., Frey, F., Schrader, H. & Eckold, G. (1991). *On the proto-to-clino-/orthoenstatite phase transformation: single-crystal X-ray and inelastic neutron investigation*. *Phys. Chem. Mineral.* **17**, 629–635.

Bradley, C. J. & Cracknell, A. P. (1972). *The Mathematical Theory of Symmetry in Solids*, pp. 51–76. Oxford: Clarendon Press.

Brämer, R. (1975). *Statistische Probleme der Theorie des Parakristalls. Acta Cryst.* A**31**, 551–560.

Brämer, R. & Ruland, W. (1976). *The limitations of the paracrystalline model of disorder. Macromol. Chem.* **177**, 3601–3617.

Bubeck, E. & Gerold, V. (1984). *An X-ray investigation in the small and wide angle range from G.P.I. zones in Al–Cu*. In *Microstructural Characterization of Materials by Non-Microscopical Techniques*, edited by N. H. Andersen, M. Eldrup, N. Hansen, R. J. Jensen, T. Leffers, H. Lilholt, O. B. Pedersen & B. N. Singh. Roskilde: Risø National Laboratory.

Burandt, B., Komorek, M., Schnabel, W., Press, W. & Boysen, H. (1992). *High resolution X-ray investigations on the supersatellite reflections of labradorite. Z. Kristallogr.* **200**, 141–156.

Butler, B. D., Haeffner, D. R., Lee, P. L. & Welberry, T. R. (2000). *High-energy X-ray diffuse scattering using Weissenberg flat-cone geometry*. *J. Appl. Cryst.* **33**, 1046–1050.

Butler, B. D. & Welberry, T. R. (1992). *Calculation of diffuse scattering from simulated disordered crystals: a comparison with optical transforms*. *J. Appl. Cryst.* **25**, 391–399.

Caglioti, G., Paoletti, A. & Ricci, R. (1958). *Choice of collimators for a crystal spectrometer for neutron diffraction. Nucl. Instrum. Methods*, **3**, 223–226.

Campbell, B. J., Welberry, T. R., Broach, R. W., Hong, H. & Cheetham, A. K. (2004). *Elucidation of zeolite microstructure by synchrotron X-ray diffuse scattering. J. Appl. Cryst.* **37**, 187–192.

Cenedese, P., Bley, F. & Lefebvre, S. (1984). *Diffuse scattering in disordered ternary alloys: neutron measurements of local order in a stainless steel $Fe_{0.56}Cr_{0.21}Ni_{0.23}$. Acta Cryst.* A**40**, 228–240.

Collongues, R., Fayard, M. & Gautier, F. (1977). *Ordre et désordre dans les solides. J. Phys. (Paris) Colloq.* **38**(C7), Suppl.

Comes, R. & Shirane, G. (1979). *X-ray and neutron scattering from one-dimensional conductors.* In *Highly Conducting One Dimensional Solids*, edited by J. T. Devreese, R. P. Evrard & V. E. Van Doren, ch. 2. New York: Plenum.

Conradi, E. & Müller, U. (1986). *Fehlordnung bei Verbindungen mit Schichtstrukturen. II. Analyse der Fehlordnung in Wismuttriiodid. Z. Kristallogr.* **176**, 263–269.

Convert, P. & Forsyth, J. B. (1983). *Position-Sensitive Detectors of Thermal Neutrons.* London: Academic Press.

Cooper, M. J. & Nathans, R. (1968*a*). *The resolution function in neutron diffractometry. II. The resolution function of a conventional two-crystal neutron diffractometer for elastic scattering. Acta Cryst.* A**24**, 481–484.

Cooper, M. J. & Nathans, R. (1968*b*). *The resolution function in neutron diffractometry. III. Experimental determination and properties of the elastic two-crystal resolution function. Acta Cryst.* A**24**, 619–624.

Courville-Brenasin, J. de, Joyez, G. & Tchoubar, D. (1981). *Méthode d'ajustement automatique entre courbes experiméntale et calculée dans les diagrammes de diffraction de poudre. Cas des solides à structure lamellaire. I. Développement de la méthode. J. Appl. Cryst.* **14**, 17–23.

Cowley, J. M. (1950*a*). *X-ray measurement of order in single crystals of Cu_3Au. J. Appl. Phys.* **21**, 24–36.

Cowley, J. M. (1950*b*). *An approximate theory of order in alloys. Phys. Rev.* **77**, 664–675.

Cowley, J. M. (1976*a*). *Diffraction by crystals with planar faults. I. General theory. Acta Cryst.* A**32**, 83–87.

Cowley, J. M. (1976*b*). *Diffraction by crystals with planar faults. II. Magnesium fluorogermanate. Acta Cryst.* A**32**, 88–91.

Cowley, J. M. (1981). *Diffraction Physics*, 2nd ed. Amsterdam: North-Holland.

Cowley, J. M. & Au, A. Y. (1978). *Diffraction by crystals with planar faults. III. Structure analysis using microtwins. Acta Cryst.* A**34**, 738–743.

Cowley, J. M., Cohen, J. B., Salamon, M. B. & Wuensch, B. J. (1979). *Modulated Structures. AIP Conference Proceedings*, No. 53. New York: AIP.

Dederichs, P. H. (1973). *The theory of diffuse X-ray scattering and its application to the study of point defects and their clusters. J. Phys. F*, **3**, 471–496.

Dolling, G., Powell, B. M. & Sears, V. F. (1979). *Neutron diffraction study of the plastic phases of polycrystalline SF_6 and CBr_4. Mol. Phys.* **37**, 1859–1883.

Dorner, B. & Comes, R. (1977). *Phonons and structural phase transformation.* In *Dynamics of Solids and Liquids by Neutron Scattering*, edited by S. Lovesey & T. Springer, ch. 3. *Topics in Current Physics*, Vol. 3. Berlin: Springer.

Dorner, C. & Jagodzinski, H. (1972). *Entmischung im System SnO_2–TiO_2. Krist. Tech.* **7**, 427–444.

Dubernat, J. & Pezerat, H. (1974). *Fautes d'empilement dans les oxalates dihydratés des métaux divalents de la série magnésienne (Mg, Fe, Co, Ni, Zn, Mn). J. Appl. Cryst.* **7**, 387–393.

Edwards, O. S. & Lipson, H. (1942). *Imperfections in the structure of cobalt. I. Experimental work and proposed structure. Proc. R. Soc. London Ser. A*, **180**, 268–277.

Egami, T. (1990). *Atomic correlations in non-periodic matter*. *Mater. Trans. JIM*, **31**, 163–176.

Egami, T. (2004). *Local crystallography of crystals with disorder. Z. Kristallogr.* **219**, 122–129.

Egami, T. & Billinge, S. J. L. (2003). *Underneath the Bragg Peaks: Structural Analysis of Complex Materials.* Oxford: Pergamon Press.

Emery, V. J. & Axe, J. D. (1978). *One-dimensional fluctuations and the chain-ordering transformation in $Hg_{3-\delta}AsF_6$. Phys. Rev. Lett.* **40**, 1507–1511.

Endres, H., Pouget, J. P. & Comes, R. (1982). *Diffuse X-ray scattering and order–disorder effects in the iodine chain compounds N,N′-diethyl-N,N′-dihydrophenazinium iodide, $E_2PI_{1.6}$ and N,N′-dibenzyl-N,N′-dihydrophenazinium iodide, $B_2PI_{1.6}$. J. Phys. Chem. Solids*, **43**, 739–748.

Epstein, J., Welberry, T. R. & Jones, R. (1982). *Analysis of the diffuse X-ray scattering from substitutionally disordered molecular crystals of monoclinic 9-bromo-10-methylanthracene. Acta Cryst.* A**38**, 611–618.

Estermann, M. & Steurer, W. (1998). *Diffuse scattering data acquisition techniques. Phase Transit.* **67**, 165–195.

Fender, B. E. F. (1973). *Diffuse scattering and the study of defect solids.* In *Chemical Applications of Thermal Neutron Scattering*, edited by B. T. M. Willis, ch. 11. Oxford University Press.

Flack, H. D. (1970). *Short-range order in crystals of anthrone and in mixed crystals of anthrone–anthraquinone. Philos. Trans. R. Soc. London Ser. A*, **266**, 583–591.

Fontaine, D. de (1972). *An analysis of clustering and ordering in multicomponent solid solutions. I. Stability criteria. J. Phys. Chem. Solids*, **33**, 297–310.

Fontaine, D. de (1973). *An analysis of clustering and ordering in multicomponent solid solutions. II. Fluctuations and kinetics. J. Phys. Chem. Solids*, **34**, 1285–1304.

Forst, R., Jagodzinski, H., Boysen, H. & Frey, F. (1987). *Diffuse scattering and disorder in urea inclusion compounds $OC(NH_2)_2 + C_nH_{2n+2}$. Acta Cryst.* B**43**, 187–197.

Fouret, P. (1979). *Diffuse X-ray scattering by orientationally disordered solids.* In *The Plastically Crystalline State*, edited by J. N. Sherwood, ch. 3. New York: John Wiley.

Frey, F. (1997). *Diffuse scattering by domain structures.* In *Local Structure from Diffraction*, edited by S. J. L. Billinge & M. F. Thorpe. New York: Plenum Press.

Frey, F. (2003). *Disorder diffuse scattering of crystals and quasicrystals.* In *Particle Scattering, X-ray Diffraction, and Microstructure of Solids and Liquids*, edited by M. Ristig & K. Gernoth. Heidelberg: Springer.

Frey, F. & Boysen, H. (1981). *Disorder in cobalt single crystals. Acta Cryst.* A**37**, 819–826.

Frey, F., Jagodzinski, H. & Steger, W. (1986). *On the phase transformation zinc blende to wurtzite. Bull. Minéral. Crystallogr.* **109**, 117–129.

Frey, F. & Weidner, E. (2002). *Diffraction by domains in decagonal Al-Co-Ni quasicrystals. J. Alloys Compd.* **342**, 105–109.

Frey, F. & Weidner, E. (2003). *Disorder in decagonal quasicrystals. Z. Kristallogr.* **218**, 160–169.

Fultz, B. & Howe, J. M. (2002). *Transmission Electron Microscopy and Diffractometry of Materials*, ch. 9. Heidelberg: Springer.

Gehlen, P. & Cohen, J. B. (1965). *Computer simulation of the structure associated with local order in alloys. Phys. Rev. A*, **139**, 844–855.

Georgopoulos, P. & Cohen, J. B. (1977). *The determination of short range order and local atomic displacements in disordered binary solid solutions. J. Phys. (Paris) Colloq.* **38**(C7), 191–196.

Gerlach, P., Schärpf, O., Prandl, W. & Dorner, B. (1982). *Separation of the coherent and incoherent scattering of C_2Cl_6 by polarization analysis. J. Phys. (Paris) Colloq.* **43**(C7), 151–157.

Gerold, V. (1954). *Röntgenographische Untersuchungen über die Aushärtung einer Aluminium–Kupfer-Legierung mit Kleinwinkel-Schwenkaufnahmen. Z. Metallkd.* **45**, 593–607.

Gibbons, P. C. & Kelton, K. F. (1993). *Arcs of diffuse scattering in icosahedral glass models. J. Non-Cryst. Solids*, **153&154**, 165–171.

Goff, J. P., Hayes, W., Hull, S., Hutching, M. T. & Clausen, K. N. (1999). *Defect structure of yttria-stabilized zirconia and its influence on the ionic conductivity at elevated temperatures. Phys. Rev. B*, **59**, 14202–14219.

Goldman, A. I., Guryan, C. A., Stephens, P. W., Parsey, J. M. Jr, Aeppli, G., Chen, H. S. & Gayle, F. W. (1988). *Diffuse scattering from the icosahedral phase alloys. Phys. Rev. Lett.* **61**, 1962–1965.

Gragg, J. E., Hayakawa, M. & Cohen, J. B. (1973). *Errors in qualitative analysis of diffuse scattering from alloys. J. Appl. Cryst.* **6**, 59–66.

Guinier, A. (1942). *Le mécanisme de la précipitation dans un cristal de solution solide métallique. Cas des systémes aluminum–cuivre et aluminum–argent. J. Phys. Radium*, **8**, 124–136.

Guinier, A. (1963). *X-ray Diffraction in Crystals, Imperfect Solids and Amorphous Bodies.* San Francisco: Freeman.

Halla, F., Jagodzinski, H. & Ruston, W. R. (1953). *One-dimensional disorder in dodecahydrotriphenylene, $C_{18}H_{24}$. Acta Cryst.* **6**, 478–488.

Harada, J., Iwata, H. & Ohshima, K. (1984). *A new method for the measurement of X-ray diffuse scattering with a combination of an energy dispersive detector and a source of white radiation. J. Appl. Cryst.* **17**, 1–6.

Harburn, G., Miller, J. S. & Welberry, T. R. (1974). *Optical-diffraction screens containing large numbers of apertures. J. Appl. Cryst.* **7**, 36–38.

Harburn, G., Taylor, C. A. & Welberry, T. R. (1975). *An Atlas of Optical Transforms.* London: Bell.

Hashimoto, S. (1974). *Correlative microdomain model for short range ordered alloy structures. I. Diffraction theory. Acta Cryst.* A**30**, 792–798.

Hashimoto, S. (1981). *Correlative microdomain model for short range ordered alloy structures. II. Application to special cases. Acta Cryst.* A**37**, 511–516.

Hashimoto, S. (1983). *Correlative microdomain model for short range ordered alloy structures. III. Analysis for diffuse scattering from quenched CuAu alloy. Acta Cryst.* A**39**, 524–530.

Hashimoto, S. (1987). *Intensity expression for short-range order diffuse scattering with ordering energies in a ternary alloy system. J. Appl. Cryst.* **20**, 182–186.

Haubold, H. G. (1975). *Measurement of diffuse X-ray scattering between reciprocal lattice points as a new experimental method in determining interstitial structures. J. Appl. Cryst.* **8**, 175–183.

Hayakawa, M. & Cohen, J. B. (1975). *Experimental considerations in measurements of diffuse scattering. Acta Cryst.* A**31**, 635–645.

Hendricks, S. B. & Teller, E. (1942). *X-ray interference in partially ordered layer lattices. J. Chem. Phys.* **10**, 147–167.

Hohlwein, D., Hoser, A. & Prandl, W. (1986). *Orientational disorder in cubic $CsNO_2$ by neutron powder diffraction. Z. Kristallogr.* **177**, 93–102.

Hosemann, R. (1975). *Micro paracrystallites and paracrystalline superstructures. Macromol. Chem.* Suppl. 1, pp. 559–577.

Hosemann, R. & Bagchi, S. N. (1962). *Direct Analysis of Diffraction by Matter.* Amsterdam: North-Holland.

Iizumi, M. (1973). *Lorentz factor in single crystal neutron diffraction. Jpn. J. Appl. Phys.* **12**, 167–172.

Ishii, T. (1983). *Static structure factor of Frenkel–Kontorova-systems at high temperatures. Application to K-hollandite. J. Phys. Soc. Jpn*, **52**, 4066–4073.

Jagodzinski, H. (1949*a*). *Eindimensionale Fehlordnung und ihr Einfluss auf die Röntgeninterferenzen. I. Berechnung des Fehlordnungsgrades aus den Röntgeninterferenzen. Acta Cryst.* **2**, 201–208.

Jagodzinski, H. (1949*b*). *Eindimensionale Fehlordnung und ihr Einfluss auf die Röntgeninterferenzen. II. Berechnung der fehlgeordneten dichtesten Kugelpackungen mit Wechsel wirkungen der Reichweite 3. Acta Cryst.* **2**, 208–214.

Jagodzinski, H. (1949*c*). *Eindimensionale Fehlordnung und ihr Einfluss auf die Röntgeninterferenzen. III. Vergleich der Berechungen mit experimentellen Ergebnissen. Acta Cryst.* **2**, 298–304.

Jagodzinski, H. (1954). *Der Symmetrieeinfluss auf den allgemeinen Lösungsansatz eindimensionaler Fehlordnungsprobleme. Acta Cryst.* **7**, 17–25.

Jagodzinski, H. (1963). *On disorder phenomena in crystals.* In *Crystallography and Crystal Perfection*, edited by G. N. Ramachandran, pp. 177–188. London: Academic Press.

Jagodzinski, H. (1964*a*). *Allgemeine Gesichtspunkte für die Deutung diffuser Interferenzen von fehlgeordneten Kristallen.* In *Advances in Structure Research by Diffraction Methods*, Vol. 1, edited by R. Brill & R. Mason, pp. 167–198. Braunschweig: Vieweg.

Jagodzinski, H. (1964*b*). *Diffuse disorder scattering by crystals.* In *Advanced Methods of Crystallography*, edited by G. N. Ramachandran, pp. 181–219. London: Academic Press.

Jagodzinski, H. (1968). *Fokussierende Monochromatoren für Einkristallverfahren? Acta Cryst.* B**24**, 19–23.

Jagodzinski, H. (1972). *Transformation from cubic to hexagonal silicon carbide as a solid state reaction. Kristallografiya*, **16**, 1235–1246.

Jagodzinski, H. (1987). *Diffuse X-ray scattering from crystals.* In *Progress in Crystal Growth and Characterization*, edited by P. Krishna, pp. 47–102. Oxford: Pergamon Press.

Jagodzinski, H. & Haefner, K. (1967). *On order–disorder in ionic non-stoichiometric crystals. Z. Kristallogr.* **125**, 188–200.

Jagodzinski, H. & Hellner, E. (1956). *Die eindimensionale Phasenumwandlung des $RhSn_2$. Z. Kristallogr.* **107**, 124–149.

Jagodzinski, H. & Korekawa, M. (1965). *Supersatelliten im Beugungsbild des Labradorits $(Ca_2Na)(Si_2Al)_2O_8$. Naturwissenschaften*, **52**, 640–641.

Jagodzinski, H. & Korekawa, M. (1973). *Diffuse X-ray scattering by lunar minerals. Geochim. Cosmochim. Acta Suppl.* 4, **1**, 933–951.

Jagodzinski, H. & Laves, R. (1947). *Über die Deutung der Entmischungsvorgänge in Mischkristallen unter besonderer Berücksichtigung der Systeme Aluminium–Kupfer und Aluminium–Silber. Z. Metallkd.* **40**, 296–305.

Jagodzinski, H. & Penzkofer, B. (1981). *A new type of satellite in plagioclases. Acta Cryst.* A**37**, 754–762.

James, R. W. (1954). *The Optical Principles of Diffraction of X-rays*, ch. X. London: Bell.

Janner, A. & Janssen, T. (1980*a*). *Symmetry of incommensurate crystal phases. I. Commensurate basic structures. Acta Cryst.* A**36**, 399–408.

Janner, A. & Janssen, T. (1980*b*). *Symmetry of incommensurate crystal phases. II. Incommensurate basic structures. Acta Cryst.* A**36**, 408–415.

Janssen, T. & Janner, A. (1987). *Incommensurability in crystals. Adv. Phys.* **36**, 519–624.

Jaric, M. V. & Nelson, D. R. (1988). *Diffuse scattering from quasicrystals. Phys. Rev. B*, **37**, 4458–4472.

Jefferey, J. W. (1953). *Unusual X-ray diffraction effects from a crystal of wollastonite. Acta Cryst.* **6**, 821–826.

Jones, R. C. (1949). *X-ray diffraction by randomly oriented line gratings. Acta Cryst.* **2**, 252–257.

Kaiser-Bischoff, I., Boysen, H., Frey, F., Hoffmann, J.-U., Hohlwein, D. & Lerch, M. (2005). *The defect structure of Y- and N-doped zirconia. J. Appl. Cryst.* **38**, 139–146.

Kakinoki, J. & Komura, Y. (1954). *Intensity of X-ray diffraction by a one-dimensionally disordered crystal. I. General derivation in the cases of 'Reichweite' s = 0 and s = 1. J. Phys. Soc. Jpn*, **9**, 169–183.

Kakinoki, J. & Komura, Y. (1965). *Diffraction by a one-dimensionally disordered crystal. I. The intensity equation. Acta Cryst.* **19**, 137–147.

Kalning, M., Dorna, V., Press, W., Kek, S. & Boysen, H. (1997). *Profile analysis of the supersatellite reflections in labradorite – A synchrotron X-ray diffraction study. Z. Kristallogr.* **212**, 545–549.

Keen, D. A. & Nield, V. M. (2004). *Diffuse Neutron Scattering from Crystalline Materials.* Oxford University Press.

Kitaigorodsky, A. I. (1984). *Mixed Crystals. Springer Series in Solid State Science*, Vol. 33, chs. 6.4, 6.5, 8.4. Berlin: Springer.

Klug, H. P. & Alexander, L. E. (1954). *X-ray Diffraction Procedures.* New York: John Wiley.

Korekawa, M. (1967). *Theorie der Satellitenreflexe.* Habilitationsschrift der Naturwissenschaftlichen Fakultät der Universität München, Germany.

Korekawa, M. & Jagodzinski, H. (1967). *Die Satellitenreflexe des Labradorits. Schweiz. Mineral. Petrogr. Mitt.* **47**, 269–278.

Krivoglaz, M. A. (1969). *Theory of X-ray and Thermal Neutron Scattering by Real Crystals.* Part I. New York: Plenum.

Krivoglaz, M. A. (1996*a*). *Diffuse Scattering of X-rays and Neutrons by Fluctuations*. Berlin: Springer.

Krivoglaz, M. A. (1996*b*). *X-ray and Neutron Diffraction in Nonideal Crystals*. Berlin: Springer.

Lechner, R. E. & Riekel, C. (1983). *Application of neutron scattering in chemistry.* In *Neutron Scattering and Muon Spin Rotation. Springer Tracts in Modern Physics*, Vol. 101, edited by G. Höhler, pp. 1–84. Berlin: Springer.

Lefebvre, J., Fouret, R. & Zeyen, C. (1984). *Structure determination of sodium nitrate near the order–disorder phase transition. J. Phys. (Paris)*, **45**, 1317–1327.

Lei, J., Wang, R., Hu, Ch. & Ding, D. (1999). *Diffuse scattering from decagonal quasicrystals. Phys. Rev. B*, **59**, 822–828.

McGreevy, R. L. (2001). *Reverse Monte Carlo modelling. J. Phys. Condens. Matter*, **13**, R877–R913.

McGreevy, R. L. & Pusztai, L. (1988). *Reverse Monte Carlo simulation: a new technique for the determination of disordered structures. Mol. Simul.* **1**, 359–367.

Mardix, S. & Steinberger, I. T. (1970). *Tilt and structure transformation in ZnS. J. Appl. Phys.* **41**, 5339–5341.

Martorana, A., Marigo, A., Toniolo, L. & Zenetti, R. (1986). *Stacking faults in the β-form of magnesium dichloride. Z. Kristallogr.* **176**, 1–12.

Matsubara, E. & Georgopoulos, P. (1985). *Diffuse scattering measurements with synchrotron radiation: instrumentation and techniques. J. Appl. Cryst.* **18**, 377–383.

Metropolis, N., Rosenbluth, A. W., Rosenbluth, M. N., Teller, A. H. & Teller, E. (1953). *Equation of state calculations by fast computing machines. J. Chem. Phys.* **21**, 1087–1092.

Micu, A. M. & Smith, J. C. (1995). *SERENA: a program for calculating X-ray diffuse scattering intensities from molecular dynamics trajectories. Comput. Phys. Commun.* **91**, 331–338.

More, M., Lefebvre, J. & Hennion, B. (1984). *Quasi-elastic coherent neutron scattering in the disordered phase of CBr_4. Experimental evidence of local order and rotational dynamics of molecules. J. Phys. (Paris)*, **45**, 303–307.

More, M., Lefebvre, J., Hennion, B., Powell, B. M. & Zeyen, C. (1980). *Neutron diffuse scattering in the disordered phase of CBr_4. I. Experimental. Elastic and quasi-elastic coherent scattering in single crystals. J. Phys. C*, **13**, 2833–2846.

Moss, D. S., Harris, G. W., Wostrack, A. & Sansom, C. (2003). *Diffuse X-ray scattering from molecular crystals. Crystallogr. Rev.* **9**, 229–277.

Moss, S. C. (1966). *Local order in solid alloys.* In *Local Atomic Arrangements Studied by X-ray Diffraction*, edited by J. B. Cohen & J. E. Hilliard, ch. 3, pp. 95–122. New York: Gordon and Breach.

Müller, H. (1952). *Die eindimensionale Umwandlung Zinkblende-Wurtzit und die dabei auftretenden Anomalien. Neues Jahrb. Mineral. Abh.* **84**, 43–76.

Neder, R. B., Frey, F. & Schulz, H. (1990). *Diffraction theory for diffuse scattering by correlated microdomains in materials with several atoms per unit cell. Acta Cryst.* A**46**, 792–798.

Nield, V. M. & Keen, D. A. (2001). *Diffuse Neutron Scattering from Crystalline Materials*. Oxford Science Publications.

Nield, V. M., Keen, D. A. & McGreevy, R. L. (1995). *The interpretation of single-crystal diffuse scattering using reverse Monte Carlo modelling. Acta Cryst.* A**51**, 763–771.

Niimura, N. (1986). *Evaluation of data from 1-d PSD used in TOF method. J. Phys. (Paris) Colloq.* **47**(C5), Suppl., 129–136.

Niimura, N., Chataka, T., Ostermann, A., Kurihara, K. & Tanaka, I. (2003). *High resolution neutron protein crystallography. Hydrogen and hydration in proteins. Z. Kristallogr.* **218**, 96–107.

Niimura, N., Ishikawa, Y., Arai, M. & Furusaka, M. (1982). *Applications of position sensitive detectors to structural analysis using pulsed neutron sources. AIP Conference Proceedings*, Vol. 89, *Neutron Scattering*, edited by J. Faber, pp. 11–22. New York: AIP.

Ohshima, K. & Harada, J. (1986). *X-ray diffraction study of short-range ordered structure in a disordered Ag–15 at.% Mg alloy. Acta Cryst.* B**42**, 436–442.

Ohshima, K., Harada, J., Morinaga, M., Georgopoulos, P. & Cohen, J. B. (1986). *Report on a round-robin study of diffuse X-ray scattering. J. Appl. Cryst.* **19**, 188–194.

Ohshima, K. & Moss, S. C. (1983). *X-ray diffraction study of basal-(ab)-plane structure and diffuse scattering from silver atoms in disordered stage-2 $Ag_{0.18}TiS_2$. Acta Cryst.* A**39**, 298–305.

Ohshima, K., Watanabe, D. & Harada, J. (1976). *X-ray diffraction study of short-range order diffuse scattering from disordered Cu–29.8% Pd alloy. Acta Cryst.* A**32**, 883–892.

Overhauser, A. W. (1971). *Observability of charge-density waves by neutron diffraction. Phys. Rev. B*, **3**, 3173–3182.

Pandey, D., Lele, S. & Krishna, P. (1980*a*). *X-ray diffraction from one dimensionally disordered 2H-crystals undergoing solid state transformation to the 6H structure. I. The layer displacement mechanism. Proc. R. Soc. London Ser. A*, **369**, 435–439.

Pandey, D., Lele, S. & Krishna, P. (1980*b*). *X-ray diffraction from one dimensionally disordered 2H-crystals undergoing solid state transformation to the 6H structure. II. The deformation mechanism. Proc. R. Soc. London Ser. A*, **369**, 451–461.

Pandey, D., Lele, S. & Krishna, P. (1980*c*). *X-ray diffraction from one dimensionally disordered 2H-crystals undergoing solid state transformation to the 6H structure. III. Comparison with experimental observations on SiC. Proc. R. Soc. London Ser. A*, **369**, 463–477.

Patterson, A. L. (1959). *Fourier theory.* In *International Tables for X-ray Crystallography*, Vol. II, ch. 2.5. Birmingham: Kynoch Press.

Peisl, J. (1975). *Diffuse X-ray scattering from the displacement field of point defects and defect clusters. J. Appl. Cryst.* **8**, 143–149.

Perez-Mato, J. M., Aroyo, M., Hlinka, J., Quilichini, M. & Currat, R. (1998). *Phonon symmetry selection rules for inelastic neutron scattering. Phys. Rev. Lett.* **81**, 2462–2465.

Petricek, V., Maly, K., Coppens, P., Bu, X., Cisarova, I. & Frost-Jensen, A. (1991). *The description and analysis of composite crystals. Acta Cryst.* A**47**, 210–216.

Pflanz, S. & Moritz, W. (1992). *The domain matrix method: a new calculation scheme for diffraction profiles. Acta Cryst.* A**48**, 716–727.

Pouget, J.-P. (2004). *X-ray diffuse scattering as precursor of incommensurate Peierls transitions in one-dimensional organic transfer conductors. Z. Kristallogr.* **219**, 711–718.

Prandl, W. (1981). *The structure factor of orientational disordered crystals: the case of arbitrary space, site, and molecular point-group. Acta Cryst.* A**37**, 811–818.

Press, W. (1973). *Analysis of orientational disordered structures. I. Method. Acta Cryst.* A**29**, 252–256.

Press, W., Grimm, H. & Hüller, A. (1979). *Analysis of orientational disordered structures. IV. Correlations between orientation and position of a molecule. Acta Cryst.* A**35**, 881–885.

Press, W. & Hüller, A. (1973). *Analysis of orientational disordered structures. II. Examples: Solid CD_4, p-D_2 and $NDBr_4$. Acta Cryst.* A**29**, 257–263.

Proffen, Th. & Neder, R. B. (1999). *DISCUS, a program for diffuse scattering and defect-structure simulations – update. J. Appl. Cryst.* **32**, 838–839.

Proffen, Th. & Welberry, T. R. (1997). *Analysis of diffuse scattering via reverse Monte Carlo technique: a systematic investigation. Acta Cryst.* A**53**, 202–216.

Radons, W., Keller, J. & Geisel, T. (1983). *Dynamical structure factor of a 1-d harmonic liquid: comparison of different approximation methods. Z. Phys. B*, **50**, 289–296.

Rahman, S. H. (1993). *The local domain configuration in partially ordered $AuCu_3$. Acta Cryst.* A**49**, 68–79.

Rietveld, H. M. (1969). *A profile refinement method for nuclear and magnetic structures. J. Appl. Cryst.* **2**, 65–71.

Rosshirt, E., Frey, F. & Boysen, H. (1991). *Disorder diffuse scattering in K-hollandite. Neues Jahrb. Mineral. Abh.* **1**, 101–115.

Rosshirt, E., Frey, F., Boysen, H. & Jagodzinski, H. (1985). *Chain ordering in $E_2PI_{1.6}$ (5,10-diethylphenazinium iodide). Acta Cryst.* B**41**, 66–76.

Sabine, T. M. & Clarke, P. J. (1977). *Powder neutron diffraction – refinement of the total pattern. J. Appl. Cryst.* **10**, 277–280.

Scaringe, P. R. & Ibers, J. A. (1979). *Application of the matrix method to the calculation of diffuse scattering in linearly disordered crystals. Acta Cryst.* A**35**, 803–810.

Schmatz, W. (1973). *X-ray and neutron scattering on disordered crystals.* In *Treatise on Materials Science and Technology*, Vol. 2, edited by H. Hermans, ch. 3.1. New York: Academic Press.

Schmatz, W. (1983). *Neutron scattering studies of lattice defects: static properties of defects.* In *Methods of Experimental Physics, Solid State: Nuclear Physics*, Vol. 21, edited by J. N. Mundy, S. J. Rothman, M. J. Fluss & L. C. Smedskajew, ch. 3.1. New York: Academic Press.

Schulz, H. (1982). *Diffuse X-ray diffraction and its application to materials research.* In *Current Topics in Materials Science*, edited by E. Kaldis, ch. 4. Amsterdam: North-Holland.

Schwartz, L. H. & Cohen, J. B. (1977). *Diffraction from Materials.* New York: Academic Press.

Schweika, W. (1998). *Diffuse scattering and Monte Carlo simulations*. *Springer Tracts in Modern Physics*, Volume 141, edited by G. Höhler. Heidelberg: Springer.

Schweika, W. (2003). *Time-of-flight and vector polarization analysis for diffuse scattering. Physica B*, **335**, 157–163.

Schweika, W. & Böni, P. (2001). *The instrument DNS: Polarization analysis for diffuse neutron scattering. Physica B*, **297**, 155–159.

Sherwood, J. N. (1979). *The Plastically Crystalline State.* New York: John Wiley.

Smaalen, S. van (2004). *An elementary introduction to superspace crystallography. Z. Kristallogr.* **219**, 681–691.

Smaalen, S. van, Lamfers, H.-J. & de Boer, J. L. (1998). *Diffuse scattering and order in quasi-one-dimensional molecular crystals. Phase Transit.* **67**, 277–294.

Sparks, C. J. & Borie, B. (1966). *Methods of analysis for diffuse X-ray scattering modulated by local order and atomic displacements.* In *Atomic Arrangements Studied by X-ray Diffraction*, edited by J. B. Cohen & J. E. Hilliard, ch. 1, pp. 5–50. New York: Gordon and Breach.

Springer, T. (1972). *Quasielastic Neutron Scattering for the Investigation of Diffuse Motions in Solid and Liquids. Springer Tracts in Modern Physics*, Vol. 64. Berlin: Springer.

Steurer, W. & Frey, F. (1998). *Disorder diffuse scattering from quasicrystals. Phase Transit.* **67**, 319–361.

Takaki, Y. & Sakurai, K. (1976). *Intensity of X-ray scattering from one-dimensionally disordered crystal having the multilayer average structure. Acta Cryst.* A**32**, 657–663.

Tibbals, J. E. (1975). *The separation of displacement and substitutional disorder scattering: a correction for structure factor ratio variation. J. Appl. Cryst.* **8**, 111–114.

Turberfield, K. C. (1970). *Time-of-flight diffractometry.* In *Thermal Neutron Diffraction*, edited by B. T. M. Willis. Oxford University Press.

Vainshtein, B. K. (1966). *Diffraction of X-rays by Chain Molecules.* Amsterdam: Elsevier.

Varn, D. P., Canright, G. S. & Crutchfield, J. P. (2002). *Discovering planar disorder in closed-packed structures from X-ray diffraction: Beyond the fault model. Phys. Rev. B*, **66**, 174110–174113.

Warren, B. E. (1941). *X-ray diffraction in random layer lattices. Phys. Rev.* **59**, 693–699.

Warren, B. E. (1969). *X-ray Diffraction.* Reading: Addison-Wesley.

Weber, T. & Bürgi, H.-B. (2002). *Determination and refinement of disordered crystal structures using evolutionary algorithms in combination with Monte Carlo methods. Acta Cryst.* A**58**, 526–540.

Weber, Th. (2005). *Cooperative evolution – a new algorithm for the investigation of disordered structures via Mont Carlo modelling. Z. Kristallogr.* **220**, 1099–1107.

Weber, Th., Boysen, H. & Frey, F. (2000). *Longitudinal positional ordering of n-alkane molecules in urea inclusion compounds. Acta Cryst.* B**56**, 132–141.

Weidner, E., Frey, F. & Hradil, K. (2001). *Transient ordering states in decagonal Al-Co-Ni and Al-Cu-Co-Si phases. Philos. Mag.* **201**, 2375–2389.

Weidner, E., Frey, F., Lei, J.-L., Pedersen, B., Paulmann, C. & Morgenroth, W. (2004). *Disordered quasicrystals: diffuse scattering in decagonal Al-Ni-Fe. J. Appl. Cryst.* **37**, 802–807.

Welberry, T. R. (1983). *Routine recording of diffuse scattering from disordered molecular crystals. J. Appl. Phys.* **16**, 192–197.

Welberry, T. R. (1985). *Diffuse X-ray scattering and models of disorder. Rep. Prog. Phys.* **48**, 1543–1593.

Welberry, T. R. (2004). *Diffuse X-ray Scattering and Models of Disorder*. Oxford University Press.

Welberry, T. R. & Butler, B. D. (1994). *Interpretation of diffuse X-ray scattering via models of disorder. J. Appl. Cryst.* **27**, 205–231.

Welberry, T. R. & Glazer, A. M. (1985). *A comparison of Weissenberg and diffractometer methods for the measurement of diffuse scattering from disordered molecular crystals. Acta Cryst.* A**41**, 394–399.

Welberry, T. R., Goossens, D. J., Haeffner, D. R., Lee, P. L. & Almer, J. (2003). *High-energy diffuse scattering on the 1-ID beamline at the Advanced Photon Source. J. Synchrotron Rad.* **10**, 284–286.

Welberry, T. R. & Proffen, Th. (1998). *Analysis of diffuse scattering from single crystals via the reverse Monte Carlo technique. I. Comparison with direct Monte Carlo. J. Appl. Cryst.* **31**, 309–317.

Welberry, T. R., Proffen, Th. & Bown, M. (1998). *Analysis of single-crystal diffuse X-ray scattering via automatic refinement of a Monte Carlo model. Acta Cryst.* A**54**, 661–674.

Welberry, T. R. & Siripitayananon, J. (1986). *Analysis of the diffuse scattering from disordered molecular crystals: application to 1,4-dibromo-2,5-diethyl-3,6-dimethylbenzene at 295 K. Acta Cryst.* B**42**, 262–272.

Welberry, T. R. & Siripitayananon, J. (1987). *Analysis of the diffuse scattering from disordered molecular crystals: application to 1,3-dibromo-2,5-diethyl-4,6-dimethylbenzene at 295 K. Acta Cryst.* B**43**, 97–106.

Welberry, T. R. & Withers, R. L. (1987). *Optical transforms of disordered systems displaying diffuse intensity loci. J. Appl. Cryst.* **20**, 280–288.

Welberry, T. R. & Withers, R. L. (1990). *Optical transforms of disordered systems containing symmetry-related scattering sites. J. Appl. Cryst.* **23**, 303–314.

Wilke, W. (1983). *General lattice factor of the ideal paracrystal. Acta Cryst.* A**39**, 864–867.

Wilson, A. J. C. (1942). *Imperfections in the structure of cobalt. II. Mathematical treatment of proposed structure. Proc. R. Soc. London Ser. A*, **180**, 277–285.

Wilson, A. J. C. (1949). *X-ray diffraction by random layers: ideal line profiles and determination of structure amplitudes from observed line profiles. Acta Cryst.* **2**, 245–251.

Wilson, A. J. C. (1962). *X-ray Optics*, 2nd ed., chs. V, VI, VIII. London: Methuen.

Windsor, C. G. (1982). *Neutron diffraction performance in pulsed and steady sources.* In *Neutron Scattering. AIP Conference Proceedings*, Vol. 89, edited by J. Faber, pp. 1–10. New York: AIP.

Wolff, P. M. de (1974). *The pseudo-symmetry of modulated crystal structures. Acta Cryst.* A**30**, 777–785.

Wolff, P. M. de, Janssen, T. & Janner, A. (1981). *The superspace groups for incommensurate crystal structures with a one-dimensional modulation. Acta Cryst.* A**37**, 625–636.

Wong, S. F., Gillan, B. E. & Lucas, B. W. (1984). *Single crystal disorder diffuse X-ray scattering from phase II ammonium nitrate, NH_4NO_3. Acta Cryst.* B**40**, 342–346.

Wooster, W. A. (1962). *Diffuse X-ray Reflections from Crystals*, chs. IV, V. Oxford: Clarendon Press.

Wu, T. B., Matsubara, E. & Cohen, J. B. (1983). *New procedures for qualitative studies of diffuse X-ray scattering. J. Appl. Cryst.* **16**, 407–414.

Yessik, M., Werner, S. A. & Sato, H. (1973). *The dependence of the intensities of diffuse peaks on scattering angle in neutron diffraction. Acta Cryst.* A**29**, 372–382.

Young, R. A. (1975). Editor. *International discussion meeting on studies of lattice distortions and local atomic arrangements by X-ray, neutron and electron diffraction. J. Appl. Cryst.* **8**, 79–191.

Zernike, F. & Prins, J. A. (1927). *Die Beugung von Röntgenstrahlen in Flüssigkeiten als Effekt der Molekülanordnung. Z. Phys.* **41**, 184–194.